Behavior and Modeling of Partially Restrained Beam-Girder Connections

by

Clinton Owen Rex

Dissertation submitted to the Faculty of
The Virginia Polytechnic Institute and State University
in partial fulfillment of the requirements for the degree of

Doctor of Philosophy in Civil Engineering

submitted to Advisory Committee

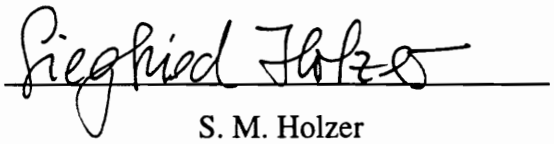

S. M. Holzer

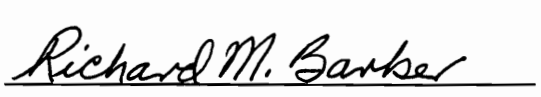

R. M. Barker

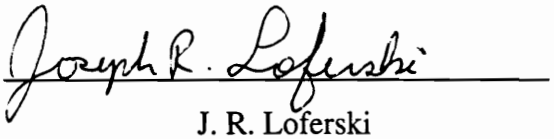

J. R. Loferski

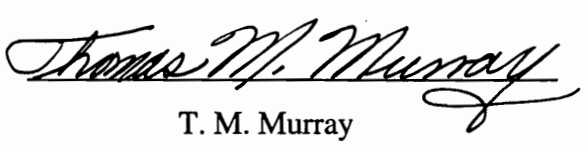

T. M. Murray

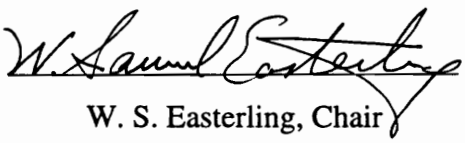

W. S. Easterling, Chair

CHARLES E. VIA, JR., DEPARTMENT OF CIVIL ENGINEERING
VIRGINIA POLYTECHNIC INSTITUTE AND STATE UNIVERSITY
BLACKSBURG, VA

December, 1996

Keywords: Steel, Connections, Composite, Partially-Restrained, Semi-Rigid, Beam-Girder

C. 2

LD
5655
V855
1996
R49
c.2

BEHAVIOR AND MODELING OF PARTIALLY RESTRAINED BEAM-GIRDER CONNECTIONS

by

Clinton Owen Rex

W. Samuel Easterling, Chairman

Civil Engineering

ABSTRACT

Beams in a typical steel framed floor design are assumed to have pinned supports for purposes of design. In reality, the connections between the beams and girders in a steel framed floor system are not pinned. The design bending moments and deflections of the attached beam could be reduced if the true rotational restraint provided by the beam-girder connections could be included in the design. The connection rotational restraint is characterized by the moment-rotation behavior. Consequently, a method for approximating the moment-rotation behavior of the beam-girder connection is required before the beneficial effects of the true connection rotational restraint can be considered in design.

Experimental and analytical research on the moment-rotation behavior of a specific type of beam-girder connection is presented in this dissertation. The primary objective of this research is to develop a component model of the connection that can be used to approximate the moment-rotation behavior. The component model is based on the hypothesis that the connection behavior can be modeled as a combination of the connection component behaviors. The connection components are the fundamental pieces of the connection such as bolts, shear studs, and welds. In general, the component model can be very computationally intensive. Consequently, a secondary objective of this research is to develop a connection model that is simpler to use.

Behavior models for each of the connection components are presented and/or developed. These models are derived from a combination of existing literature, experimental and analytical research, and basic mechanics. Next, a method of combining the component behaviors into a connection model that can be used to approximate the moment-rotation behavior is developed. Results from experimental research on the moment-rotation behavior of the beam-girder connection are then used to verify the model. Finally, a simplified model of the beam-girder connection is developed. This model is based on the same hypothesis as the component model; however, through a combination of assumptions, simplifications, and the results of parametric studies the simplified model becomes far less computationally intensive than the full component model.

ACKNOWLEDGMENTS

I would like to thank Dr. W. Samuel Easterling for initiating this research and for entrusting me with the responsibility for its successful completion. I also want to thank him for providing me with a variety of opportunities to expand my abilities and broaden my horizons. I want to thank Dr. Thomas M. Murray for his guidance, support, and for providing me with an education in steel which is most likely unparalleled by any other university. Both of these men have gone above the call of duty to help ensure that the time I spent at Virginia Tech was the best experience possible both in and out of the classroom.

I would like to thank the Structures Division faculty for each of their contributions to my education. In particular, Dr. Richard Barker and Dr. Siegfried Holzer for serving on my committee. I would also like to thank Dr. Joseph Loferski for serving on my committee. Thanks also to my fellow Research Assistants, both old and new; including, Angela Terry, Ron Rodkey, David Gibbings, John Lyons, Budi Widjaja, Ron Shope, Joe Howard, and Michelle Rambo-Roddenberry who were all of great assistance when asked to help and who I wish all the best. A thanks is also given to Dennis Huffman and Brett Farmer for their assistance in the fabrication of test specimens and construction of test setups.

A special thank you goes to my family for always inspiring me to continue my education and for providing constant support. I want to especially thank my parents for providing me with two outstanding examples of remarkable people.

A very special thank you goes to my wife Karen for all the little and big things she did to help me complete my education (including attaching instruments and bringing me dinner late at night). Without the stability, happiness, and understanding she gave me from start to finish I would never had completed this degree.

An additional thank you is extended to The American Institute of Steel Construction, The American Iron and Steel Institute, and The National Science Foundation for sponsoring this research.

TABLE OF CONTENTS

LIST OF FIGURES

LIST OF TABLES

TABLE OF NOMENCLATURE

α = Bolt tension coefficient; Angle of fracture surface in the fillet weld

a = Distance from center of plate to the caliper; Factor for locating center of resistance (0 if weld in compression, 0.345 if weld in tension); also the distance from the weld line to the centerline of the bolts in a single plate shear connection

A_0 = Initial cross-sectional area of tensile test specimen

α_1 = Correction factor for reinforcing bond; angle from geometric bearing stiffness model

α_2 = Correction factor for loading time period; angle from geometric bearing stiffness model

α_1, α_4, α_3 = Parametric modifiers for the curvature parameter

A_b = Area of the bolt based on nominal diameter

A_{bt} = Tensile area of a bolt

A_{bv} = Shear area of a bolt

A_{ceff} = Effective concrete area in tension

A_r = Area of reinforcing steel

A_{sc} = Area of the shear stud based on the nominal shear stud diameter

A_w = Effective area of weld throat

β = Steel correction factor

β_1, β_2, β_3, β_4, β_5 = Parametric terms used for determining curvature parameter

C_1 = Tension coefficient for determining slip load

C_1, C_2, C_3 = Constants for parabolic representation of Load-Strain behavior of slab

C_{bb} = Bolt bending stiffness coefficient

C_{bbr} = Bolt bearing stiffness coefficient

C_{bs} = Bolt shearing stiffness coefficient

C_{pbr} = Plate bearing stiffness coefficient

COV = Coefficient of variation

δ = Deformation

$\delta_{failure}$ = Deformation at failure

δ_{slab1} = Deformation at first critical point of reinforced concrete slab behavior

δ_{stud1} = Deformation at first critical point of shear stud behavior

$\delta_{0.5Qsol}$ = Stud deformation at a load of 0.5 Q_{sol}

Δ = Deformation; Plate deformation which is defined as the elongation of the hole

$\overline{\Delta}$ = Normalized deformation

Δ_0 = maximum deformation for a weld with $\theta = 0$

Δ_1 = Reference deformation for Richard Equation

Δ_f = Deformation at fracture of fillet weld; Failure deformation (in.)

$\overline{\Delta}_f$ = Normalized failure deformation

Δ_{fu} = Deformation at which frictional resistance is considered zero

Δ_{last} = Deformation at last key point in multi-linear load-deformation behavior

$\Delta\delta$ = Change in deformation

Δ_{max} = Test deformation at maximum test load

ΔR = Change in resistance

Δ_u = Deformation at ultimate load of fillet weld

Δ_s = Deformation when a major slip occurs

d_b = Bolt diameter

d_{bar} = Reinforcing bar diameter

d_h = Hole diameter

d_{m16} = Nominal diameter of a M16 bolt (16mm)

d_{sh} = Diameter of the shear stud shank

d_{stud} = Nominal shear stud diameter

D = Leg size of fillet weld (in.)

D_a = Leg size of fillet weld at seat angle

D_p = Leg size of fillet weld at shear plate

DCDT = Displacement potentiometer

ε = Strain or strain rate

ε_1, ε_2 = Strain values at key points for Load-Strain behavior of slab

ε_{cr} = Concrete tensile cracking strain

ε_{yr} = Strain in reinforcing steel at yield

e = Base of natural logarithm

E = Modulus of elasticity for steel, 29,000 ksi

E_c = Modulus of elasticity of concrete

ϕ_{ult} = Ultimate rotation capacity of connection

f_b = Bearing stress

f_c = Concrete stress

f_{ns} = Net section tensile stress

f'_c = Compressive strength of the concrete

f_{cr} = Tensile cracking stress of concrete

F = Bolt tension force

F_b = Bearing stress

F_{exx} = Nominal weld electrode strength

F_{exxa} = Electrode strength used for the fillet weld at the seat angle

F_{exxp} = Electrode strength used for the fillet weld at the shear plate

F_u = Ultimate tensile stress

F_{ub} = Ultimate stress of the bolt steel

F_{usc} = Shear stud steel tensile strength

F_{vb} = Ultimate shear stress of the bolt steel

F_y = Yield stress

F_{ya} = Seat angle steel yield strength

F_{ua} = Seat angle steel tensile strength

F_{yf} = Beam flange steel yield strength

F_{uf} = Beam flange steel tensile strength

F_{yp} = Shear plate steel yield strength

F_{up} = Shear plate steel tensile strength

F_{yr} = Reinforcing steel yield strength

F_{ur} = Reinforcing steel tensile strength

F_{yw} = Beam web steel yield strength

F_{uw} = Beam web steel tensile strength

G = Shear modulus for steel, 11,200 ksi

h = Elastic center of rotation

h_r = Height of the deck rib

H = Web bolt load resistance in horizontal direction

H_s = Shear stud height after welding

I_b = Moment of inertia of the bolt

IC = Instantaneous center of rotation

ICX = X Distance from vertical baseline to the IC

ICY = Y Distance from horizontal baseline to the IC

k = Shear deformation shape correction factor, 4/3 for a circle, 1.2 for a rectangle

k_b = Stiffness coefficient to account for edge and bolt spacing

k_t = Stiffness coefficient to account for plate thickness

K = Elastic stiffness coefficient for Richard Equation

K_1 = Parameter in Richard Equation

K_1, K_2 = First and second slope associated with key points for Load-Strain behavior of slab

K_b = Bolt stiffness

K_{br} = Bearing stiffness

K_f = Frictional stiffness

K_{fi} = Frictional initial stiffness

K_{fp} = Frictional final stiffness

K_i = Initial stiffness

K_{ia} = Initial stiffness of seat angle

K_{islab} = Initial stiffness of reinforced composite slab in tension

K_{iw} = Initial stiffness of web bolt

K_p = Plastic stiffness parameter for Richard Equation; also plate stiffness

K_{pb} = Plate bending stiffness; also the plastic stiffness of web bolts

K_{pbr} = Plate bearing stiffness

K_{pi} = Plate initial stiffness

K_{pr} = Plastic stiffness of reinforced slab

K_{ps} = Plastic stiffness of shear studs

K_{pslab} = Plastic stiffness of reinforced composite slab in tension

K_{pv} = Plate shearing stiffness

K_v = Shearing stiffness

λ = Regression coefficient for Fisher Equation

L = Distance from the center of the plate to the face of the test rig

L_0 = Initial length of tensile test specimen

L_1, L_2, L_3 = Lengths of reinforcing bar in regions 1, 2, and 3

L_{ah} = Horizontal length of the outstanding angle leg

L_{av} = Vertical distance between the top of the angle and the assumed point of contact between the angle and the girder web

L_c = Clear end distance

L_e = End distance

L_{e1} = End distance for plate 1

L_{e2} = End distance for plate 2

L_{eff} = Effective length of reinforced concrete slab for deformation calculations

L_{eh} = Horizontal distance from the bolt centerline to the end of the beam

L_f = Final length of tensile test specimen

L_{w0} = Length of fillet weld that runs parallel to the load

L_{w90} = Length of fillet weld that runs transverse to the load

μ = Coefficient of friction

μ = Regression coefficient for Fisher Equation; also coefficient of friction

M_0 = Moment capacity for Richard Equation

M_{ult} = Ultimate moment capacity of connection

n = Curvature parameter for Richard Equation

N_a = Number of bolts attaching the seat angle to the beam flange

N_{bars} = Number of reinforcing bars

N_r = Number of shear studs per deck rib

N_{studs} = Number of effective shear studs

N_w = Number of bolts in the web

P = Tensile test load

P_0 = Strength of weld loaded at $\theta = 0$

P_1, P_2, P_3 = Loads in regions 1, 2, and 3 of a reinforcing bar

P_a = Horizontal bolt pitch of seat angle bolts

POT = Displacement potentiometer

P_θ = Strength of weld loaded at angle θ

PR = Partially Restrained

P_{slab1} = Load resistance at first critical point of reinforced concrete slab behavior

P_{stud1} = Load resistance at first critical point of shear stud behavior

P_w = Vertical bolt pitch

θ = Angle of load with respect to the longitudinal axis of a fillet weld

Q = Shear stud load

Q_{base} = Basic shear stud strength for a weak position stud

Q_{sol} = The strength for a single shear stud

R = Resistance; Load

ρ = Weld deformation ratio

R_0 = Reference load for Richard Equation

R_1 = Reference load for Richard Equation

R_1, R_2, R_3, R_4 = Load values at key points for Load-Strain behavior of slab

R_f = Slip load

R_{last} = Resistance at last key point in multi-linear load-deformation behavior

R_n = Nominal strength

R_{nb} = Bolt strength

R_{nh} = Nominal strength of web bolt in the horizontal direction

R_{np} = Plate strength

R_{np1} = Strength of plate 1

R_{np2} = Strength of plate 2

R_{nslab} = Composite slab strength

R_{nv} = Nominal strength of web bolt in the vertical direction

R_o = Reference load for Richard Equation

R_{oa} = Intercept of K_2 with ordinate axis

$R_{transition}$ = Transition load

R_{ult} = Maximum test load

S = Bolt spacing

S_0 = Distance from the girder centerline to the nearest shear stud on the beam

S_{bar} = Reinforcing bar spacing

SR = Strength ratio of plate strength over bolt strength

SRF = Stud reduction factor used to account for metal decking

S_{stud} = Shear stud spacing parallel to the beam

ST = Displacement potentiometer

τ = Regression coefficient for Fisher Equation

t = Thickness of main plates

t' = Thickness of lap plates

t_1 = Thickness of the thinner of two plates in a lap plate connection

t_2 = Thickness of the thicker of two plates in a lap plate connection

t_a = Seat angle thickness

t_f = Bottom beam flange thickness

t_p = Plate thickness

t_p = Shear plate thickness

t_w = Beam web thickness

V = Web bolt load resistance in vertical direction

V_{ult} = Ultimate shear capacity of connection

W_a = Seat angle width

w_c = Unit weight of concrete

W_p = Shear plate width

w_r = Width of the deck rib

Ψ_1, Ψ_2, Ψ_3, Ψ_4 = Parametric ratios used for determining the curvature parameter

Y_b = Distance from the top of the seat angle to the center of the bottom bolt

Y_{con} = Total depth of composite slab

Y_j = Vertical distance from web bolt j to top of seat angle

Y_r = Vertical distance from top of seat angle to centerline of reinforcing steel

1. Introduction

Three changes in steel design over the last 30-40 years have allowed engineers to design longer beam spans in steel framed floors. First, composite steel-concrete floor system technology has developed which allows designers to use the synergy of tying the two floor components (the beam and the concrete slab) together to span longer distances. Second, the plastic section analysis and design procedures found in the AISC Load and Resistance Factor Design Specification (*Load and* 1986) has allowed an additional increase in span length for the same section over AISC Allowable Stress Design (*Specification for* 1989) procedures. Third, high strength steel, particularly A572Gr50 steel, is becoming more readily available and at a cost comparable with A36 steel.

As the beam designs become longer and shallower serviceability design criteria such as floor deflection and vibration are, in many cases, controlling the beam design (Zandonini, 1989). Currently most beams in steel framed floor systems are designed with the assumption that the beam end connections can be treated as simple supports. In reality, no connection behaves as a simple support. Each type of connection possesses some degree of rotational restraint. If this restraint is included in the beam design then both beam design moments and deflections are reduced and an overall improvement in the structural efficiency is achieved.

Before the true rotational restraint of beam connections can be included in the design there has to be a way of calculating (i.e. modeling) the connection moment-rotation behavior. This behavior determines the degree of continuity that can be achieved in the floor system. Connections with relatively small moment resistance result in a discontinuous floor system while connections with relatively high moment resistance result in a floor system that is nearly continuous. In terms of reducing design moments and deflections, a continuous floor system is the best situation. However, the connection details required to ensure full moment restraint are complex and expensive compared to simple connections. Using connections with moment resistance that lies somewhere

between these two extremes results in a floor that is between a discontinuous and continuous system. The connection details required to achieve partial continuity can be very simple and economical while still providing a significant amount of rotational restraint. This type of connection was previously termed a "semi-rigid" connection. More recently, these connections are called "partially-restrained" (PR) connections.

Research into PR beam-girder connections began at Virginia Tech (VT) in the spring of 1993. This research was conducted as part of a larger research program that has the main objective of developing innovative floor designs. The objective of the research on PR beam-girder connections was to develop a connection model for a particular type of bare steel and composite beam-girder connection. The details for the proposed PR beam-girder connection are discussed in the following section.

A bare steel PR connection is a connection that provides rotational restraint through the steel details of the connection such as bolts, welds, plates, and angles. A composite PR connection is a connection that combines the strength of the steel connection details with the strength of the composite floor slab to develop rotational restraint. It is important that any connection model be able to approximate the moment-rotation behavior of both bare steel and composite PR beam-girder connections. This is primarily because the majority of composite beams are built using un-shored construction techniques. Consequently, connections associated with these beams will be subject to two distinct stages of loading. First, before the concrete hardens, the bare steel connection provides the only rotational resistance to the beam end. This is a very important loading stage for composite beams and being able to model the bare steel connection in this stage of loading provides a significant potential for economy. Second, after the concrete hardens, the composite slab helps provide the rotational restraint for all subsequently applied loads.

1.1 Proposed PR Beam-Girder Connection

Before the moment-rotation behavior of a beam-girder connection can be investigated the primary details of the connection have to be known. In choosing the details of the beam-girder connection, used in this study, the following were considered:

- The bare steel connection is to provide enough rotational restraint to significantly improve the design of the steel beam during the construction loading stages.
- The subsequent composite connection must have sufficient ductility to allow proper moment redistribution required for the development of a plastic collapse mechanism.
- The cost of labor is proportionally much higher than the cost of materials. Consequently, the connection details must be simple so that fabrication and erection efforts are not significantly increased compared to current practice.
- If the connection is to be readily accepted into practice the connection details should be similar to current details.
- Erection tolerances must be accommodated.

Currently, the three most commonly used beam-girder connections are double angle, single plate (shear tab), and single angle connections. Of these three connections the single plate connection was considered to be the best. First, double angle connections were not considered because of safety considerations. Next, when comparing a single angle connection to a single plate connection it is clear that the single angle connection would be inherently more flexible than the single plate connection because of angle flexure.

Prior to the current study, four PR connections were evaluated by conducting full scale tests (Rex, 1994). The four connections are shown in Figure 1. The first connection is a typical single plate connection. The next three connections represent modifications to the first in an attempt to improve the rotational resistance of both the bare steel and the composite connections. The testing procedure used for each of these connections provided information about both the bare steel and composite connections.

Based on the results of the preliminary investigation and discussions with an advisory group made up of a design engineer, steel fabricator, and steel erector the details of the proposed connection were chosen as shown in Figure 2. The reader will note that these details are similar to the details of Connection #2 from the preliminary investigation. The details can be broken into two major groups: details associated with the steel connection and details associated with the composite slab.

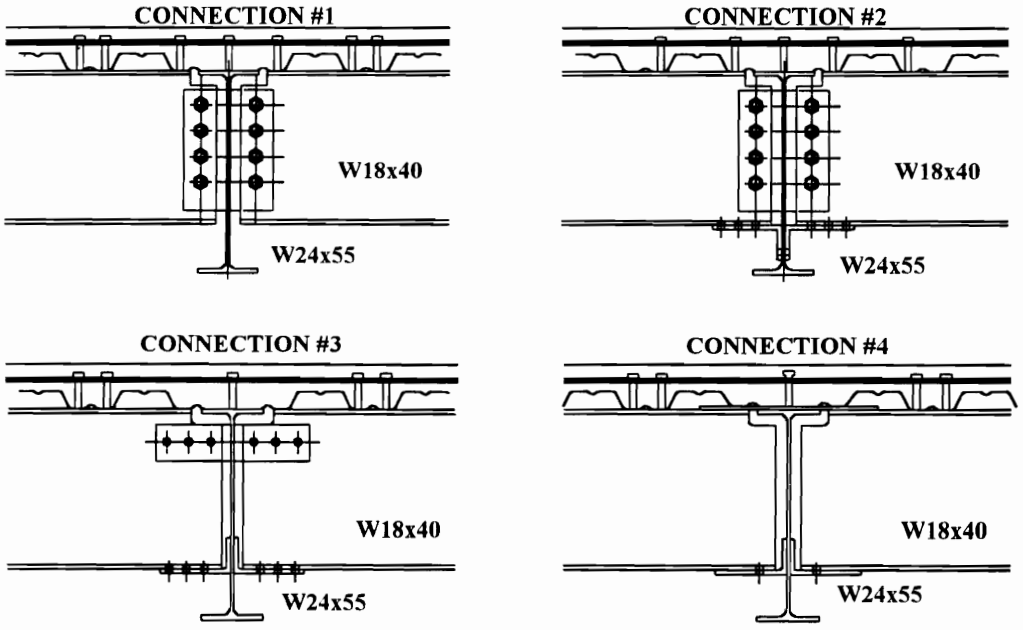

Figure 1 Preliminary Beam-Girder Connections

The steel connection consists of a typical single plate shear connection and an un-stiffened seat angle connection. There were basically two reasons for choosing the steel connection details of Connection #2. First, based on the results of first four PR connection tests, it was determined that the bottom flange of the beam had to be restrained to provide increased stability of the flange and to provide a bare steel connection with sufficient rotational restraint to improve beam design during the construction loading stage. This consideration eliminated Connection #1. Second, the only connection element that carries the vertical shear in both Connections #3 and #4 is the seat angle. The current

method for designing un-stiffened seat angles for shear (*Manual of,* 1993) did not seem applicable to these connection configurations because of differences in how load is introduced into the seat angle; and, development of a new method was beyond the scope of the current research. This consideration eliminated Connections #3 and #4.

The composite slab consists of #4 Grade 60 reinforcing steel, round headed shear studs, composite steel decking, and concrete. The reinforcing steel is specifically given as #4 Grade 60 for two primary reasons:

- All experimental tests of composite connections, composite slabs, and reinforcing steel conducted at VT (in conjunction with this research) have used #4 Grade 60 bars
- The #4 bar is believed to be an effective size for reinforcing thin composite slabs

Round headed shear studs were chosen because they are the most common type of shear connector used today. Composite steel decking was included because most steel framed floor systems use a composite steel deck. The direction of the decking was chosen to be consistent with the typical direction of the steel deck with respect to filler beams.

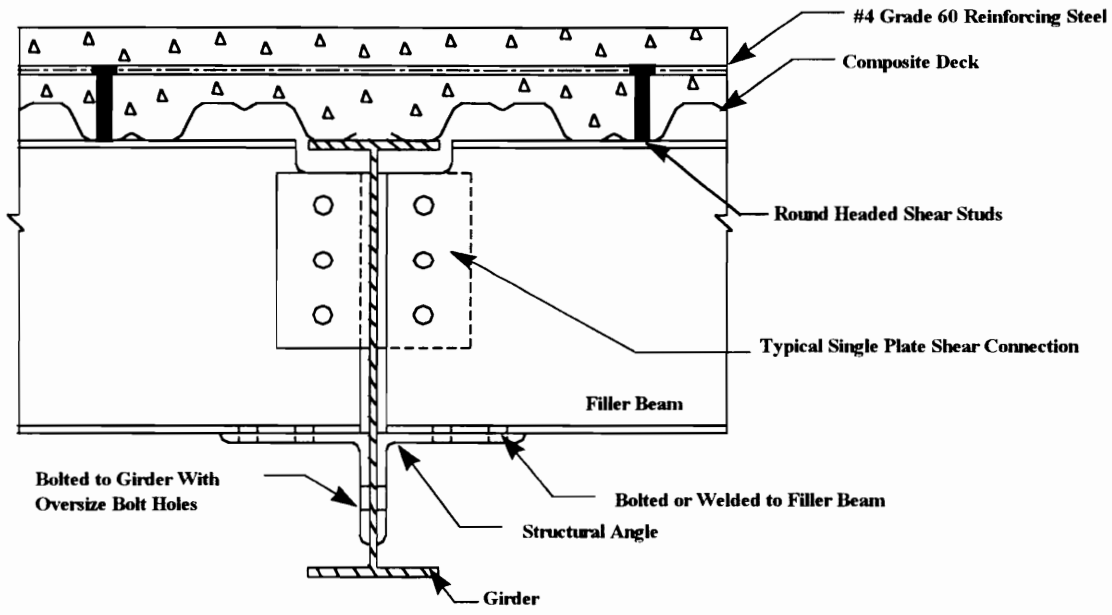

Figure 2 Details of Proposed Beam-Girder Connection

1.2 Objectives and Methods

The primary objective of the research presented in this dissertation was to develop a component model of the proposed PR beam-girder connection that can be used to approximate its moment-rotation behavior. The component model is based on the hypothesis that the connection behavior can be modeled as a combination of the connection component behaviors. The connection components are the fundamental pieces of the connection such as bolts, shear studs, and welds. The primary components are illustrated in Figure 3. In general, a component model can be very computationally intensive. Consequently, a secondary objective of this research was to develop a connection model that is simpler to use. These objectives are achieved through three major steps.

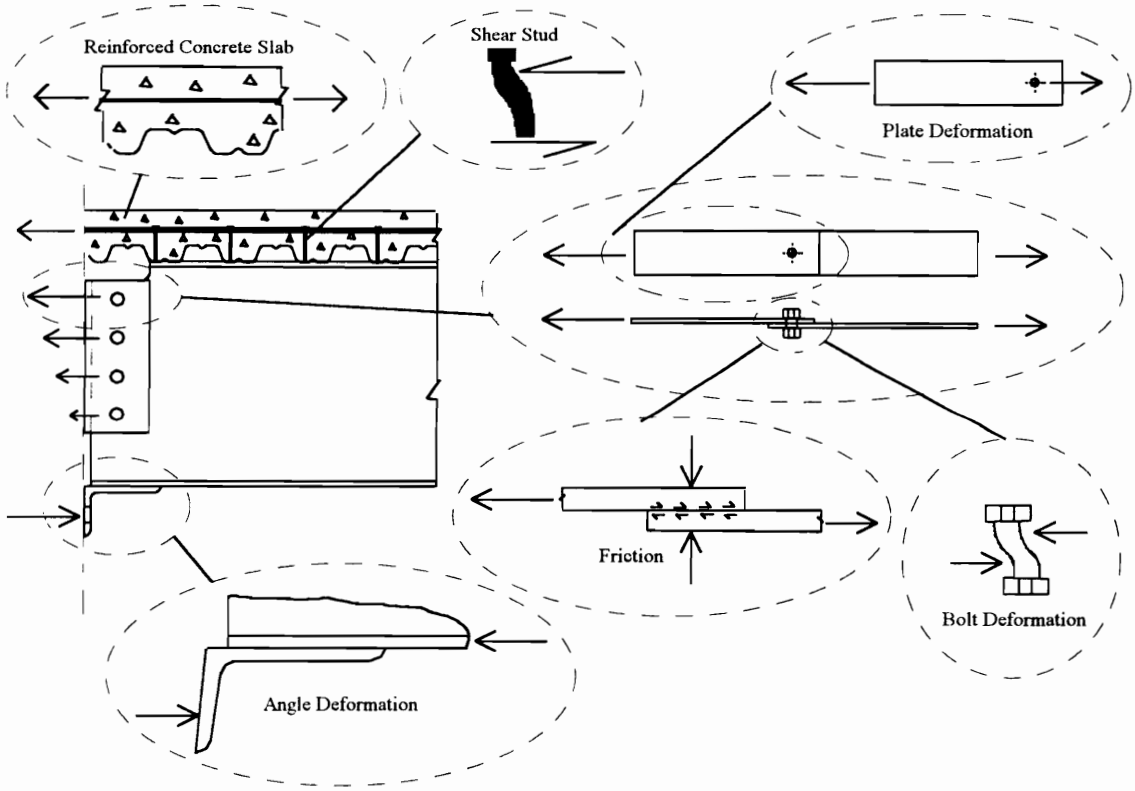

Figure 3 Component Model of Proposed Beam-Girder Connection

First, behavior models for each of the connection components were determined. The behavior models were derived from a combination of existing literature, experimental and analytical research, and basic mechanics. Existing literature that considered the behavior of any of the connection components is reviewed. For some components, there is sufficient information available in the literature to provide a behavior model. For these components, additional experimental research, analytical research, and data analysis was conducted to develop a component behavior model.

Second, a method of combining the component behaviors into a connection model that can be used to approximate the moment-rotation behavior was developed. This method is based on the ultimate strength analysis for eccentrically loaded bolt groups given in the AISC Manual Vol. II (*Manual of*, 1993). The results of this model are then verified against experimental moment-rotation data for steel and composite PR beam-girder connections.

Third, the component model provides a very general approach to connection analysis which is not (ideally) limited by the range of parameters that have been included in experimental test programs. However, this flexibility comes at the price of complexity. In general, a component model is fairly complex to apply and requires a computer program to readily implement. Consequently, as a final step, a simpler model for approximating the steel and composite connection moment-rotation behavior is developed. This model is based on the same hypothesis as the component model; however, through a combination of assumptions, simplifications, and the results of parametric studies the simplified model becomes far less computationally intensive than the full component model.

1.3 Literature Review

Two types of literature were considered applicable to the current research. First, general literature dealing with the topic of steel and/or composite PR connections was reviewed. At the time of the review, no literature dealing with PR beam-girder connections was found. However, literature dealing with PR beam-column connections

was found. Although the details of this literature are not specifically applicable to the current research, they do, in general, provide some important knowledge about the behavior of steel and composite PR connections. A review of this literature was previously presented in Rex (1994).

Second, literature dealing with the behavior of the connection components was reviewed. Review of this literature is presented in the applicable sections of this dissertation where the topic of the literature is being discussed. This is done for clarity.

1.4 Forward

The steps outlined in the Objectives and Methods constituted a large volume of work. This work has been reported in detail in six separate reports (Rex and Easterling, 1996(a,b,c,d,e,f)). This dissertation is a summary of the work presented in the six reports. Each of the following chapters is a summary of a report. These chapters are titled as follows:

- Behavior and Modeling of Mild and Reinforcing Steel,
- Behavior and Modeling of a Reinforced Composite Slab as Part of a PR Composite Beam-Girder Connection,
- Behavior and Modeling of a Single Plate Bearing on a Single Bolt,
- Behavior and Modeling of a Single Bolt Lap Plate Connection,
- Behavior and Modeling of PR Steel Beam-Girder Connections, and
- Behavior and Modeling of PR Composite Beam-Girder Connections.

Behavior models for some of the connection components are presented and/or developed in the first four chapters. Additional required component behavior models and a method of combining the components into a connection model are developed in the last two chapters. The connection model is also verified against experimental results and a simplified model of the steel and composite connection is developed in the last two chapters.

In each chapter a short introduction to the particular topic is given which is intended to show the reader the relationship between the topic and the overall objectives of this dissertation. The introduction is followed by a statement of the objectives and methods used to achieve the objectives for each topic. This is followed by a summary of the work conducted on the particular topic. Finally, each chapter is concluded with a summary, conclusions, and recommendations section. Because each chapter is concluded with this section there is not a summary, conclusions, and recommendations section for the dissertation as a whole.

2. Behavior and Modeling of Mild and Reinforcing Steel

This chapter summarizes the report by Rex and Easterling (1996(a)) on the behavior of mild and reinforcing steel.

2.1 Introduction

2.1.1 General

The two most fundamental components of a PR composite beam-girder connection are mild steel and reinforcing steel. The plates, angles, beams, and girders are fabricated from mild steel and the composite slab contains reinforcing steel. Before any type of connection analysis can be conducted the stress-strain behavior of the steel must be understood and quantified.

Because PR connections can undergo large inelastic deformations, a simple approximation using elastic-plastic stress-strain behavior may lead to incorrect connection analysis results. Consequently, an approximate stress-strain behavior which includes all major parts of the actual stress-strain curve is needed. Currently, there is little guidance available for quantifying the full stress-strain behavior of either mild or reinforcing steels. In addition, new methods used for manufacturing mild and reinforcing steel have resulted in changing yield and tensile strengths of these steels. The full extent of these changes is currently unclear.

The purpose of this part of the study was to develop methods for approximating the full stress-strain behavior and to determine current values of the mean yield and tensile strengths for mild and reinforcing steel. The most commonly used mild structural steels are ASTM A36 and ASTM A572Gr50 steel. In addition, all research by the writer on composite beam-girder connections only utilizes #4 Grade 60 reinforcing bars. Consequently, this report only deals with these particular steels.

2.1.2 Objectives And Methods

There were three primary objectives for this study

- Provide a quantified approximation of the stress-strain behavior of A36 and A572Gr50 mild steels in terms of yield and tensile strengths,
- Provide a quantified approximation of the stress-strain behavior for #4 Grade 60 reinforcing bars in terms of yield and tensile strengths, and
- Determine appropriate values of the yield and tensile strengths of A36, A572Gr50, and #4 Grade 60 reinforcing steel based on currently supplied steel.

The methods used to achieve the objectives included:

- Existing information on the stress-strain behavior of mild and reinforcing steels was gathered.
- Existing tensile test data on mild and reinforcing steel including mill data and data from tensile tests conducted at VT was gathered.
- Special tensile tests designed to quantify the full stress-strain behavior of mild and reinforcing steel were conducted.
- The data was compared and contrasted to develop solutions for the objectives.

2.2 Mild Steel Stress-Strain Behavior

Four sources of information were used to develop an approximation to stress-strain behavior of A36 and A572Gr50 steels: existing data on mild steel stress strain behavior, mill survey of plate and angle steel properties, existing data from tensile tests conducted at VT, and the results of special tensile tests designed to obtain information on the full stress-strain behavior.

2.2.1 Existing Data

Two studies on the behavior of mild steel were found in the literature Galambos and Ravindra (1978) and Read and Frank (1993). When the LRFD design method for steel structures was being developed, Galambos and Ravindra (1978) studied the

properties of hot rolled steel. They considered three sources of data: mill test data, data found in papers designed to determine specific steel properties, and papers that reported steel properties but where the focus was on some other feature of structural steel design. The results (of interest for this study) are summarized as follows (note that the coefficient of variation (COV) is calculated by dividing the standard deviation by the mean):

- Mean elastic modulus = 29,000 ksi, COV = 6%,
- Mean yield stress for flanges in rolled shapes = 1.05 Specified Yield Stress, COV = 10%, and
- Mean yield stress for plates and webs of rolled shapes = 1.10 Specified Yield Stress, COV = 11%.

The use of recycled steel in recent years has changed the characteristics of structural steel. A mill survey was conducted (Read and Frank, 1993) to evaluate the properties of steel currently being supplied. Mill test data for rolled W sections from six steel companies was analyzed for a 12 month period. The results of a statistical analysis of the data for A36 and A572Gr50 steel, which included some 57,930 mill tests, are summarized in Table 1.

Table 1 Results of 1990 Mill Survey (Read and Frank, 1993)

	Steel Grade	A36	A572
	Number of Data	36,570	13,536
Yield Stress			
	Mean (ksi)	49.2	57.6
	COV	10%	9%
Ultimate Stress			
	Mean (ksi)	68.5	75.6
	COV	7%	8%
Ultimate/Yield			
	Mean	1.39	1.31
	COV	8%	6%

2.2.2 Mill Survey of Angles and Plates

Mill tests reporting yield stress, ultimate stress, percent elongation, and chemical analysis for hot rolled angles and plates were supplied by a steel mill for this research. These tests covered approximately a six month time period from June 25, 1995 to December 20, 1995. The mill that supplied the mill test data uses electric arc furnaces and scrap steel to produce the angles and plates.

Data from the mill test reports was entered into a commercial database program and analyzed with a commercial spreadsheet program. The data included 15 angle shapes and 40 plate shapes. The data also included 14 grades of steel. Only A36 and A572Gr50 steels were included in the analysis. A summary of the mean steel properties are presented in Table 2 below.

Table 2 Mean Values From Mill Survey On Plates And Angles

	F_y		F_u		% Elongation		F_u/F_y		No. of
	AVG (ksi)	COV	AVG (ksi)	COV	AVG	COV	AVG	COV	Data Points
A36 Structural Angles	46.1	6.3%	67.3	5.5%	34.9	5.6%	1.46	3.2%	174
A36 Plates	45.7	7.5%	67.2	6.8%	32	10.0%	1.47	5.6%	586
A572Gr50 Structural Angles	57.7	6.8%	79.3	6.2%	30.4	9.5%	1.37	1.8%	18
A572Gr50 Plates	54.7	4.8%	77.1	5.0%	29.6	9.5%	1.41	4.6%	32
A36 Angles & Plates	45.8	7.3%	67.2	6.5%	32.7	9.8%	1.47	5.2%	760
A572Gr50 Angles & Plates	55.8	6.2%	77.9	5.6%	29.9	9.5%	1.4	4.0%	50

As seen in Table 2, the properties for A36 angles differed very little from those for A36 plates. Consequently, it does not seem necessary to distinguish between angles and plates when considering A36 steel properties. The properties for A572Gr50 angles did differ somewhat from those for A572Gr50 plates. There were only 50 mill test reports available for A572Gr50 angles and plates. The small number of tests is the likely reason for the difference seen in the properties between A572Gr50 angles and plates. Consequently, distinguishing between angles and plates when considering A572Gr50 steel is also not considered necessary.

2.2.3 Tensile Tests Conducted at Virginia Tech

There were two sources of tensile test data from VT. First, all readily available data from tensile tests performed by the writer and other researchers at VT was collected and compiled. The amount of stress-strain data available varied depending on the particular tensile test. Tensile tests for plates and angles made of A36 steel and wide flange shapes made from A572Gr50 steel were found. Second, special tensile tests were performed to better define the full stress-strain behavior.

Typical tensile tests measure strain data up to when yielding begins and occasionally up to when strain hardening begins. To determine additional strain values needed to define an adequate approximation of the stress-strain curve, special tensile tests that report the full stress-strain behavior were performed on 42 mild steel coupons. These tests were conducted according to ASTM A370 (1988). The 42 mild steel coupons came from rolled steel plate that had a nominal grade A36. This plate was purchased at varying times from a local supplier. Because of this and the fact that the plate thickness varied it is assumed that these coupons came from different steel heats. The resulting data from both the existing and special tensile tests is summarized in Table 3. Note that the yield stress was determined using the 0.2% offset method (Beer and Johnston, 1981) and the percent elongation was determined in accordance with ASTM A370 (1988).

Table 3 Stress-Strain Data From Tests Conducted At VT On Mild Steel

	Elastic Modulus (ksi)	Yield Stress 0.2% Offset (ksi)	Strain @ Start of Strain Hardening	Stress @ 5% Strain % of F_u	Stress @ 10% Strain % of F_u	Ultimate Stress (ksi)	Strain @ Ultimate Stress	Rupture Stress % of F_u	% Elongation (8" Gage)	F_u/F_y
A36 & A572Gr50										
No. Data	58	100	64	64	53	101	42	62	101	100
Mean	30050	45.9	0.0219	84.6%	95.7%	67.2	0.1894	83.3%	29.6%	1.47
COV	17.5%	6.7%	25.3%	2.5%	1.4%	5.8%	9.8%	6.6%	6.6%	4.9%
A36 Angles & Plates										
No. Data	48	90	54	54	53	90	42	52	90	90
Mean	30528	45.9	0.0210	84.9%	95.7%	67.8	0.1894	83.0%	29.8%	1.48
COV	17.3%	6.9%	18.5%	2.3%	1.4%	5.5%	9.8%	6.9%	3.9%	4.3%
A572Gr50 WF Sections										
No. Data	10	10	10	10		11		10	11	10
Mean	27757	46.0	0.0264	83.1%		62.7		85.2%	28.5%	1.36
COV	16.8%	5.3%	37.4%	3.0%		2.4%		4.7%	17.5%	4.0%

2.2.4 Development of Multi-Linear Stress-Strain Approximation

A multi-linear approximation of the stress-strain behavior of A36 and A572Gr50 steels is developed in the two following sections. In the first section, mean values of the yield and ultimate stress are recommended. In the second section, values which quantify the other key points needed to describe the full stress-strain behavior are recommended.

2.2.4.1 Mean Values of Yield And Ultimate Stress

Yield and ultimate stress values are probably the most important values for defining the stress-strain behavior. All the data collected on the mean values of the yield and ultimate stress for A36 and A572Gr50 steels is summarized in Table 4.

Table 4 Mean Values of Yield and Ultimate Stress Data For Mild Steel

	F_y (ksi)	F_u (ksi)	F_u/F_y	No. Data
A36 Mild Steel				
Tensile Tests on Wide Flange Shapes				
Mill Survey (Read and Frank 1993)	49.2	68.5	1.39	36570
Tensile Tests on Plates & Angles				
Mill Survey	45.8	67.2	1.47	760
Tensile Tests Conducted @ VT	45.9	67.8	1.48	90
A572 Gr. 50 Mild Steel				
Tensile Tests on Wide Flange Shapes				
Mill Survey (Read and Frank 1993)	57.6	75.6	1.31	13536
Tensile Tests Conducted @ VT	46.0	62.7	1.36	10
Tensile Tests on Plates & Angles				
Mill Survey	55.8	77.9	1.40	50

When considering A36 mild steel there is a difference in mean yield stress values between wide flange shapes and plates and angles. It is unclear why this difference exits. Despite the difference in the yield stress values, there is very little difference in the ultimate stress values. Because of the significant difference between the yield for wide flange shapes and for plates and angles, a distinction must be made between the two groups of shapes.

When considering A572Gr50 mild steel, there is a large difference for both yield and ultimate stress values for wide flange shapes between the mill survey by Read and Frank (1993) and the data found from tensile tests at VT. This difference is attributed to the particularly small number of data from tensile tests conducted at VT, and it is assumed that a larger base of data would tend to give values more in line with those determined by Read and Frank (1993). However, for the tensile tests conducted at VT it should be noted that the mean value of 46 ksi for the yield and 62.7 ksi for the ultimate are below the minimum required values for this grade of steel. The reason for this is unknown. When comparing wide flange shape properties to angle and plate properties, there is a very small difference between the yield and ultimate stress values; consequently, it is suggested that no distinction be made between the different shapes.

2.2.4.2 Other Key Stress-Strain Values

In addition to the yield and ultimate stress values other key values, are required to properly represent the stress-strain behavior. These values include:

- The modulus of elasticity,
- Strain at start of strain hardening,
- Two stress-strain points between start of strain hardening and the ultimate stress,
- The strain at ultimate stress (percent elongation), and
- The stress and strain at rupture.

A summary of these key values is presented in Table 5. The data presented are the mean values without regard to steel grade or shape. A separate analysis of the data determined that such distinctions were not necessary. The 5% and 10% strain levels were chosen based on a visual inspection of the typical stress-strain behavior. The stresses at these strain levels and at rupture have been normalized by the ultimate stress of the steel.

Table 5 Mean Values For Key Stress-Strain Strain Points For Mild Steel

	Galambos & Ravindra (1978)	Plate & Angle Mill Survey	Tensile Tests Conducted @ VT
Modulus of elasticity (ksi)	29000	-	30000
Strain @ start of strain hardening (in./in.)	-	-	0.0219
Stress @ 5% strain (normalized by F_u)	-	-	0.846
Stress @ 10% strain (normalized by F_u)	-	-	0.957
Strain @ ultimate stress (in./in.)	-	-	0.1894
Stress @ rupture (normalized by F_u)	-	-	0.833
Strain @ rupture (in./in.)	-	0.325	0.296

The only values that can be compared between sources are the modulus of elasticity and the strain at rupture. The commonly accepted value of the elastic modulus for mild steel is 29,000 ksi. The difference between this and what was determined from tensile tests at VT can be attributed to the small number of tests and the lack of accuracy with which the extensometer used can measure small strains. Consequently, the commonly accepted value of 29,000 is recommended. The difference in rupture strains is small and can easily be attributed to the wide variability seen in percent elongation measurements. A value of 30% is easily justifiable.

2.3 Reinforcing Steel

The suggested stress-strain behavior of #4 Grade 60 reinforcing bars was based on three sources of information; existing data on Grade 60 reinforcing steel stress-strain behavior, existing data from tensile tests conducted at VT, and the results of special tensile tests designed to obtain information on the full stress-strain behavior.

2.3.1 Existing Knowledge

There were two sources of information on the stress-strain behavior of #4 Grade 60 reinforcing steel found in the literature. A mill survey by Mirza and MacGregor (1979) determined the following results for Grade 60 reinforcing steel.

- Yield Stress: Mean = 71 ksi, COV = 9.3%

- Ultimate Stress: Mean = 110.8 ksi, COV = 8.73%
- Elastic Modulus: Mean = 29,200 ksi, COV = 3.3%

Four of the key points of an ideal stress-strain curve for grade 60 reinforcing bars, as given by Wang and Salmon (1985), are shown in Table 6.

Table 6 Ideal Stress Strain Points For Grade 60 Reinforcing Steel

Point	Stress (ksi)	Strain (in/in)
Yield	60	0.002
Begin Strain Hardening	60	0.01
Ultimate	110	0.08
Rupture	95	0.125

2.3.2 Tensile Tests Conducted at Virginia Tech

There were two sources of tensile test data from VT. First, all readily available data from tensile tests performed by the writer and other researchers at VT was collected and compiled. The amount of stress-strain data available varied depending on the particular tensile test. Second, special tensile tests were performed to better define the full stress-strain behavior.

Typical tensile tests only measure enough strain data to determine the steel yield stress and occasionally extend into the start of the strain hardening region. To determine additional strain values needed to define an adequate multi-linear representation of the stress-strain curve, special tensile tests that report the full stress-strain behavior were performed on 20 reinforcing steel coupons. These tests were conducted according to ASTM A370 (1988). The 20 reinforcing steel coupons were taken from #4 Grade 60 bars. These bars were all purchased at the same time from a local supplier. Although not guaranteed, because these bars came from the same supplier at the same time and are all the same size and grade it is very likely they all came from the same heat of steel. The resulting data from both the existing and special tensile tests is summarized in Table 7.

Table 7 Stress-Strain Data From Tests Conducted At VT On Reinforcing Steel

	Elastic Modulus (ksi)	Yield Stress 0.2% Offset (ksi)	Strain @ Start of Strain Hardening	Stress @ 3% Strain % of F_u	Stress @ 7% Strain % of F_u	Ultimate Stress (ksi)	Strain @ Ultimate Stress	Rupture Stress % of F_u	% Elongation (2" Gage)	F_u/F_y
No. Data	24	25	24	24	20	25	20	24	21	25
Mean	32451	70.5	0.0074	83.2%	97.6%	114.6	0.1010	83.7%	16.7%	1.63
COV	17.5%	2.7%	20.4%	1.2%	0.6%	1.9%	6.0%	5.8%	10.8%	2.5%

2.3.3 Development of Multi-Linear Stress-Strain Approximation

A multi-linear approximation of the stress-strain behavior of #4 Grade 60 Reinforcing bars is developed in the two following sections. In the first section, mean values of the yield and ultimate stress are considered. In the second section, values which quantify the other key points needed to describe the full stress-strain behavior are considered.

2.3.3.1 Mean Values of Yield And Ultimate Stress

Yield and ultimate stress values are probably the most important values for defining the stress-strain behavior. Data on the mean values of the yield and ultimate stress for #4 Grade 60 reinforcing steel is summarized in Table 8.

Table 8 Mean Values of Yield and Ultimate Stress for Reinforcing Steel

	F_y (ksi)	F_u (ksi)	F_u/F_y	No. Data
Mill Survey (Mirza & MacGregor	71.0	110.8	1.56	3042
Tensile Tests Conducted @ VT (#4 Bars)	70.5	114.6	1.63	25

Review of Table 8 shows there is very little difference between the yield stress values from the two sources; however, there is a small difference in the ultimate stress values. This is attributed to the fact the tests at VT are believed to come from the same heat and same bar size while the mill survey data comes from a much larger number of

heats and bar sizes. Consequently, the yield and ultimate stress values based on the mill survey by Mirza and MacGregor (1979) are suggested.

2.3.3.2 Other Key Stress-Strain Values

In addition to the yield and ultimate stress values other key values are required to properly represent the stress-strain behavior. These values include:

- The modulus of elasticity,
- Strain at start of strain hardening,
- Two stress-strain points between start of strain hardening and the ultimate stress,
- The strain at ultimate stress (percent elongation), and
- The stress and strain at rupture.

A summary of the mean values of key points is presented in Table 9. The 3% and 7% strain levels were chosen based on a visual inspection of the typical stress-strain behavior. The stresses at these strain levels and at rupture have been normalized by the ultimate stress of the steel for each specimen.

Table 9 Mean Values For Key Stress-Strain Strain Points For Reinforcing Steel

	Mirza & MacGregor (1979)	Wang & Salmon (1985)	Tensile Tests Conducted @ VT
Modulus of elasticity (ksi)	29200	30000	32500
Strain @ start of strain hardening (in./in.)	-	0.01	0.0074
Stress @ 3% strain (normalized by F_u)	-	-	0.832
Stress @ 7% strain (normalized by F_u)	-	-	0.976
Strain @ ultimate stress (in./in.)	-	0.08	0.101
Stress @ rupture (normalized by F_u)	-	-	0.837
Strain @ rupture (in./in.)	-	0.125	0.167

A comparison of the data presented in Table 9 reveals some minor differences between the three sources. For the most part these differences may be explained by the limited variety of reinforcing steel used in the tensile tests conducted at VT. However, the source of the ideal stress-strain behavior given by Wang and Salmon (1985) is not known. Consequently, it is difficult to say which set of values is more accurate. Currently, the

values for strain and stress based on the tensile tests at VT are recommended. For the modulus of elasticity a value of 29,000 ksi seems justifiable and is consistent with common practice.

2.4 Summary and Recommendations

2.4.1 Summary

Currently available information on the stress-strain behavior of mild and reinforcing steels was gathered. A mill survey of plates and angles made of A36 and A572Gr50 steels was conducted. Data from tensile tests conducted at VT on A36, A572Gr50, and #4 Grade 60 steels was collected. Special tensile tests on A36 and #4 Grade 60 steels were conducted. Based on this data, quantified approximations of the full stress-strain behavior for these steels were developed. The multi-linear approximations that use six key points. These approximations are summarized in Figures 4 and 5. In addition, reasonable estimates for the yield and tensile strengths of these steels are suggested based on current mean yield and tensile strength values.

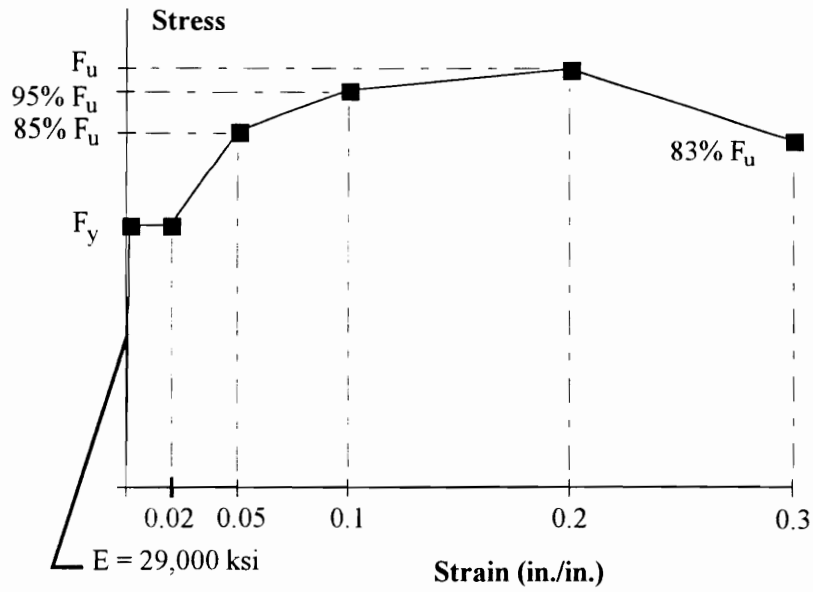

Figure 4 Multi-Linear Approximation For Mild Steel Stress-Strain Behavior

The following guidelines are suggested for determining F_y and F_u if either or both are unknown:

A36 Steel

F_y & F_u Unknown		
Use Nominal Values	$F_y = 36$	$F_u = 58$
Or Use Mean Values		
Wide Flange Shapes	$F_y = 49.2$	$F_u = 68.5$
Plates & Angles	$F_y = 45.8$	$F_u = 67.3$
F_y or F_u Unknown		
Use Mean F_u/F_y Values		
Wide Flange Shapes	$F_y = Fu/1.39$	$F_u = 1.39\ Fy$
Plates & Angles	$F_y = Fu/1.47$	$F_u = 1.47\ Fy$

A572Gr50 Steel

F_y & F_u Unknown		
Use Nominal Values	$F_y = 50$	$F_u = 65$
Or Use Mean Values	$F_y = 57.6$	$F_u = 75.6$
F_y or F_u Unknown		
Use Mean F_u/F_y Values	$F_y = F_u/1.31$	$F_u = 1.31\ F_y$

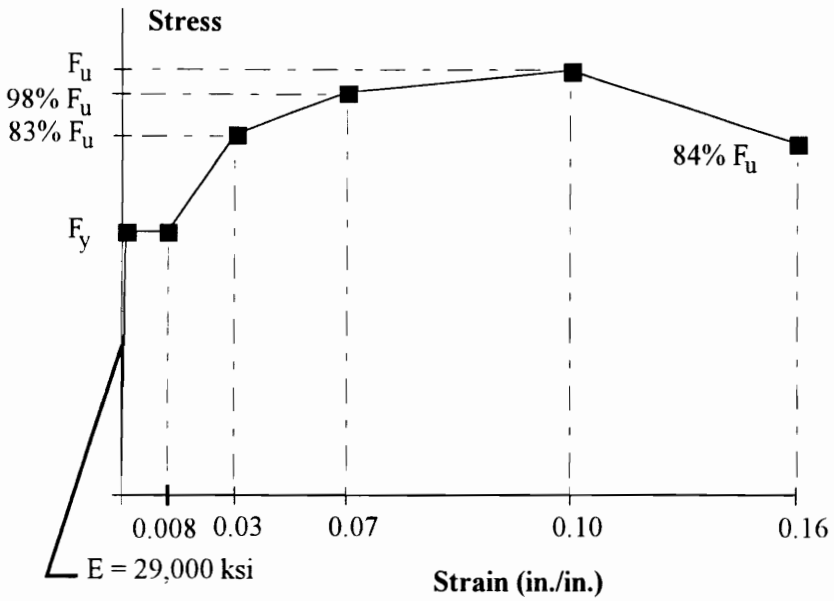

Figure 5 Multi-Linear Approximation For Reinforcing Steel Stress-Strain Behavior

If F_y and or F_u are unknown then the mean values 71 ksi and 111 ksi respectively are recommended for the #4 Grade 60 reinforcing steel.

2.4.2 Recommendations

The accuracy with which an approximation to the stress-strain behavior is needed depends on the intended use of the behavior. In many cases, highly accurate approximations are not necessary because the intended use is fairly insensitive to small variations in the behavior.

If the intended use is very sensitive to small variations in the approximate material behavior then the following recommendations are given:

A much larger base of data needs to be collected.

A statistical study of this data should be conducted to find the following for each key point of the stress-strain behavior:

- The mean value
- The shape of the variation
- Confidence interval values

The results of such a study would allow investigators to properly account for the effects that the variation in the steel behavior has on their particular work.

3. Behavior and Modeling of a Reinforced Composite Slab As Part of a PR Composite Beam-Girder Connection

This chapter summarizes the report by Rex and Easterling (1996(b)) on the behavior and modeling of a reinforced composite slab as part of a PR composite beam-girder connection.

3.1 Introduction

3.1.1 General

The primary hypothesis of this dissertation is that a PR composite beam-girder connection can be modeled as a combination of connection components. The reinforced composite slab is one of these components; consequently, a behavior model of the reinforced composite slab is needed. Specifically, a behavior model of the axial force-deformation behavior of the slab under tension is needed. A study of reinforced composite slab behavior is presented in this chapter along with a development of a behavior model.

The hypothesis of this study is that the force-deformation behavior of the composite slab can be modeled as a combination of three fundamental connection components: concrete, reinforcing steel, and shear studs (i.e. a component model of the slab as shown in Figure 6). This is consistent with the hypothesis of modeling the overall connection. Based on this hypothesis, it is assumed that if the behavior of the fundamental composite slab components can be modeled then the behavior of the overall composite slab can also be modeled.

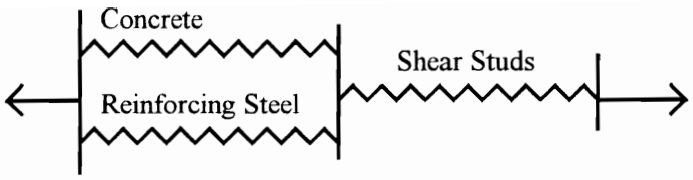

Figure 6 Component Model Of Reinforced Composite Slab

3.1.2 Objectives And Methods

The objective of this study is to prove that the axial force-deformation behavior of a reinforced composite slab under tension can be modeled as a combination of three fundamental composite slab components: concrete, reinforcing steel, and shear studs. There are three major steps needed to achieve this objective:

- Define the behavior of the fundamental components
- Develop a method of combining the fundamental component behaviors to create an approximation to the composite slab force-deformation behavior
- Verify the approximation against experimental results

First, to define the behavior of the fundamental components, available literature and data on the behavior of concrete tension stiffening, reinforcing steel, and shear studs was collected and analyzed. Based on this analysis and comparisons to the experimental results (from the reinforced composite slab tests discussed later), methods for approximating the behavior of these elements were developed.

Second, using the component model of the slab, shown previously in Figure 6, and the fundamental component behaviors, a method of creating a multi-linear approximation of the composite slab force-deformation behavior is developed. Based on the multi-linear approximation, a method of representing the behavior with a continuous non-linear equation is also developed.

Third full-scale reinforced composite slab tests were conducted. These tests were conducted for two reasons:

- To provide additional information needed during the first two steps

- To provide experimental data that can be used to verify that the approximate force-deformation behaviors adequately represent the "true" behavior (assuming the "true" behavior can be equated to experimental behavior)

3.2 Experimental Investigation of the Force-Deformation Behavior of Reinforced Composite Slabs

The experimental investigation will be presented first because the experimental data is referred to in the later parts of this study. The goal of the experimental investigation was to isolate and measure the behavior of reinforced composite slabs in a composite connection. The flexural strength of the slab is assumed to be small compared to the overall moment strength of the connection; consequently, only the axial force-deformation behavior in tension is of interest.

3.2.1 Test Specimens

Six composite slab test specimens were used in this study. Each specimen consisted of a reinforced composite slab which was attached to two beam sections (later referred to as test beams) by means of shear studs. The details of all the test specimens were similar except for the location and number of shear studs.

- Slab #1 5 studs in positions A, B, C, E, G
- Slab #2 5 studs in positions A, B, C, D, E
- Slab #3 4 studs in positions B, C, E, G
- Slab #4 4 studs in positions A, B, C, E
- Slab #5 3 studs in positions C, E, G
- Slab #6 3 studs in positions B, C, E

These stud positions along with the other details of the test specimens are presented in Figure 7.

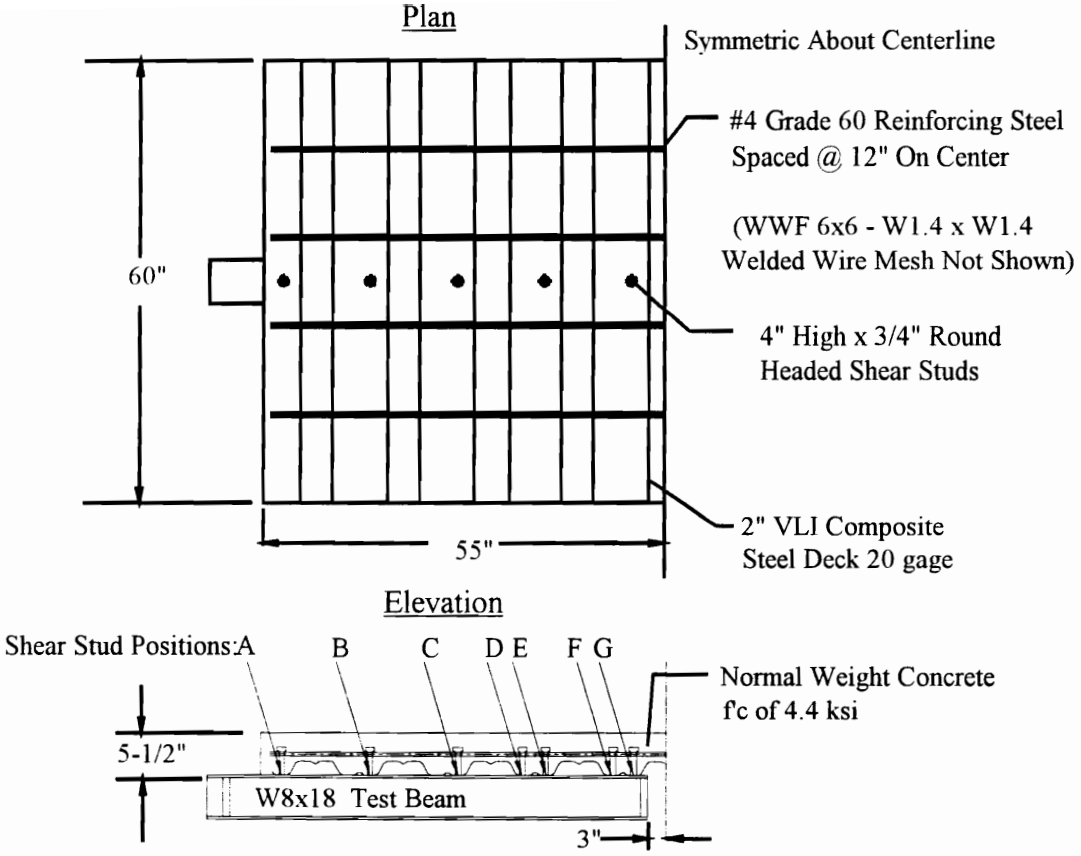

Figure 7 Test Specimens

3.2.2 Instrumentation

There were essentially two sets of instrumentation. To achieve the primary goal of the experimental investigation, one set was used to measure the axial force-deformation behavior of the composite slab. This consisted of measuring the axial elongation of the reinforced slab and slip between the slab and the test beams with displacement gages. In addition, the applied load was measured with a load cell. The second set was used to directly measure the force in the reinforcing steel. This was done by strain gauging the reinforcing steel and then calibrating the strain gage readings to force in the bars.

3.2.3 Test Setup

The details of the test setup used for the last four of the six slab tests are shown in Figure 8. The first of the slab tests had the loading ram pushing directly on the rotation frame beam and there was no tube section across the fixed end of the specimen. The second of the slab tests did not have the tube section across the fixed end of the specimen. These two modifications to the setup were made to avoid premature failure of the test specimens. This is discussed later in more detail.

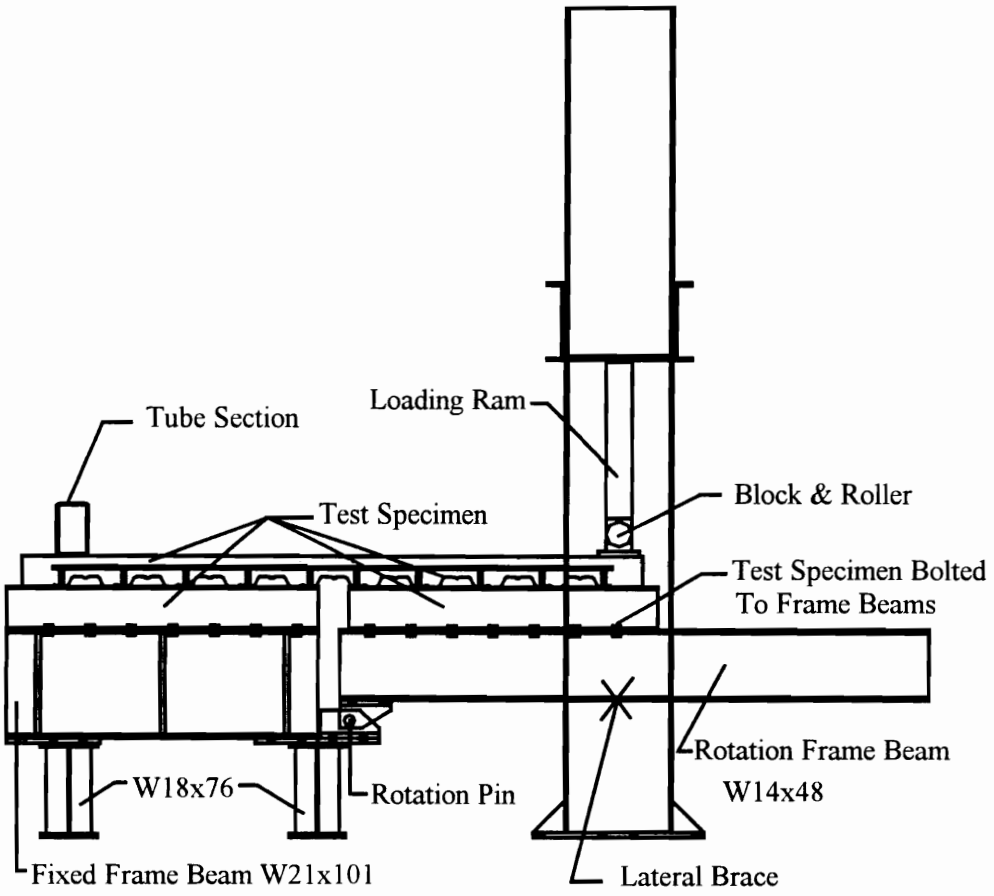

Figure 8 Test Setup

3.2.4 Test Procedure

The rotation frame beam had to be supported at its free end when a test specimen was not attached. This support was left in place until the start of the test. Typically all instrumentation would be zeroed and then the temporary support would be removed. The weight of the rotation beam and half the test specimen was carried by the composite slab at this stage. The specimen would then be pre-loaded and unloaded. Occasionally after unloading some of the instrumentation would be adjusted and re-zeroed. The test loading would then start. The loading was initially controlled by load increments and later by displacement increments. The test was ended when the test was deemed to have undergone excessive deformations or when there was a shear stud failure.

3.2.5 Test Setup Problems

Slab #5 and Slab #6 failed prematurely because of separation between the composite slab and the test beams near the ends of the slab. These two slabs were the first two slabs tested and the test setup did not restrain this separation. To eliminate this problem the load ram and a large tube section were placed onto the top of the specimen. Because vertical separation of the slab from the beam is not consistent with actual service conditions, Slabs #5 and #6 have been removed from further consideration in the test results and analysis.

3.2.6 Slab Tension Force Vs. Slab Deformation

The tension force in the slab was determined by summing moments about the rotation pin shown in Figure 8. The slab deformation is defined as the horizontal deformation at the level of the reinforcing steel. The deformation included axial elongation of the slab as well as slip between the slab and the test beam. The slab tension force vs. deformation results for Slab #1 through #4 are plotted in Figure 9.

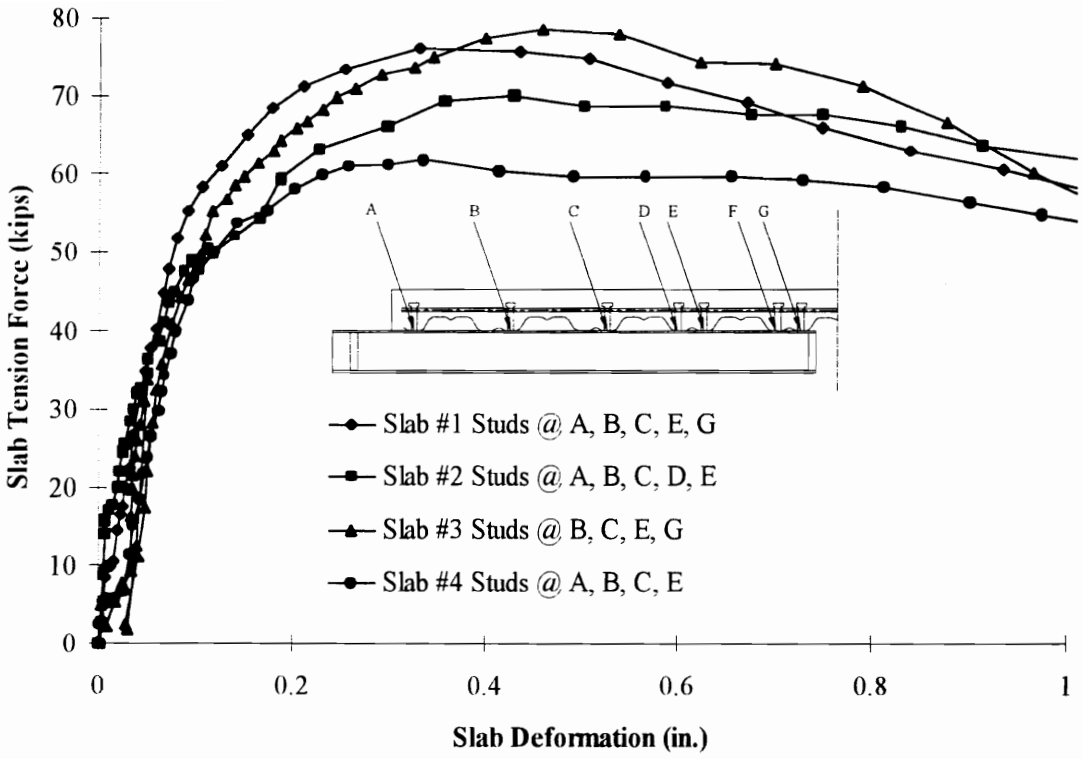

Figure 9 Slab Tension Force Vs. Deformation Behavior

The maximum tension forces for Slabs #1 through #4 were 76.0, 70.0, 78.3, and 61.8 kips respectively. The reinforcing steel yielded in each test specimen; but, the maximum tension force was limited by shear stud failure for all tests.

Two conclusions can be reached by considering these maximum forces and by reviewing Figure 9. First, by comparing Slab #1 to Slab #3 it is clear that the extra shear stud in position "A" in Slab #1 had little to no effect on the overall force-deformation behavior. This can also be concluded by comparing Slab #3 to Slab #4. Second, by comparing Slab #1 to Slab #2 it is clear that a shear stud in position "E" is not as effective as a shear stud in position "G".

3.2.7 Slab Force Vs. Shear Stud Slip

The slab force vs. stud slip measurements for Slab #3 are shown in Figure 10. Although not identical, most force vs. stud slip relationships followed the same basic trends seen in Figure 10. The designations in Figure 10 refer to the stud position and which side of the test specimen the stud was on. For example "G Fix" means the stud was in location "G" on the fixed side of the test specimen.

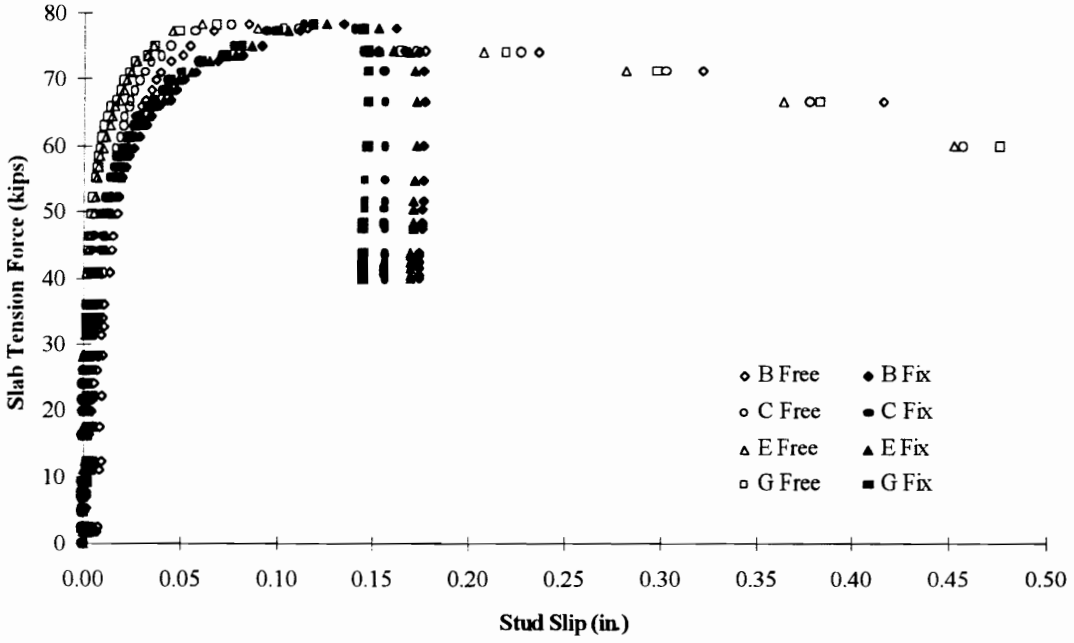

Figure 10 Slab Force Vs. Shear Stud Slip

The typical trend was for the studs on both sides of the specimen to deform fairly evenly. The stud response would start to soften at approximately 75% of the maximum force. The response was still fairly similar on each side of the specimen although in two cases it appeared that the side where the studs failed seemed to have a slightly stiffer response than the opposite side. After the maximum force was reached the studs on one side of the specimen started to loose load carrying capacity and incurred large deformations (i.e. these studs failed). The opposite side maintained a constant level of deformation as the slab force decreased and deformation increased on the failure side.

The slab deformation measurements were the combined deformations of both sides (fixed side and rotation side) of the test specimen. Before the maximum force was reached both sides of the specimen were deforming and the deformation measurements could be attributed to deformations on both sides. However, because of the typical behavior of one side failing and the other side not, deformation measurements taken after the maximum force was reached are mainly attributable to only one side of the specimen deforming. This observation is important for later analysis of the force-deformation behavior.

3.3 Behavior of Composite Slab Components

There are three fundamental components that determine the behavior of the reinforced composite slab: reinforcing steel, concrete, and shear studs. Because the reinforcing steel and concrete act together in resisting tensile forces, a method of predicting the force-deformation behavior of the combination (a reinforced concrete slab) will be developed. This development is followed by a development for modeling the shear stud behavior.

3.3.1 Behavior of a Reinforced Concrete Slab in Tension

The behavior of the reinforced concrete in tension is comprised of the behavior of the reinforcing steel and the tension stiffening effects that the concrete has on the reinforcing steel. The following sections present a method for modeling the stress-strain behavior of the reinforcing and for considering the tension stiffening effects that the concrete has on the reinforcing. This is followed by the development of a method for determining the force-deformation behavior of the reinforced concrete slab.

3.3.1.1 Reinforcing Steel Stress-Strain Behavior

A normalized stress-strain behavior for Grade 60 #4 reinforcing steel was developed and is presented in Chapter 2 of this dissertation.

3.3.1.2 Concrete Tension Stiffening

The concrete in a composite beam-girder connection is typically going to be in tension because of the negative moment resistance provided by the connection. This concrete is normally assumed to have no tensile strength. In reality, the concrete has significant strength before cracking and after cracking it has a stiffening effect on the reinforcing steel.

After cracking, the concrete cannot carry force across the cracks. This force has to be carried by the reinforcing steel. However, between cracks the concrete can carry force. This reduces the force in the reinforcing steel and consequently reduces the axial deformations in the reinforcing steel. This effect on the reinforcing steel is called concrete tension stiffening (Collins and Mitchell, 1991).

One way to account for the stiffening effect the concrete has on the reinforcing steel is to model the concrete as an axially loaded member acting in parallel with the reinforcing steel. The concrete is represented with a special stress-strain behavior and the strain in the concrete is assumed to be the same as the strain in the reinforcing steel (i.e., no slip between the reinforcing steel and the concrete surrounding it). By combining the force resisted by the reinforcing steel with the force resisted by the fictitious concrete element the real effect of concrete tension stiffening can be satisfactorily represented.

One stress-strain model for concrete tension behavior both before and after concrete cracking is given by Collins and Mitchell (1991).

For: $\varepsilon_c \leq \varepsilon_{cr}$

$$f_c = E_c \varepsilon \qquad \text{(Eq 1)}$$

For: $\varepsilon_c > \varepsilon_{cr}$ (Tension stiffening)

$$f_c = \frac{\alpha_1 \alpha_2 f_{cr}}{1 + \sqrt{500\ \varepsilon_c}} \qquad \text{(Eq 2)}$$

Where:

$$f_{cr} = \frac{4\sqrt{1000\ f'_c}}{1000}$$

$$\varepsilon_{cr} = \frac{4\sqrt{1000\ f'_c}}{1000\ E_c} = \text{Strain at which concrete cracks}$$

$E_c = w_c^{1.5}\ \sqrt{f'_c}$ (*Load and*, 1993)

f'_c = Compressive strength of concrete (ksi)

w_c = Unit weight of concrete (pcf)

The factor α_1 accounts for bond characteristics of reinforcement and is equal to 1.0 for deformed reinforcing bars. The factor α_2 accounts for the loading time period. It is equal to 1.0 for short-term monotonic loads and 0.7 for sustained and/or repeated loads.

Equation 2 is a curve that was fit through test data. Equation 2 and the test data are presented in Figure 11, along with a multi-linear representation. The data for Figure 11 is based on Figure 4-16 of Collins and Mitchell (1991).

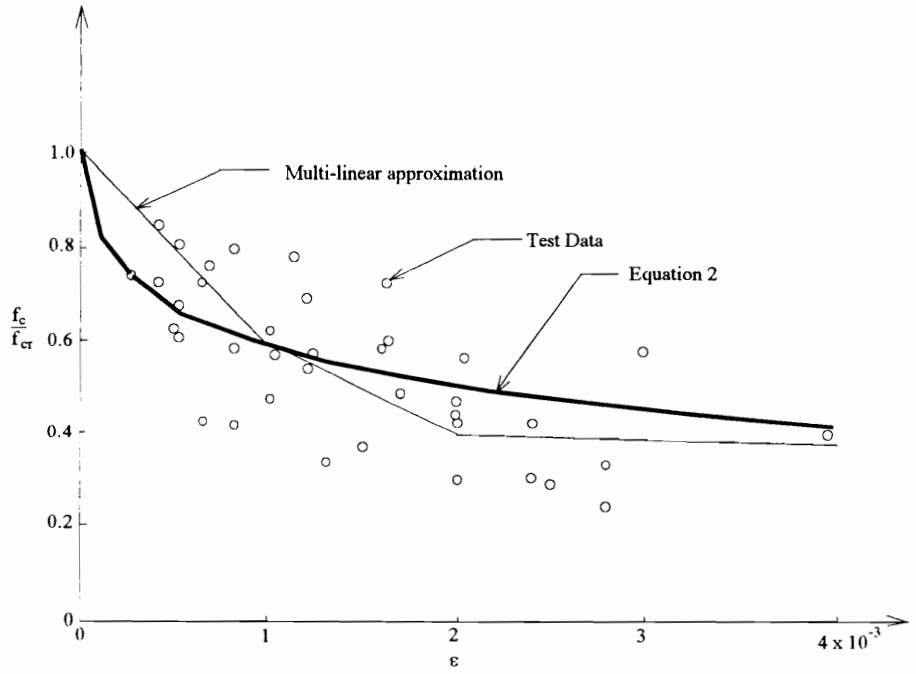

Figure 11 Concrete Tension Stiffening Stress-Strain Behavior

Comparison of Equation 2 with the test data shows good agreement except for the very small strains where Equation 2 tends to be conservative. In addition, at a 10% strain value (average strain associated with the reinforcing steel reaching ultimate stress) the

stress given by Equation 2 is not zero. This could result in estimated concrete slab forces in excess of the ultimate strength of the reinforcing steel which clearly cannot occur. For these reasons the multi-linear representation given in Table 10 will be used.

Table 10 Recommended Concrete Tension Stiffening Stress-Strain Behavior

Strain	Stress
f_{cr} / E_c	f_{cr}
0.001	0.6 f_{cr}
0.002	0.4 f_{cr}
0.008	0.3 f_{cr}
0.1	0

3.3.1.3 Reinforced Concrete Slab Force

The force in the reinforced concrete slab will initially be almost exclusively carried by the concrete as there is typically much more concrete area than reinforcing steel area. After the concrete cracks, the tensile force at the cracks must be carried exclusively by the reinforcing steel; however, the model which accounts for the tension stiffening effect treats the concrete and reinforcing steel as two elements in parallel and does not consider the true discontinuity of the concrete at the cracks. The force in the reinforcing steel can be determined by multiplying the steel stress by the steel area.

The force in the concrete is determined by multiplying the concrete stress by the effective area of concrete (A_{ceff}). Before cracking A_{ceff} is the gross area (i.e. the effective width of the slab by the depth of the slab minus the height of the steel decking). After concrete cracking the area is the effective area around each reinforcing bar, which is suggested by Collins and Mitchell (1991) to be a block of concrete centered about the reinforcing bar with a height and width of 15 times the bar diameter. The writer assumes that if the full effective concrete area is not available (as is the case for thin composite slabs or close reinforcing spacing) that the portion of this area that is available should be used instead. This can be put into equation form as

$$A_{ceff} = \left\{ \min \left| \begin{matrix} 15\, d_{bar} \\ Y_{con} - h_r \end{matrix} \right\} \right\} \left\{ \min \left| \begin{matrix} 15\, d_{bar} \\ S_{bar} \end{matrix} \right\} \right\} \quad \text{(Eq 3)}$$

Where:

d_{bar} = Reinforcing bar diameter

Y_{con} = Total depth of the composite slab from bottom of deck to top of slab

h_r = Depth of the composite steel decking

S_{bar} = Reinforcing bar spacing

Rather than dealing with two distinct effective areas (one before cracking and one after cracking) a conservative assumption of using A_{ceff} as defined in Equation 3 was made.

3.3.1.4 Reinforced Concrete Slab Deformation

A method for determining the deformation associated with the reinforced concrete slab for a given strain level is still needed before a force-deformation behavior can be determined for the reinforced concrete slab. To determine the deformation of the reinforcing steel and concrete there must be some effective length (L_{eff}) by which the calculated strains can be multiplied. The geometry of a typical reinforced composite slab is considered to determine the effective length. The important parts of this geometry are shown in Figure 12.

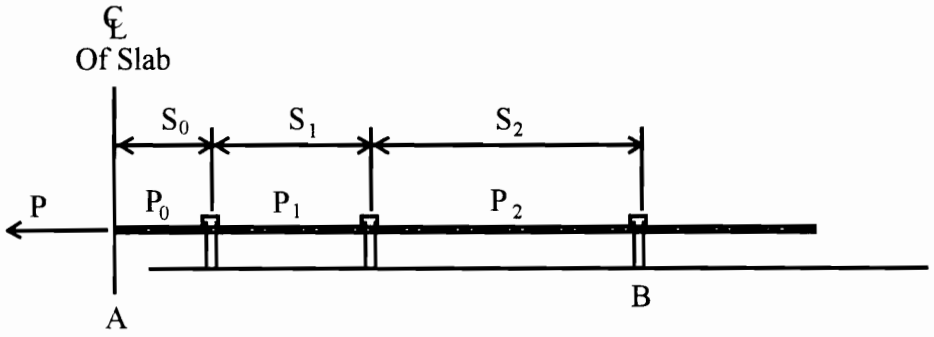

Figure 12 Typical Geometry For Elastic Effective Length of Reinforcing Steel

In Figure 12, S_0, S_1, and S_2 are the distances from the centerline of the composite slab to the first shear stud and then the shear stud spacing, respectively. P_0, P_1, and P_2

represent the forces carried by the reinforcing steel in each section and P is the total force carried by the reinforcing steel at the center line of the slab.

If it is assumed that each stud resists an equal load and that shear lag between the reinforcing bars is not significant then P_0 is P, P_1 is 2/3 P, and P_2 is 1/3 P. The elastic deformations of the reinforcing steel from point A to point B is then given by

$$\delta = \frac{P}{A_r E}\frac{(3S_0 + 2S_1 + S_2)}{3} \quad \text{(Eq 4)}$$

This can be replaced by

$$\delta = \frac{P}{A_r E} L_{eff} \quad \text{(Eq 5)}$$

Where

$$L_{eff} = \frac{(3S_0 + 2S_2 + S_3)}{3} \quad \text{(Eq 6)}$$

In general, for N_{studs}, L_{eff} is given by

$$L_{eff} = [N_{studs}\, S_0 + (N_{studs} - 1)S_1 + \ldots + S_{N_{studs}-1}]/N_{studs} \quad \text{(Eq 7)}$$

The same logic can be used for the concrete.

The above assumes elastic deformations. For concrete, when the force exceeds the cracking force and for reinforcing steel when the force exceeds the yield force, the above effective length is no longer valid. For convenience it is assumed that both the concrete and reinforcing steel elements have the same effective lengths and that the above effective length is valid until the reinforcing steel yields. Consequently, any variation in effective length that occurs when the concrete cracks is ignored.

Once the reinforcing steel has yielded, the above effective length can no longer be used. Because the force in the reinforcing steel and the concrete between the center of the slab and the first shear stud is the highest, the reinforcing steel will yield here first. The deformations that occur after yielding are much larger than the elastic deformations. For this reason the effective length after yielding is assumed to be S_0 until the ultimate stress of the steel is reached. Because necking of the reinforcing is typically very localized, the

effective length after the ultimate stress is taken as one or two inches if deformations beyond the ultimate stress of the reinforcing steel are desired.

3.3.2 Behavior of Shear Studs

The following presents the development and/or verification of procedures to estimate both the strength and load-deformation behavior of round headed shear studs. The development and/or verification is based on an analysis of existing literature and data on shear studs. The data came from 36 pushout tests conducted at VT and reported in Lyons et al (1994) and Sublett et al (1992).

3.3.2.1 Strength of Shear Studs

Today almost all steel-concrete composite floor systems use a profiled steel decking. The shear studs are welded to the tops of the steel beams through the steel decking and are placed in the ribs of the decking pattern. Because of a stiffener that is present in most commonly used deck patterns, the shear stud cannot be placed in the center of the rib. Easterling et al (1993) deemed studs welded on one side of the rib weak position studs and the other side strong position studs. The designation of weak or strong depends on the relative direction of the force in the concrete. These relationships are shown schematically in Figure 13.

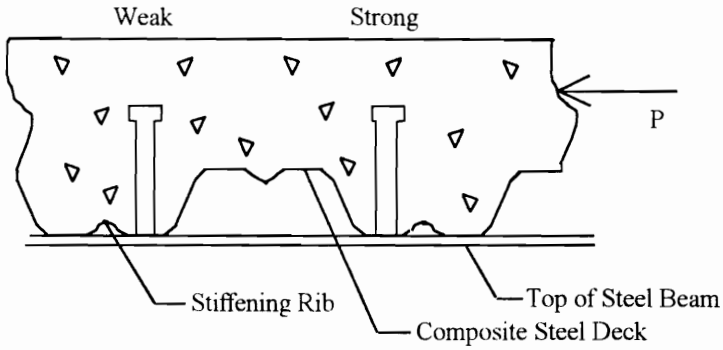

Figure 13 Weak and Strong Position Shear Stud Locations (Easterling et al 1993)

Strength prediction equations for shear studs were first developed for solid slabs. Later, when composite slabs were becoming more common, strength reduction equations were developed to account for possible reductions in strength resulting from the differences between the solid slab and the composite slab. There are a large number of shear stud strength prediction equations and strength reduction equations available. A recent review of these equations is found in Lyons et al (1994).

Both Lyons et al (1994) and Sublett et al (1992) concluded that none of the current strength prediction equations adequately predict the strength of studs in steel deck (weak and strong positions). Consequently, some modifications to the current strength prediction equations are needed. For simplicity these modifications will be made to the current AISC Specification (*Load and*, 1993) provisions.

3.3.2.1.1 Modifications To Current AISC Equations For Strong Position Studs

Two recommendations have been made to improve the accuracy of the current prediction equations given in the AISC Specification (*Load and*, 1993). Easterling et al (1993) recommended that an upper limit of 0.75 be used when calculating the stud reduction factor (SRF) with AISC Specification (*Load and*, 1993) equation I3-1. In addition, Lyons et al (1994) recommended that the upper limit on the shear stud strength be 0.8 A_{sc} F_u rather than A_{sc} F_u as is currently given by AISC Specification (*Load and*, 1993) equation I5-1.

These two suggested modifications were evaluated against the shear stud strength data from 23 pushout tests collected from Lyons et al (1994) and Sublett et al (1992). The ratio of the test strength over the predicted strength was considered. Two predicted strengths were calculated, one with and one without the suggested modifications. The ratio of test over predicted was 0.96 with a COV of 10% if the suggested modifications were included. The ratio of test over predicted was 0.77 with a COV of 10% if the suggested modifications were not included. Based on this analysis it appears that the suggested modifications are warranted.

3.3.2.1.2 Modifications To Current AISC Equations For Weak Position Studs

No suggested modifications were found in the literature to the current prediction equations given in the AISC Specification (*Load and*, 1993) for weak position studs. Because weak position studs typically have concrete failures, a modification to the SRF equation seems appropriate. In addition, Lyons et al (1994) suggested that the strength of a single stud in the weak position was a combination of load carried by the shear stud and load carried by the steel deck. The load carried by the deck was developed by the attachment of the deck to the steel beam that occurs at the weld collar around the shear stud. The author also showed that this deck strength could be approximated by using equations for spot welds found in the AISI Specification (*Load and*, 1991). Consequently, an additional modification that includes the effect of deck strength may be warranted.

First, consider the effect of deck strength. A summary of the results from 13 pushout tests that had weak position studs is presented in Table 11. The deck strength was calculated with the AISI Specification (*Load and*, 1991) equations using measured deck properties. Review of columns 1 and 3 of Table 11 indicates that the increases in the deck strength correlate well with the increases in shear stud test strength (i.e. the test strength increases because of increased deck strength given that other parameters are held constant). This was the same conclusion reached by Lyons et al (1994).

Next, consider putting an upper limit on the SRF equation. This modification is consistent with that used for the strong position studs. To determine an appropriate upper limit, the deck strength needs to be removed from the test strength; however, because the minimum deck gage typically used is 22 gage, it is recommended that only the increase in strength resulting from deck gages thicker than 22 gage be removed. This is how the base strength was determined in Table 11. The base strength was then divided by the predicted strength based on the AISI Specification (*Load and*, 1991) to determine an appropriate upper limit on the SRF. The average SRF was determined to be 0.53. A value of 0.5 seems justifiable.

Table 11 Weak Position Shear Stud Strength and Deck Strength

Test Strength (kips)	Deck Gage	Deck Strength (kips)	Base Strength (kips)	AISC Strength (kips)	SRF
11.15	22	2.37	11.15	19.93	0.56
10.96	22	2.37	10.96	19.93	0.55
12.46	22	2.37	12.46	19.93	0.63
11.56	20	3.19	10.74	19.93	0.54
12.79	20	3.19	11.97	19.93	0.60
13.66	20	3.19	12.84	19.93	0.64
14.8	18	5.62	11.55	19.93	0.58
13.62	18	5.62	10.37	19.93	0.52
15.06	16	7.07	10.36	19.93	0.52
13.66	20	3.19	12.84	28.39	0.45
12.87	20	3.19	12.05	28.19	0.43
12.92	20	3.19	12.10	27.92	0.43
14.75	20	3.19	13.93	27.92	0.50

3.3.2.1.3 Concrete in Tension Vs. Compression

Almost all the equations developed and research done deals with shear studs that are in concrete which is in compression. The concrete in the region of a composite beam-girder connection is normally in tension. The effect of the concrete being in tension on the strength of shear studs is not currently well understood. Johnson et al (1969) conducted push-off tests of solid slab specimens in which the concrete was in tension. Based on the results of these tests a reduction in strength of 20% compared to the shear stud strength in concrete that is in compression was suggested. Because these were solid slab specimens it is difficult to determine whether a similar reduction would be suitable for specimens with metal deck.

The only basis for determining whether tension or compression in the concrete had any effect on the shear stud strength is the data from the composite slab tests presented in Section 3.2. Considering pushout tests with similar parameters to those for the slab tests the average shear stud strength for strong and weak position studs is 20 kips and 12.7 kips respectively. Adding up these strengths for the weak and the strong position studs and only considering the effective studs (i.e. no studs in position "A") the estimated stud

strength is 80, 72.5, 80, and 60 kips for Slabs #1 through #4. The ratio of slab test strength to these estimated strengths are 0.95, 0.97, 0.98, 1.03 for Slabs #1 through #4 respectively. This seems to indicate that the fact that the concrete is in tension has little if any detrimental effects on the shear stud strength when the studs are in composite steel deck.

3.3.2.1.4 Summary of Recommended Shear Stud Strength

The following summarizes the current AISC Specification (*Load and*, 1993) equations with the recommended modifications.

$$Q_{sol} = SRF\ 0.5\ A_{sc}\ (f'_c\ E_c)^{0.5} \leq 0.8\ A_{sc}\ F_{usc} \qquad \text{(Eq 8)}$$

Where

Q_{sol} = The strength for a single shear stud (kips)

A_{sc} = Area of the shear stud based on the nominal shear stud diameter (in^2)

f'_c = Compressive strength of the concrete (ksi)

F_{usc} = Shear stud steel tensile strength (typically taken as 60 ksi)

E_c = Modulus of elasticity of concrete = $w_c^{1.5}\ \sqrt{f'_c}$ (*Load and*, 1993) (ksi)

w_c = Unit weight of concrete (pcf)

SRF = Stud reduction factor, given by

$$SRF = \frac{0.85}{\sqrt{N_r}}(w_r/h_r)[(H_s/h_r) - 1.0] \leq \begin{matrix} 0.75 \text{ For Strong Position Studs} \\ 0.5 \text{ For Weak Position Studs} \end{matrix} \qquad \text{(Eq 9)}$$

Where

N_r = Number of shear studs per deck rib

H_s = Shear stud height after welding

h_r = Height of the deck rib

w_r = Width of the deck rib

The strength given by Equation 8 can be increased for weak position shear studs to account for increased strength associated with deck gages above 22 gage. This

modification factor is given in Table 12. Caution should be exercised when adding the modification factor for two reasons:

- By adding the factor, it is assumed that the weld collar around the shear stud is sufficient to properly attach the deck to the beam
- Lyons et al (1994) showed that the increased strength associated with thicker deck gages tends to degrade in the later stages of the load-deformation behavior

Table 12 Weak Position Shear Stud Strength Modifiers

Deck Gage	Modification Factor (kips)
22	0.00
20	0.82
18	3.25
16	4.70

3.3.2.2 Load-Deformation Behavior Of Shear Studs

Three analytical models for predicting the load-deformation behavior of shear studs were found: Buttry (1965). Ollgaard, et al (1971), Oehlers and Coughlan (1986). All three of the above analytical models were evaluated against the push-off test data for strong and weak position shear studs. Many of the pushout tests exhibited a softening in the load-deformation response after the peak load was attained but before failure. Because none of the above models attempt to include this softening only data up to the point where test softening occurred was included in the evaluation. The maximum measured test load was used for Q_{sol} in the analytical expressions. The evaluation was carried out by calculating the ratio of the test load over the predicted load for each analytical method and for each load-deformation point. The results of the evaluation are summarized in Table 13.

Table 13 Evaluation of Load-Deformation Behavior Models

	Buttry		Ollgaard		Oehlers & Coughlan	
	Weak	Strong	Weak	Strong	Weak	Strong
Mean	1.25	1.30	0.98	1.08	3.92	4.01
COV	122%	76%	17%	23%	315%	187%
No. Points	271	595	271	595	271	595
Maximum	22.61	19.79	1.97	2.59	172.78	141.41
Minimum	0.12	0.00	0.02	0.00	0.79	0.01

Of the three analytical models Ollgaard (1971) appears to fit the test data the best. Both Buttry (1965) and Oehlers and Coughlan (1986) typically under predict the load. In addition, visual comparisons of the data with the estimates showed that the initial stiffness estimate by Oehlers and Coughlan clearly underestimates the initial stiffness seen in this test data.

If the load-deformation behavior after the initiation of softening occurs is not of interest then clearly using Ollgaard's analytical model appears to be justifiable. However, if the load-deformation behavior after initiation of softening is of interest then none of the analytical models considered so far would be suitable in the later stages of the load-deformation behavior. The refinement required to include the load softening effect is not believed necessary at this point and therefore Ollgaard's analytical model is recommended for use up to the average failure deformations of 0.36-in. and 1.1-in. for strong position and weak position studs respectively. This model is given by:

$$Q = Q_{sol}\left[1 - e^{-18\delta}\right]^{2/5} \qquad \text{(Eq 10)}$$

3.4 Methods of Representing The Load-Deformation Behavior of A Reinforced Composite Slab

Any point of the load-deformation behavior of the reinforced composite slab can now be determined by using the component model shown previously in Figure 6 and the behavior models for the reinforcing , concrete, and shear studs just developed. However,

rather than represent the load-deformation behavior with a large number of load-deformation points, it is desirable to represent the behavior with simpler approximations.

3.4.1 Multi-Linear Representation

A multi-linear representation of the composite slab force-deformation behavior can be obtained by determining a variety of key load-deformation points and then connecting them with straight line segments. Because the deformation can be calculated directly for a given load it is suggested that various key force points be picked and then the corresponding deformations be determined. The following key forces are recommended

- Key forces for combined reinforcing steel and concrete
  1. Force when the reinforcing steel stress is at 50% F_y
  2. Force when the reinforcing steel yields
  3. Force when the reinforcing steel stress is midway between F_y and F_u
  4. Force when the reinforcing steel stress is at F_u
- Key forces for shear studs
  5. 50% of the maximum total shear stud strength
  6. 80% of the maximum total shear stud strength
  7. 94% of the maximum total shear stud strength
  8. Load at a shear stud deformation of 0.36-in.

These key points were picked because they represent transition points in the typical force-deformation behavior for either of the elements. Obviously only forces up to the strength of either the shear studs or for the reinforcing steel and concrete would be included in the multi-linear representation.

3.4.2 Continuous Representation

Sometimes it is convenient to represent the composite slab force-deformation behavior with a continuous analytical curve. The writer has chosen the Richard Equation

(Richard and Elsalti, 1991) for this purpose. A typical curve represented by the Richard Equation along with definitions of the basic equation parameters are given in Figure 14.

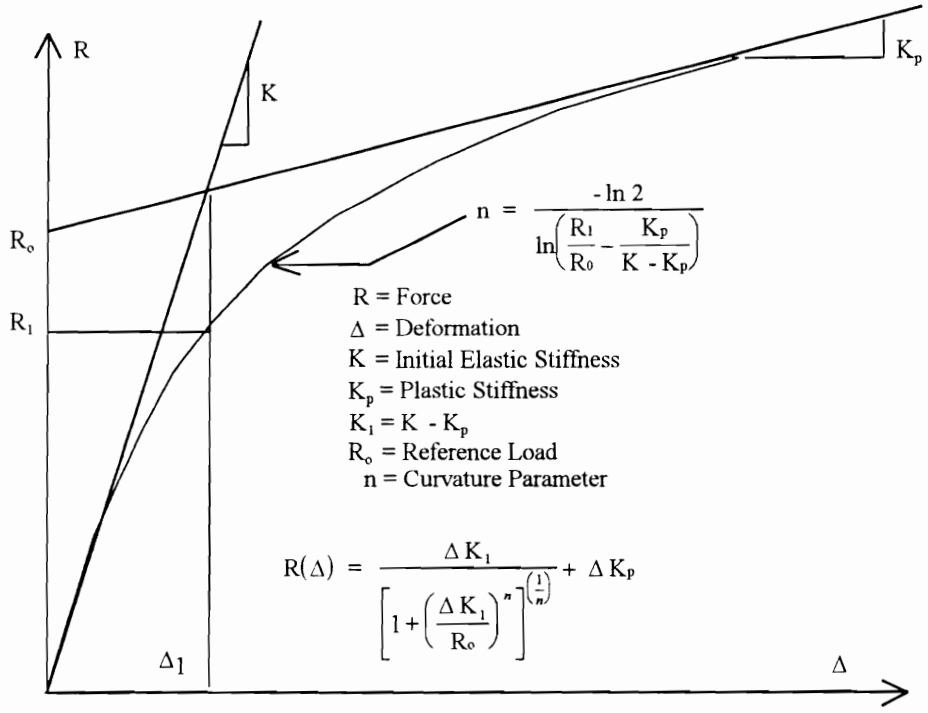

Figure 14 Richard Equation (Richard and Elsalti, 1991)

The first parameter is K (K = R / Δ), the elastic stiffness. This can be approximated by the initial stiffness of the multi-linear representation. This would be done by determining the first key point (i.e. either 50% reinforcing steel yield force or 50% Q_{sol}) and dividing the force by the deformation at that point. For P_{slab1} less than P_{stud1} this is given by

$$K = \frac{P_{slab1}}{\delta_{slab1} - \frac{\ln\left\{1 - \left(\frac{P_{slab1}}{N_{studs} Q_{sol}}\right)^{2.5}\right\}}{18}} \qquad \text{(Eq 11)}$$

Otherwise:

$$K = \frac{P_{stud1}}{0.0108 + \delta_{slab1} \frac{P_{stud1}}{P_{slab1}}} \qquad \text{(Eq 12)}$$

Where

$P_{slab1} = A_{ceff} f_c + A_r F_{yr} / 2$ = Force in reinforced concrete slab at first key point

$\delta_{slab1} = L_{eff} F_{yr} / (2 E)$ = Deformation of reinforced concrete slab at first key point

$P_{stud1} = 0.5 N_{studs} Q_{sol}$ = Load in studs at first key point

$\delta_{stud1} = 0.0108$ -in. = Stud deformation at first key point

The next parameter, K_p the plastic stiffness, can be approximated by the slope of the load-deformation behavior between the last two key points. If the reinforcing steel controls the maximum load capacity of the slab then the change in load and the change in deformation between the last two key points are given by

$$\Delta R = A_r (F_u - F_y)/2 \quad \text{(Eq 13)}$$

$$\Delta\delta = 0.07 L_{eff} \quad \text{(Eq 14)}$$

When the mean values of F_u and F_y for reinforcing steel (previously given in Chapter 1) are substituted into Equation 13 and the effective length is assumed to be S_0 then the resulting value of the plastic stiffness is given by:

$$K_{pr} = 300 A_r / S_0 \quad \text{(Eq 15)}$$

If the shear studs control the maximum load capacity of the slab then the plastic stiffness can be derived as

$$K_{ps} = 0.24 Q_{sol} \quad \text{(Eq 16)}$$

Neither K_{pr} or K_{ps} consider the additional flexibility of the other component (i.e. if the shear studs control then the added flexibility from the combined concrete and reinforcing or if the reinforcing controls then the added flexibility from the shear studs). For typical combinations of reinforcing steel and shear studs, the added flexibility can be accounted for by dividing K_{pr} or K_{ps} by two.

To determine the reference load, R_0, the plastic stiffness (K_p) and the load (R_{last}) and deformation (Δ_{last}) associated with the last key point of the multi-linear representation must be known. Once these values are known, the reference load is calculated by

$$R_0 = R_{last} - \Delta_{last} K_p \quad \text{(Eq 17)}$$

The deformation at the intercept of K and K_p is given by

$$\Delta_1 = R_0 / (K - K_p) \qquad \text{(Eq 18)}$$

The parameter R_1 is the load at deformation Δ_1. This can be determined by interpolating between points on the multi-linear representation. Typically only the first two or three key points are required to determine R_1.

Finally, the curvature parameter n is given by

$$n = \frac{-\ln 2}{\ln\left(\frac{R_1}{R_0} - \frac{K_p}{K - K_p}\right)} \qquad \text{(Eq 19)}$$

The method for determining the Richard equation parameters just outlined was verified by comparing the resulting curve to the multi-linear representation for a wide variety of composite slab variables. Overall agreement between the curve and the multi-linear representation was excellent.

3.5 Experimental Verification of The Component Method of Modeling the Slab

Multi-linear and Richard equation representations of the load-deformation behavior for Slabs #1 through #4 are compared to the test data in Figures 15 through 17. Before any comparisons between the model and the test data could be made three modifications to the test data were required. First, the initial stages of the load-deformation behavior for Slabs #1, #3 and #4 had significant "jumps" in the data. These jumps were caused by large slips between the rotation pin and the fixed side of the test setup. Slab #2 did not have these jumps because most of the slipping was prevented by using shims and by fully tightening the bolts attaching the frame beams to the rotation pin. These jumps in deformation were removed from the test data.

Second, the slab deformation determined from the tests represents the deformations from both sides of the specimen. This is true at least up to the point of maximum load when the shear studs in one side of the specimen would start to fail while the studs on the opposite side typically maintained a constant deformation. The

component model considers only one side of the composite slab. Consequently, the slab deformations up to maximum load were divided by two. Increases in deformation that occurred after the maximum load can mainly be attributed to the shear studs failing on one side of the specimen. Consequently, these deformation measurements were taken at full value and simply added to the deformation at the maximum load.

Third, shear studs in position "A" were obviously ineffective based on reviewing the results. Consequently, shear studs in position "A" were ignored for modeling purposes. This results in Slab #1 and Slab #3 being identical in terms of parameters.

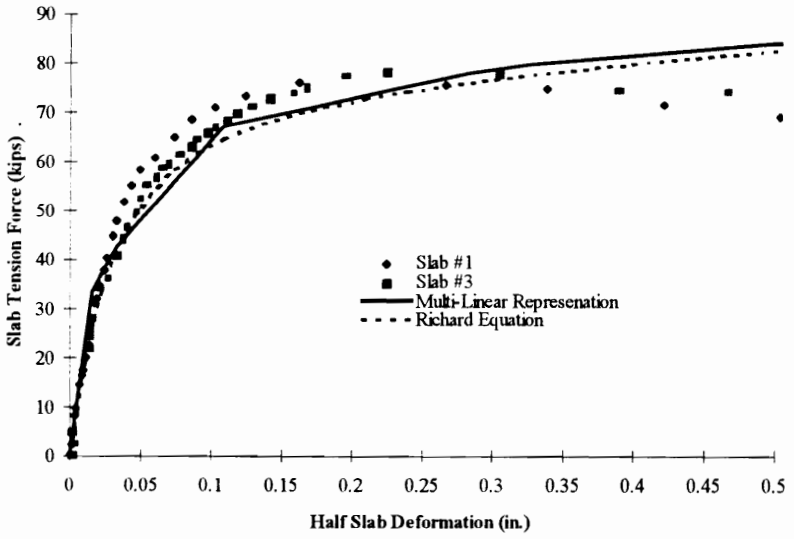

Figure 15 Model Vs. Test Results Slab #1 And #3

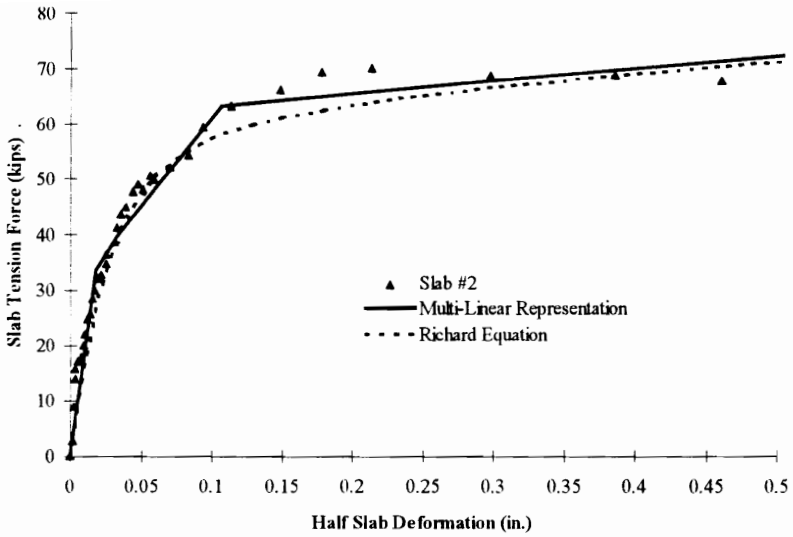

Figure 16 Model Vs. Test Results Slab #2

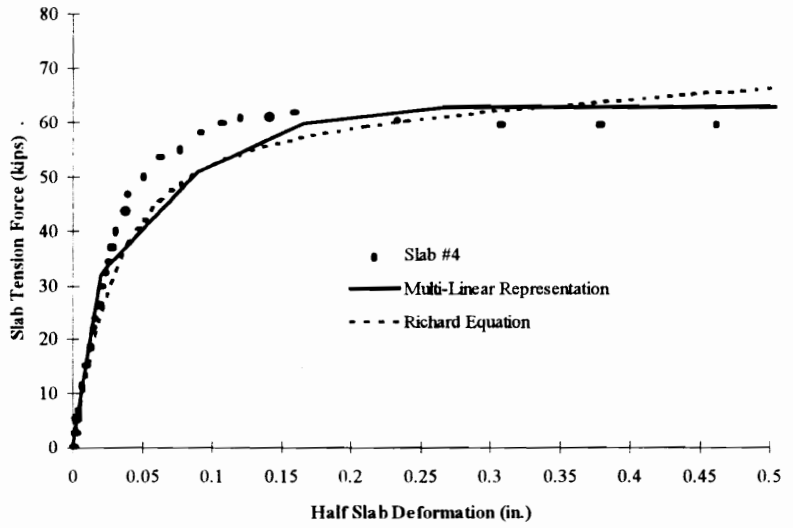

Figure 17 Model Vs. Test Results Slab #4

Review of Figure 15-17 shows favorable comparison between the model and the test results with two notable exceptions. First, the maximum force predicted with the

model was between 3% and 11% higher than the maximum force of the test. There are two sources for this difference. First, it was previously shown that the average ratio of test to predicted stud strength was 96%. Second, it was also shown that there may be a slight drop in the stud strength because the concrete is in tension rather than compression. These combined sources of error easily explain the difference between predicted and test forces. Overall, the error is still small and refinement of the model is not deemed necessary.

Second, the deformation at the maximum force does not agree well. This is mainly attributable to the fact that predicted test forces were higher than actual test forces. The difference in deformation is attributed to the increase in reinforcing steel and concrete element deformations that occurred between the maximum test force and the maximum predicted force.

Based on the above comparison between the model and the test data, it appears that the model provides a good estimate of the force-deformation behavior for the reinforced composite slab.

3.6 Summary, Conclusions and Recommendations

3.6.1 Summary

The objective of this study was to show that the axial force-deformation behavior of a reinforced composite slab under tension can be modeled as a combination of three fundamental composite slab components: concrete, reinforcing steel, and shear studs. To verify the hypothesis four steps were taken:

1. An experimental investigation of the force-deformation behavior was conducted.
2. Behavior models of the fundamental composite slab components were developed.
3. Two methods for combining the fundamental component behaviors to model the composite slab force-deformation behavior were developed. The second of these

methods develops fairly simple relationships that can be used to estimate the initial and final stiffness of the force-deformation behavior.

4. The model composite slab force-deformation behavior was evaluated against the data from the experimental investigation.

Based on the evaluation of the model behavior compared to the test behavior it appears that the axial force-deformation behavior of a reinforced composite slab under tension can be modeled as a combination of the three fundamental composite slab components.

3.6.2 Conclusions

The following conclusions were made in this chapter.

- Whether the composite slab is in tension or compression seems to have little effect on the strength of the shear studs.
- Using the AISC Specification (*Load and*, 1993) shear stud strength equations with previously suggested modifications (Easterling et al 1993 and Lyons et al 1994) for strong position studs provides a reasonably accurate estimate of the shear stud strength for studs in profiled steel deck.
- The stud reduction factor calculated using the current AISC Specification (*Load and*, 1993) should be limited to a maximum of 0.5 for studs in the weak position.

3.6.3 Recommendations

The following recommendations are made for further study of the load-deformation behavior of composite slabs.

- The behavior model developed for shear studs in this chapter was based on a very limited number of pushout tests in which a limited number of parameters were considered. Clearly, a more comprehensive study beginning with a collection and analysis of a much larger base of data is warranted.
- Further simplification of methods to determine a multi-linear representation of the slab load-deformation behavior or to determine the parameters of the Richard Equation are

needed. The methods outlined in this report are still too cumbersome for use in day to day design. Most likely, the easiest way to simplify these methods is to develop parametric equations.

- Additional composite slab tests are also recommended to provide further verification of the component model. In particular composite slab tests were the reinforcing steel fails instead of the shear studs is needed.

4. Behavior and Modeling of a Single Plate Bearing On a Single Bolt

This chapter summarizes the report by Rex and Easterling (1996(c)) on the behavior and modeling of a single plate bearing on a single bolt.

4.1 Introduction

4.1.1 General

One of the primary components of the PR composite beam-girder connection considered in this dissertation is a high strength bolt in single shear. The load-deformation behavior of this component is needed to properly model the PR connection. A component method of modeling the load-deformation behavior of a single bolt in single shear is presented in Chapter 5 of this dissertation. This component model breaks the load-deformation behavior into three basic behavior models: friction, plate bearing deformation, and bolt deformation. The development of a behavior model for the plate bearing deformations is presented in this chapter.

Plate bearing deformations occur when load is transferred by contact between the shank of the bolt and a plate bolt hole. Plate bearing deformations are the localized deformations of the plate at the point of contact with the bolt shank. These concepts are illustrated in Figure 18. A model for predicting the load vs. plate bearing deformation is needed so that the more general behavior of a single bolt in single shear can be modeled.

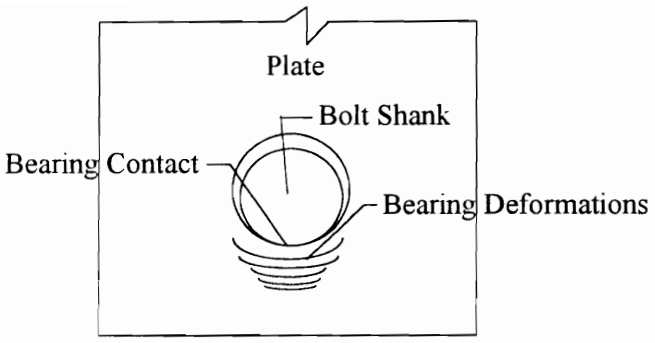

Figure 18 Single Plate Bearing On A Single Bolt

4.1.2 Objectives And Methods

The objective of the study presented in this chapter is to develop a model for approximating the load-deformation behavior associated with plate bearing. This objective is achieved by:

- Conducting an experimental investigation of a single plate bearing on a single bolt,
- Developing a model for estimating the initial stiffness of the load-deformation behavior,
- Verifying a model for estimating the strength of a single plate bearing on a single bolt, and
- Determining how the load-deformation behavior can be normalized and represented by a non-linear analytical expression.

First, an experimental investigation was conducted at VT to provide data about the strength and load-deformation behavior of a single plate bearing on a single bolt. The goal of this investigation was to experimentally isolate and measure the localized bearing load-deformation behavior and to determine failure modes and loads.

Second, one of the primary characteristics that define the load-deformation behavior is the initial stiffness. The experimental results are used to validate a finite element model of the bolt and plate. The finite element model is then used to determine the effect of varying parameters on the initial stiffness of the load-deformation behavior.

Based on the experimental and finite element results, a model for estimating the initial stiffness is developed. This model and other existing models are then evaluated against the test and finite element results.

Third, existing models for estimating the plate in bearing are evaluated. These models are evaluated against experimental data from the current study as well as from an independent study conducted at Oklahoma State University (Lewis, 1994).

Fourth, a method of normalizing the experimental load-deformation data is developed. A non-linear analytical equation is then used to approximate the behavior.

4.2 Experimental Investigation Conducted At VT

An experimental investigation was conducted to provide data for the development and verification of a method for approximating the load-deformation behavior of a single plate bearing against a single bolt. The following describes the details and results of this investigation.

4.2.1 Test Specimens

A schematic of the typical single plate specimen is shown in Figure 19. The parameters that were systematically varied included the end distance (L_e), plate thickness (t_p), bolt diameter (d_b), edge condition (sheared or sawed), and plate width. Because of an effort to use existing materials, rather than purchasing all new material, the steel properties also varied among the test specimens. A summary of these parameters is presented in Table 14.

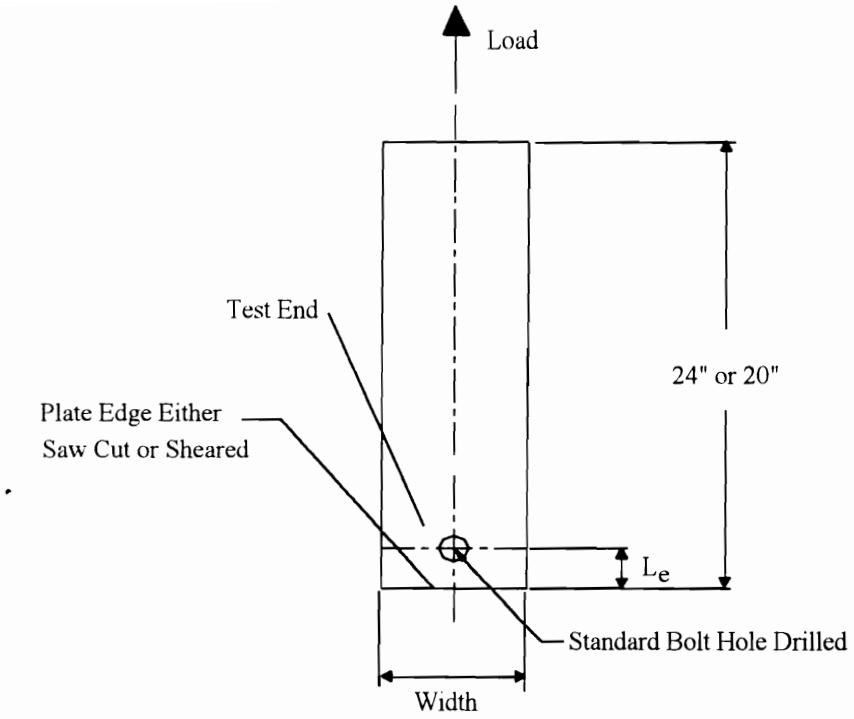

Figure 19 Test Specimen

A comparison of F_y and F_u values in Table 14 shows a wide variation in steel properties. The properties of the steel used for test specimens 1 to 28 are not typical of steels used in normal construction today. The steel used for test specimens 1 to 28 will be referred to as "high strength" and the steel used for the remaining test specimens will be referred to as "mild" for the remainder of this chapter.

Table 14 Test Specimen Parameters

Test	Bolt Diameter (in.)	Plate Thickness (in.)	Plate Width (in.)	End Distance (in.)	Edge Condition	Fy (ksi)	Fu (ksi)
1	1	0.25	4.5	1	Sawed	60	100
2	1	0.25	4.5	1	Sawed	60	100
3	1	0.25	4.5	1.5	Sawed	60	100
4	1	0.25	4.5	1.5	Sawed	60	100
5	1	0.25	4.5	2	Sawed	60	100
6	1	0.25	4.5	2	Sawed	60	100
7	1	0.25	4.5	2.5	Sawed	73.5	109
8	1	0.25	4.5	2.5	Sawed	56.5	95
9	1	0.25	4.5	3	Sawed	60	100
10	1	0.25	4.5	3	Sawed	60	100
11	1	0.25	4.5	1	Sheared	59	96.5
12	1	0.25	4.5	1	Sheared	59	96.5
13	1	0.25	4.5	2	Sheared	59	96.5
14	1	0.25	4.5	2	Sheared	59	96.5
17	1	0.25	5.4	2	Sawed	73.5	109
18	1	0.25	5.4	2	Sawed	73.5	109
19	1	0.25	3.5	2	Sawed	73.5	109
20	1	0.25	3.5	2	Sawed	73.5	109
21	0.875	0.25	4.5	2	Sawed	56.5	95
22	0.875	0.25	4.5	2	Sawed	56.5	95
23	0.75	0.25	4.5	2	Sawed	56.5	95
24	0.75	0.25	4.5	2	Sawed	56.5	95
25	0.875	0.25	4.5	1.75	Sawed	56.5	95
26	0.875	0.25	4.5	1.75	Sawed	56.5	95
27	0.75	0.25	4.5	1.5	Sawed	56.5	95
28	0.75	0.25	4.5	1.5	Sawed	60	100
29	1	0.375	5	1.5	Sheared	43.7	63.7
30	1	0.375	5	1.5	Sheared	43.7	63.7
31	1	0.5	5	1.5	Sawed	53.3	74.8
32	1	0.5	5	1.5	Sawed	51.5	74.5
33	1	0.625	5	1.3	Sawed	43.7	63.3
34	1	0.625	5	2	Sawed	43.7	63.3
35	1	0.75	5	2	Sawed	44.5	67.8
36	1	0.75	5	2	Sawed	44.5	67.8
37	1	0.375	5	1.75	Sheared	43.4	63.9
38	1	0.5	5	1.5	Sawed	51.5	74.5
39	1	0.25	5	1.5	Sawed	44.5	65.5
40	1	0.25	5	1.5	Sawed	44.5	65.5
41	1	0.25	5	1.5	Sawed	44.5	65.5
42	1	0.25	5	1	Sawed	44.5	65.5
43	1	0.25	5	1	Sawed	44.5	65.5
44	0.875	0.25	5	1	Sawed	44.5	65.5
45	0.875	0.25	5	1	Sawed	44.5	65.5
46	0.875	0.25	5	1.3125	Sawed	44.5	65.5
47	0.875	0.25	5	1.3125	Sawed	44.5	65.5
48	1	0.25	5	1	Sawed	44.5	65.5

4.2.2 Instrumentation

Two linear calipers were used to measure deformation on each side of the plate as shown schematically in Figure 20. The calipers have markings at each 0.001-in. By interpolating between these marks the deformations were read to the nearest 0.0001-in. +/- 0.00025-in.

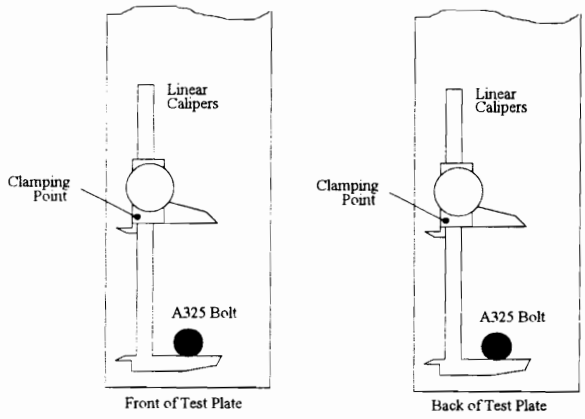

Figure 20 Displacement Instrumentation

As illustrated in Figure 20 the calipers were attached to the test plate with a small C-clamp. This fixed one edge of the caliper while the other edge was positioned so that it rested against the bottom of the bolt. The deformations determined by this setup included both elastic deformations in the plate as well as plate bearing deformations below the bolt.

4.2.3 Test Setup

The test setup used is shown schematically in Figure 21. The top and bottom of the test rig were placed in the upper and lower heads of a universal testing machine which was used to apply the load for the test.

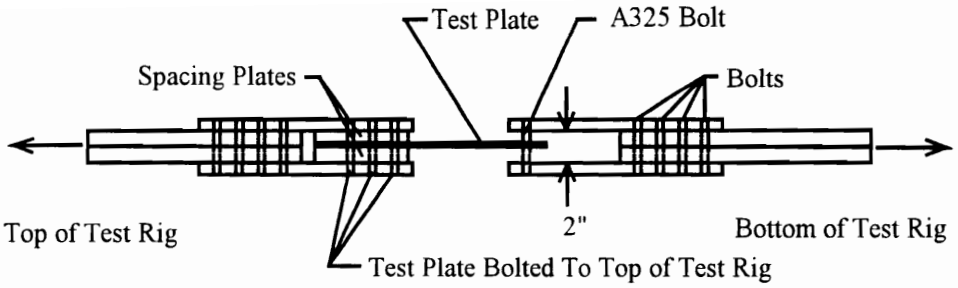

Figure 21 Test Setup

4.2.4 Test Procedure

Test specimens were loaded to 1 kip at a rate of 0.1-in./minute. The calipers were then checked to ensure they were bearing on the bottom of the bolt. The plates were then either loaded at a load rate of 2 kips/minute or at a displacement rate of 0.005-in./minute. The displacement controlled loading was used in lieu of the load controlled loading in the latter test specimens because it was found to provide better control over the test. Once the load deformation behavior started to soften the specimen was loaded at a rate of 0.04-in./minute. The initial deformation reading was taken when the load was between 2 and 3 kips. Subsequent deformation readings were initially taken at approximately every 2.5 kips. After the behavior started to soften load readings were taken at approximately every 0.05-in. of deformation.

Specimens were loaded until either the specimen failed or the limits of the test setup were reached. The primary characteristic of the plate load-deformation behavior that prompted these tests was the initial stiffness. As a result, the test setup was not designed to test all specimens to failure. Consequently, many specimens were not tested to failure but instead only initial stiffness data was obtained.

4.2.5 Results

The general test results are presented in Table 15. The initial stiffness (K_i) was determined by a best fit through the initial data (after data adjustments were made). In

addition, upper and lower bounds on the stiffness were determined by considering the precision of the deformation and load measuring devices. The first and last data points included for determining the initial stiffness were used to determine the upper and lower bounds for the initial stiffness. The precision of the load and deformation measurements were added and subtracted from the data point values. This created a box of possible load-deformation points that could have been read for each point. Upper and lower bounds on the initial stiffness were based on slopes passing from the edges of these boxes as shown in Figure 22.

The following sections describe the types of failure modes observed and adjustments that were made to the raw data. Aside from these topics, additional discussion of results is not presented here. Rather, the remaining results are discussed in the later sections of the chapter as appropriate.

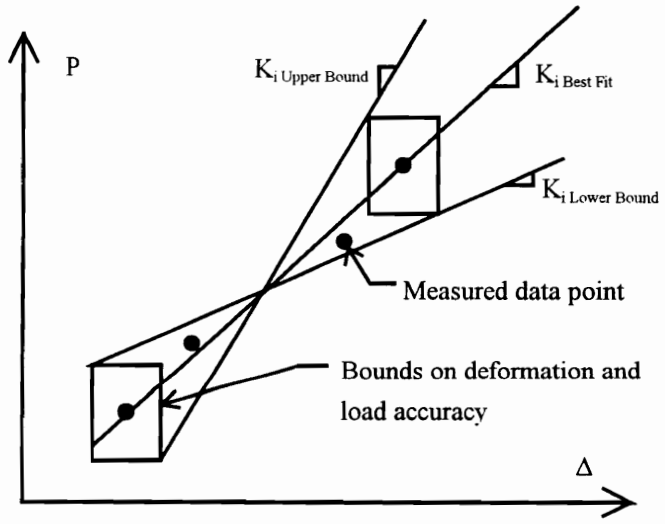

Figure 22 Upper and Lower Bounds For K_i

Table 15 General Test Results

Test	K_i Best Fit (Kips/in.)	K_i Upper (Kips/in.)	K_i Lower (Kips/in.)	R_{ult} (Kips)	Δ @ R_{ult} (in.)	Failure Mode
1	1138	1677	824	24.3	0.2374	Bearing
2	1278	1958	906	22.3	0.2498	Tearout
3	1511	1765	1336	34.2	0.4171	Splitting
4	*	*	*	33.8	0.3857	Bearing
5	1477	1866	1217	43.2	0.3291	Bearing
6	1572	1999	1277	45.6	0.2721	Curling
7	*	*	*	41.7	0.1598	Curling
8	1643	2089	1332	42.2	0.1583	Curling
9	1601	2038	1303	41.7	0.1065	Curling
10	2137	2946	1646	40.5	0.1237	Curling
11	1258	1869	910	23.8	0.2017	Splitting
12	1631	2995	1055	22.1	0.2261	Splitting
13	1542	1927	1261	41.4	0.1872	Curling
14	2057	2783	1604	42.9	0.1792	Curling
17	1777	2337	1416	42.7	0.1934	Curling
18	1403	1743	1157	44.1	0.2216	Curling
19	1573	1988	1281	37.9	0.1585	Curling
20	1457	1821	1199	35.7	0.1471	Curling
21	1124	1336	958	**	**	**
22	1172	1421	996	**	**	**
23	1098	1306	941	**	**	**
24	935	1087	813	**	**	**
25	1611	2038	1314	**	**	**
26	1189	1451	1005	**	**	**
27	*	*	*	**	**	**
28	669	753	597	**	**	**
29	1393	1701	1164	32.5	0.1557	Splitting
30	1724	2220	1375	30.7	0.2205	Splitting
31	1670	1917	1494	**	**	**
32	2779	4165	2044	**	**	**
33	2265	3096	1757	**	**	**
34	2295	2852	1920	**	**	**
35	3590	4934	2752	**	**	**
36	3531	4861	2717	**	**	**
37	1778	2335	1425	35.4	0.2115	Splitting
38	1865	2390	1512	**	**	**
39	*	*	*	25.5	0.5068	Bearing
40	*	*	*	25.9	0.5072	Bearing
41	1522	2894	963	25.7	0.4996	Bearing
42	561	667	462	16.3	0.3338	Bearing
43	1113	1484	860	16.3	0.3807	Bearing
44	902	1128	760	16.1	0.3833	Bearing
45	1056	1646	745	16.0	0.3210	Bearing
46	797	897	698	22.5	0.4472	Bearing
47	856	1099	695	22.6	0.4486	Bearing
48	388	431	349	17.3	0.3734	Bearing

* Inaccurate initial stiffness data.

** Test limited by test setup. Specimen not tested to failure.

4.2.5.1 Types of failures

Four plate failure modes were observed. These failure modes are shown schematically in Figure 23. The definitions of tearout and splitting failures are clear in Figure 23; however, the definitions of bearing and curling failures warrant further description. Bearing failure was defined as bearing deformations exceeding 0.5-in. without any substantial loss in load capacity. Plate curling was defined as the plate below the bolt buckling out of the original plane of the plate and tests were stopped when the plate had deformed far enough to cause conflicts with the test setup or there was a drop in load carrying capacity. The buckling was caused by the compression forces in the portion of the plate below the bolt.

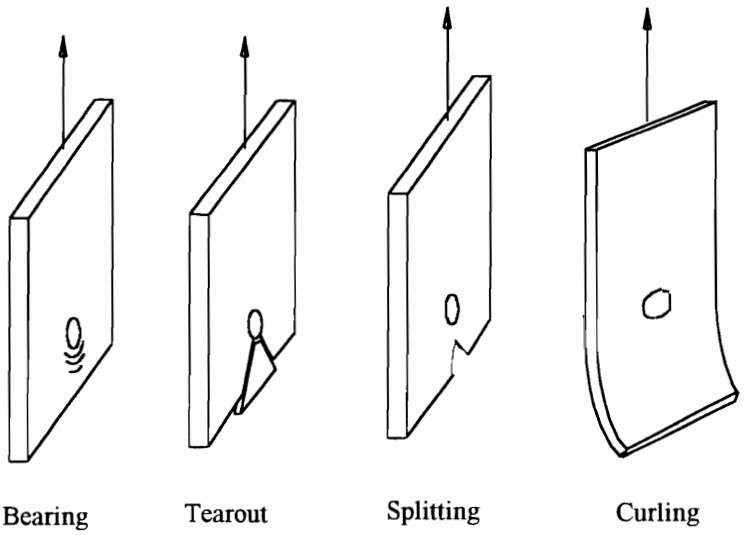

Figure 23 Typical Plate Failures

4.2.5.2 Adjustments to data

Before the raw data could be used for the development and verification of load-deformation behavior prediction models there were typically three and in some cases four types of adjustments made to the data. First, estimates of elastic plate deformations and bolt deformations were removed from the raw data. Next, the new data was used to determine the initial stiffness of the specimen. The data was then shifted based on the

initial stiffness such that the initial response passed through a point of zero load and zero deformation. Finally, in tests where excessive curling of the specimen occurred, it was sometimes necessary to remove one of the linear calipers to prevent damage. For these tests, data was adjusted for the missing caliper readings.

4.3 Initial Stiffness

The initial stiffness of the load-deformation behavior is one of the two most important quantities of the behavior. Unfortunately, it is also the hardest quantity to measure. Because of the difficulty in measuring experimental initial stiffness values, it was decided that a combination of experimental and finite element work would be used to develop and evaluate predictive models. A finite element model of the single plate bearing against the single bolt was developed and verified against the experimental data. This model was then used to conduct a parameter study. In turn, the data from the parameter study was then used to develop and evaluate predictive models.

4.3.1 Finite Element Model

A finite element model of a single plate bearing against the single bolt was developed and analyzed using the ANSYS general purpose finite element program. Two dimensional and three dimensional finite element meshes were considered. Element type and mesh density was varied to determine the most efficient modeling scheme that also compared well with the experimental results. Based on this preliminary study, a three dimensional mesh of brick elements (8 node, 24 dof) was chosen and the double symmetry of the physical problem was taken into account. A plan view of the mesh used is presented in Figure 24.

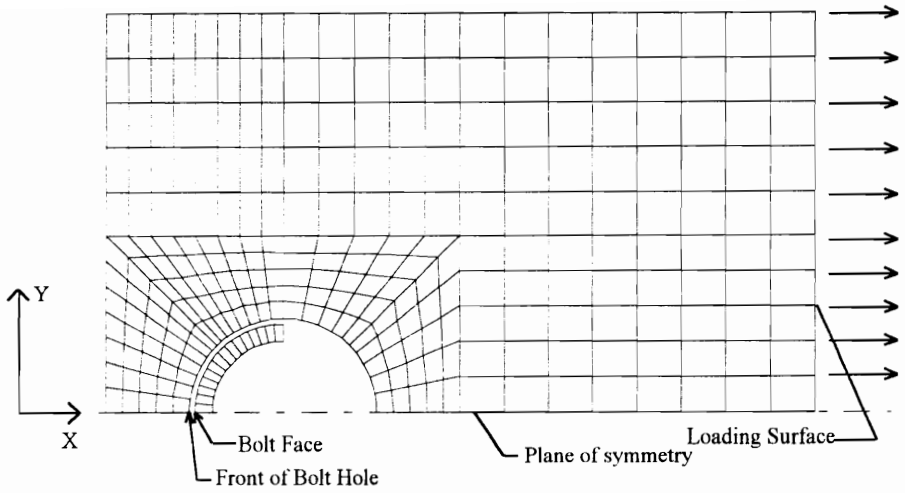

Figure 24 Typical Finite Element Mesh

Twenty finite element models were used for verification against the experimental data. These models included all the parameters that were included in the experimental tests except for edge condition which was determined to have no effect on the initial stiffness based on the results of the experimental tests. Nominal values for the geometry were used. A graphical summary of the results is presented in Figure 25. Note that the experimental test results in Figure 25 have error bars representing the upper and lower bounds on the initial stiffness which were determined based on the precision of the deformation and load measurements.

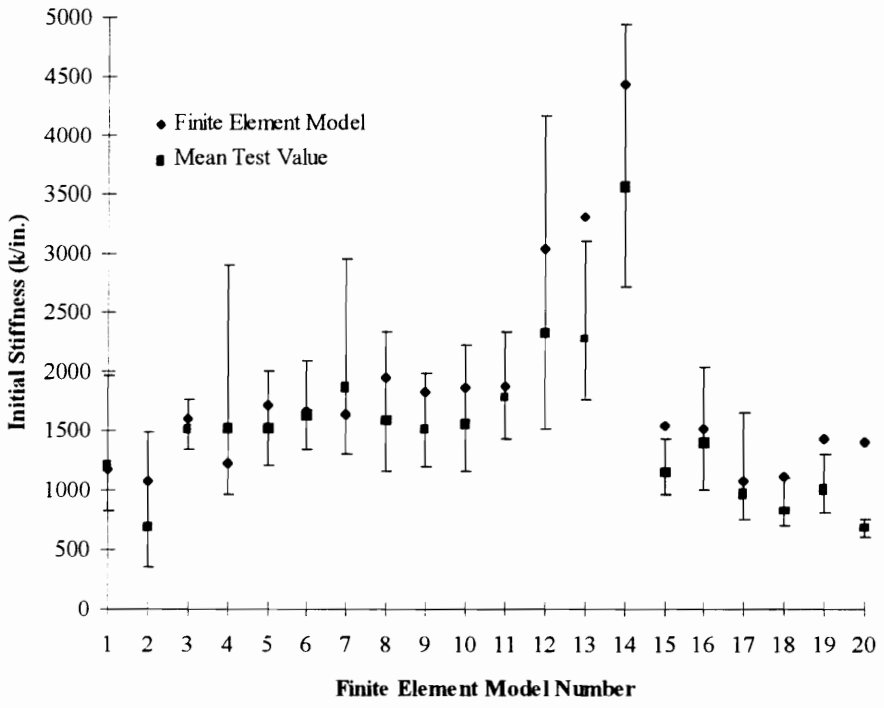

Figure 25 Finite Element Model K_i Vs. Experimental K_i

Comparison of the finite element results to the experimental test results in Figure 25 shows that all but four of the finite element results fell within the upper and lower bounds for the experimental test results. Sources of difference between finite element model and experimental test results include:

- Difference between the nominal and actual geometry
- Difficulty in experimentally measuring initial stiffness
- Variations between the actual and modeled stress-strain behavior

Overall, the agreement between the finite element results and the test results was deemed satisfactory.

An additional 140 finite element models were analyzed to investigate the effect of changing parameters. The parameters included were

- Bolt Diameter 3/4-in., 7/8-in., and 1-in.
- Plate Thickness: 1/8-in. to 1-in. in increments of 1/8-in.

- Edge Distance: 1-in. to 3-in. in increments of 1/4-in.
- Yield Stress: 35 ksi to 60 ksi in increments of 5 ksi
- Ultimate Stress: 50 ksi to 100 ksi in increments of 10 ksi

These finite element model results are used later to evaluate methods for predicting the initial stiffness.

4.3.2 Existing Prediction Models

Two models for predicting the initial stiffness of bolted joints, in which bolts are not fully tightened, were reviewed from the literature. The first of these was given in Eurocode 3 Annex J (1994). This was developed for the purpose of determining the initial stiffness of the moment-rotation behavior of bolted joints where the bolts are in shear and not fully tightened. This initial stiffness is given by:

$$K_i = 24\, k_b\, k_t\, d_b\, F_u \qquad \text{(Eq 20)}$$

Where:

$k_b = L_e / (4d_b) + .5 \leq 1.25$

$k_t = 1.5\, t_p / d_{m16} \leq 2.5$

d_{m16} = Nominal diameter of a M16 bolt (16mm)

A second expression for estimating the stiffness of bolts in butt joints with multiple bolts was developed by Tate and Rosenfeld (1946).

$$K_b = 2 /(C_{bs} + C_{bb} + C_{bbr} + C_{pbr}) \qquad \text{(Eq 21)}$$

Where:

$$C_{bs} = \frac{t + 2t'}{3GA_b} \qquad \text{(Eq 22)}$$

$$C_{bb} = \frac{8t'^3 + 16tt'^2 + 8t't^2 + t^3}{192EI_b} \qquad \text{(Eq 23)}$$

$$C_{bbr} = \frac{(t + 2t')}{Ett'} \qquad \text{(Eq 24)}$$

$$C_{pbr} = \frac{1}{t'E} + \frac{2}{tE} \quad \text{(Eq 25)}$$

And:

t' = Thickness of lap plates

t = Thickness of main plates

A review of this derivation gives the estimate of the plate bearing stiffness as

$$K_i = t_p E \quad \text{(Eq 26)}$$

4.3.3 Proposed Prediction Model

Based on the results from the finite elements models and the experimental tests it appears that the initial stiffness depends on three primary stiffness values in the plate. The stiffness associated with bending, shearing, and bearing combine to determine the final initial stiffness. The model that accounts for these three stiffness values is simply three springs in series. The final stiffness is given by

$$K_i = \frac{1}{\frac{1}{K_{br}} + \frac{1}{K_b} + \frac{1}{K_v}} \quad \text{(Eq 27)}$$

Where:

K_{br} = Bearing stiffness

K_b = Bending stiffness

K_v = Shearing stiffness

4.3.3.1 Bearing Stiffness

The physical reality of a bolt bearing on the side of a bolt hole is complex three dimensional problem involving material non-linearity. Some simplifications of the real problem have to be made to develop a model that relates the plate geometry and material to the bearing stiffness. Two assumptions were made to simplify the problem. First, the problem is assumed to be two dimensional; and second, the steel in contact with the bolt is assumed to be at its yield stress. With these two assumptions the basic problem becomes

one of geometry. The geometrical model of the problem is shown in Figure 26 where R1 and R2 are the radii of the bolt and bolt hole respectively.

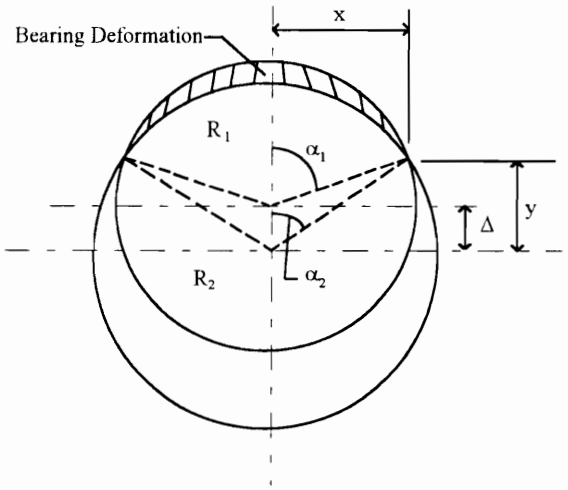

Figure 26 Bearing Stiffness Model

By assuming standard hole sizes and an initial bearing deformation of 0.004-in., the initial stiffness can be derived as:

$$K_{br} = 120\ t_p\ F_y\ d_b \qquad \text{(Eq 28)}$$

The assumed bearing deformation of 0.004-in. was based on comparisons between the resulting value of K_{br} and the results of the finite element models. Additional comparisons to finite element results showed that the relation between bolt diameter and initial stiffness was not linear as indicated in Equation 28; consequently, one modification was made to provide better correlation between the prediction method and the finite element results. The final relationship is given by:

$$K_{br} = 120\ t_p\ F_y\ d_b^{0.8} \qquad \text{(Eq 29)}$$

4.3.3.2 Bending and Shearing Stiffness

The bending and shearing stiffness are derived based on the assumption that the steel between the bolt and the end of the plate can be modeled as a rectangular elastic fixed end beam with length d_b and height $L_e - d_b/2$ as shown in Figure 27. This results in:

$$K_b = 32\ E\ t_p\ (L_e/d_b - 1/2)^3 \qquad \text{(Eq 30)}$$

$$K_v = 6.67\ G\ t_p\ (L_e/d_b - 1/2) \qquad \text{(Eq 31)}$$

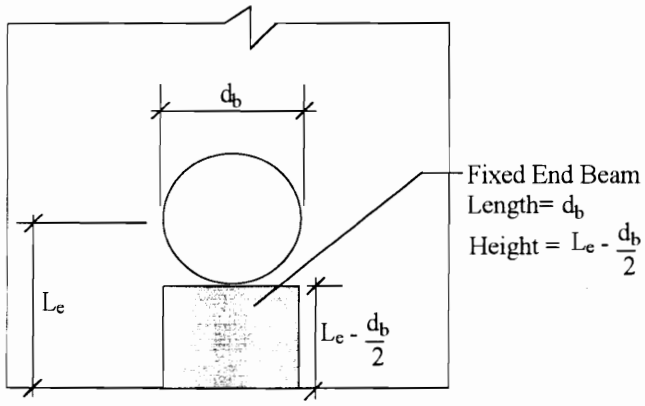

Figure 27 Bending And Shear Stiffness Model

4.3.4 Evaluation of Existing and Proposed Models

The proposed initial stiffness model (Equation 27) as well as the existing models given by EC3 Annex J (1994) and Tate and Rosenfeld (1946) were evaluated against the experimental and finite element data. The average and COV of the ratio of test and finite element initial stiffness values over the predicted values are presented in Table 16. Based on this evaluation the proposed model has the best correlation with the finite element and test data and is recommended. The reason that the predicted stiffness compared less favorably with the experimental results than with the finite element results is because the experimental results were, on average, not as stiff as the finite element results. The reason for this difference is believed to be the difficulty in measuring the initial stiffness experimentally.

Table 16 Evaluation of K_i Models, Test or Finite Element Over Predicted

Model:	Proposed	EC3 Annex J	Tate and Rosenfeld
Experimental Results			
Average	0.88	1.15	0.17
COV	23%	24%	30%
Finite Element Results			
Average	1.02	1.48	0.17
COV	5%	16%	14%

4.4 Plate Strength

Existing plate strength predictive equations were evaluated against data from two independent experimental investigations of single plates bearing on single bolts. Based on this evaluation it was determined that the plate strength equation found in the AISC Specification (*Load and*, 1993) provided the best correlation with the experimental results. In addition, an analysis of the effect of plate edge condition will show that shearing plates rather than saw cutting plates has a negative effect on the plate strength.

4.4.1 Experimental Data

There were two sources of experimental strength data. First, the data from the tests conducted at VT (discussed earlier in this chapter) was included. Of these tests, only the 20 tests that failed by bearing , tearout, or splitting were used.

Second, data from 52 tests on single plates bearing against single bolts conducted at Oklahoma State University (Lewis, 1994) were included. Variables considered in this test program included the clear distance (L_c) which was varied from 0.125 to 2.75-in., the plate thickness which varied from 0.25 to 0.75-in., and the bolt diameter which varied from 0.625 to 1-in. The plates were all 4-in. wide with standard holes and were fabricated from A36 steel. The clear distance is the distance from the front edge of the bolt hole to the free edge of the test plate.

4.4.2 Existing Plate Strength Models

All existing plate strength models treat bearing and tearout modes as one limit state. When the bolt is close to the end of the plate a tearout failure will occur. When the bolt is far away from the end of the plate, tearout only occurs after excessive bearing deformations (bearing failure) so an upper limit representing bearing failure is applied to each model.

The most common strength model for predicting tearout failure was developed by Fisher and Struik (1974). They used a simple plate shearing model to develop an equation for predicting the tearout strength of plates.

$$F_b = \frac{R_n}{d_b t_p} = 1.4\, F_u \left(\frac{L_e}{d_b} - \frac{1}{2} \right) \leq 3.0\, F_u \qquad \text{(Eq 32)}$$

The upper limit of $3.0\, F_u$ is an upper limit on the tearout strength representing a transition from tearout failure to bearing failure.

In addition to Equation 32, Fisher and Struik (1974) also recommended a simpler expression that was adopted by the AISC Specification (*Load and,* 1993). The specification states that for a single bolt in the line of force the bearing/tearout strength is given as

$$F_b = F_u \frac{L_e}{d_b} \leq 2.4\, F_u \qquad \text{(Eq 33)}$$

The reduced upper limit was adopted to limit bearing deformations as suggested by Perry (1981); however, the specification does state that an upper limit of $3.0\, F_u$ can be used instead for situations where excessive bolt hole deformation is not a concern.

Recently, there has been a proposed change in the RCSC Specification for Structural Joints Using ASTM A325 or A490 Bolts (Minutes, 1994). The proposed equation is based on a physical model similar to that used by Fisher and Struik (1974) and is given as

$$F_b = 1.2 F_u \frac{L_c}{d_b} \leq 2.4\, F_u \qquad \text{(Eq 34)}$$

Where L_c is the minimum distance from the edge of the bolt hole to the edge of the plate.

EC3 (1993) has a slightly different expression for the tearout strength. If it is assumed that the bolt steel tensile strength is greater than the plate steel tensile strength the expression given in EC3 (1993) can be rewritten as:

$$F_b = \frac{2.5}{3} F_u \frac{L_e}{d_h} \leq 2.5\, F_u \qquad \text{(Eq 35)}$$

Where d_h is the hole diameter.

4.4.3 Evaluation of Existing Models

Statistical and graphical comparisons of the strength models is presented in Table 17 and Figure 28, respectively. The values given in Table 17 are the ratio of test over the predicted. For the graphical comparison to be made two assumptions were needed. First, so that the newly proposed model could be plotted, an average d_b was assumed as 0.87-in.. This model is fairly insensitive to small changes in this value so using the average value seems justifiable. Second, so that the EC 3 model could be plotted an average value of L_e/d_b vs. L_e/d_h was determined as 0.93. Again, small variations in this ratio have little effect on the graphical results so using the average seems justifiable. Based on the statistical and graphical comparisons of the strength models it is clear that the plate strength equation found in the AISC Specification (*Load and*, 1993) provided the best correlation with the experimental results and is consequently recommended. The model recently proposed for the RCSC Specification (Minutes, 1994) is clearly over conservative compared to the test strengths for a single bolt in the line of force. However, it should be noted that the reason a new model is being considered is to try to improve strength predictions for two or more bolts in the line of force.

Table 17 Ratio of Test Strength To Predicted Strength

Model:	AISC (1993)	Fisher and Struik	RCSC Proposed	EC 3
Average	.998	1.155	1.446	1.227
COV	10%	25%	30%	12%

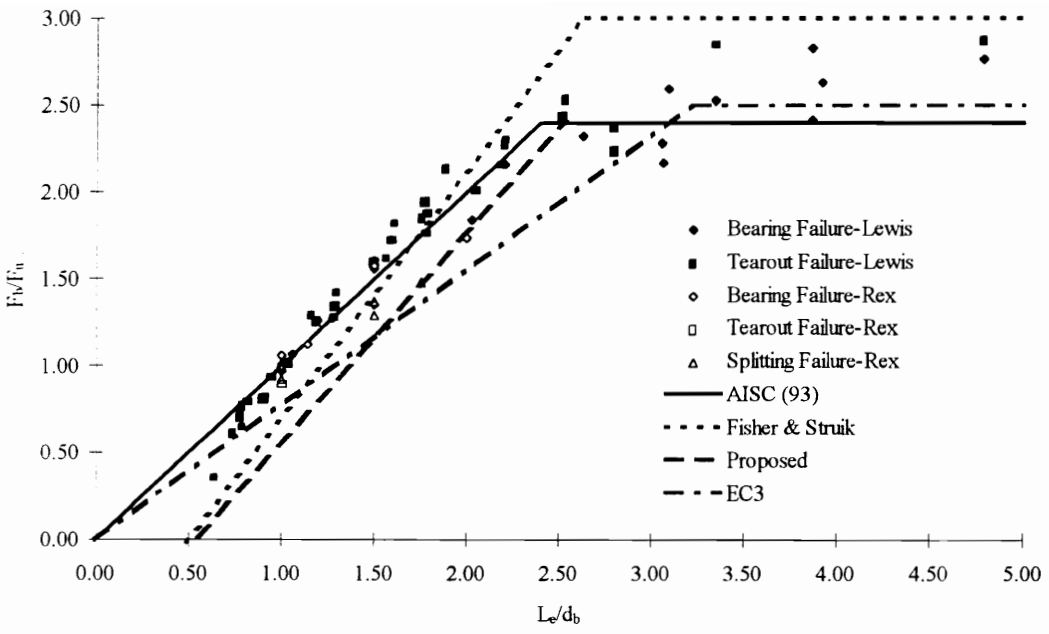

Figure 28 Normalized Bearing Stress Vs. Normalized End Distance

4.4.4 Effect of Edge Condition

The steel between the bolt hole and the cut edge of the plate acts very much like a short deep beam. The bottom of this beam is the cut edge of the plate; and, in a typical loading configuration, this edge is in high tension as a result of bending stresses. The small flaws along the cut edge of the plate tend to become stress risers. The increased stress at the tips of these flaws causes them to enlarge and eventually develop into a split in the steel that propagates toward the bolt hole.

Shearing plates rather than sawing plates tends to increase the size and number of flaws along the edge of the plate. The effect, of shearing rather than sawing, on the plate strength is not currently understood or considered in the currently available strength models.

Review of the results from the tests conducted at VT indicated three possible effects. First, the plate strength of a sheared plate is less than the plate strength of a saw cut plate; however, the reduction tends to depend on the steel strength and the end

distance. Second, sheared plates tend to fail by splitting rather than tearout. Third, the deformation when the maximum load is reached in sheared plates is reduced compared to saw cut plates. These observations are based on only a few tests and cannot be considered conclusive at this time.

4.5 Normalized Load-Deformation Behavior

A normalized load-deformation behavior for bearing was believed to be the simplest way to represent the behavior. To develop the normalized behavior, the data from each test conducted at VT which failed by bearing, tearout, or splitting was normalized by the maximum load for the test. Based on this normalized data, a method of normalizing the test deformations was then developed. After the load and deformation values were normalized, non-linear regression was used to fit the Richard Equation (Richard and Elsalti, 1991) to the data. The resulting relationship is given by:

$$\frac{R}{R_n} = \frac{1.74\,\bar{\Delta}}{\left(1 + \bar{\Delta}^{0.5}\right)^2} - 0.009\,\bar{\Delta} \qquad \text{(Eq 36)}$$

Where

R = Plate load

R_n = Plate Strength

$\bar{\Delta}$ = Normalized deformation = $\Delta\ \beta\ K_i/R_n$

Δ = Hole elongation

β = Steel correction factor = 30% / %Elongation (for typical steels taken as 1)

K_i = Initial stiffness

4.6 Summary, Conclusions, Recommendations

4.6.1 Summary

The objective of the study presented in this chapter was to develop a model for approximating the load-deformation behavior associated with plate bearing. The following steps were taken to achieve this objective:

1. An experimental investigation of a single plate bearing on a single bolt was conducted.
2. A model for estimating the initial stiffness of the load-deformation behavior was developed.
3. An existing model for predicting the plate strength was verified.
4. Using the results from steps 2 and 3, the data from step 1 was normalized and a normalized load-deformation behavior was determined using the Richard Equation.

The final form of the model for predicting the load-deformation behavior associated with plate bearing is given as:

$$\frac{R}{R_n} = \frac{1.74\,\bar{\Delta}}{\left(1 + \bar{\Delta}^{0.5}\right)^2} - 0.009\,\bar{\Delta}$$

Where

R = Plate load

R_n = Plate strength = $L_e\, t_p\, F_u \le 2.4\, d_b\, t_p\, F_u$ (*Load and,* 1993)

$\bar{\Delta}$ = Normalized deformation = $\Delta\, \beta\, K_i / R_n$

Δ = Hole elongation

β = Steel correction factor = 30% / %Elongation (for typical steels, such as A36 or A572Gr50, β is taken as 1)

K_i = Initial stiffness given by

$$K_i = \frac{1}{\frac{1}{K_{br}} + \frac{1}{K_b} + \frac{1}{K_v}}$$

Where

K_{br} = Bearing stiffness = $120\ F_y\ t_p\ d_b^{0.8}$ (units are kips and inches)

K_b = Bending stiffness = $32\ E\ t_p\ (L_e/d_b - 0.5)^3$

K_v = Shearing stiffness = $6.67\ G\ t_p\ (L_e/d_b - 0.5)$

4.6.2 Conclusions

Experimental strength values for a single plate bearing on a single bolt from two independent testing programs were compared to four existing strength models. Based on this comparison, it was concluded that the model given in the AISC Specification (*Load and,* 1993) best represents the experimental strength values.

Although not conclusive at this time, shearing rather than sawing plates does appear to have a negative effect on the nominal strength. This effect seems to be influenced by end distance and steel strength. Existing models do not account for this effect nor do they account for splitting failure strengths.

4.6.3 Recommendations

- Strength models for curling and splitting failure modes are currently not available. Curling failures are not generally seen in typical connections. Consequently, there is probably little need for a strength equation for curling failure. Splitting failures are seen in typical connections and more work needs done to develop a better understanding and a strength model for splitting failures. The effect of shearing plates rather than saw cutting plates should also be considered with respect to the splitting failures.
- The load-deformation behavior of a single plate bearing against a single bolt for a wider range of parameters should be investigated. An improved test setup needs to be developed that allow thicker plates and smaller bolt diameters to be tested to failure. In addition, bolt hole types other than standard holes should be considered.

- The larger goal of this research is to determine the load-deformation behavior of bolts in full steel connections. Ideally, there would be a direct relationship between plate width and bolt spacing in the connection. A series of simple tests could be devised to determine if there is a direct relationship between these two parameters.

5. Behavior and Modeling of Single Bolt Lap Plate Connections

This chapter summarizes the report by Rex and Easterling (1996(d)) on the behavior and modeling of single bolt lap plate connections.

5.1 Introduction

5.1.1 General

The primary hypothesis of this dissertation is that a PR beam-girder connection can be modeled as a combination of connection components. A high strength bolt in single shear is one of these components; consequently, a behavior model for this component is needed. To develop this behavior model, it has been assumed that the load-deformation behavior of the bolt in the PR connection is very similar to the load-deformation behavior of the bolt in a single bolt lap plate connection. This assumption is shown to be valid, with a couple of exceptions, in Chapter 6. Consequently, a study of the load-deformation behavior of single bolt lap plate connections is presented and a method of approximating the behavior is developed in this chapter.

The hypothesis of this study is that the load-deformation behavior of the high strength bolt in a single bolt lap plate connection can be modeled as a combination of three, more fundamental, load-deformation behaviors: friction, plate bearing, and bolt. This is consistent with the hypothesis of modeling the overall connection. Based on this hypothesis, it is assumed that if each of the more fundamental load-deformation behaviors can be approximated then the overall load-deformation behavior of the high strength bolt in a single bolt lap plate connection can be approximated by combining the more fundamental behaviors is series and parallel as shown in Figure 29.

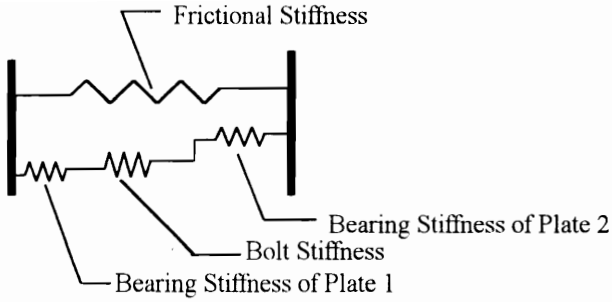

Figure 29 Component Model of High Strength Bolt in Single Shear

5.1.2 Objectives And Methods

The objective of the study presented in this chapter is to develop two models for approximating the load-deformation behavior of a high strength bolt in a single bolt lap plate connection: a component model and a parametric model. This objective is achieved by:

1. Collecting all readily available data on single bolt lap plate connection tests,
2. Evaluating existing plate and bolt strength prediction models,
3. Developing a method of approximating the load-deformation behavior of the bolt isolated from the plate and friction behaviors,
4. Developing a method of approximating the frictional behavior isolated from the plate and bolt behaviors,
5. Developing component model limits so that it can be used to predict the deformation when a single bolt lap plate connection fails,
6. Developing parametric equations to describe the full load-deformation behavior of a fully tensioned high strength bolt in a single bolt lap plate connection,
7. Evaluating models for predicting the full load-deformation behavior of a high strength bolt in a single bolt lap plate connection,

First, data from four independent test programs that studied single bolt lap plate connections is collected. This data is analyzed and modified as needed to provide a

consistent data base of experimental results for development and verification of subsequent work.

Second, existing models for predicting the plate and bolt strengths are evaluated against the experimental results. Based on this evaluation, recommendations are made about the most appropriate models.

Third, the load-deformation behavior of the bolt isolated from the plate and friction behaviors is needed for the component model of the lap plate connection. A method of approximating this behavior is developed from a combination of the experimental data and other literature. This same process is repeated to develop a method approximating the friction behavior isolated from the plate and bolt behavior.

Fifth, the component model is modified so that it can be used to predict the deformation at failure of the lap plate connection. An evaluation of these predictions against the test data is then made.

Sixth, because the component method is generally complex and computationally intensive, a simpler method of approximating the load-deformation behavior is needed. For this purpose, a parametric model is developed to approximate the load-deformation behavior of a fully tensioned high strength bolt.

Seventh, to determine how well the methods developed in this chapter (component and parametric) and existing methods approximate the load-deformation behavior of the lap plate connections, a general evaluation is made of each method against the experimental data.

5.2 Experimental Data For Single Bolt Lap Plate Connections

Four experimental investigations of single bolt lap plate connection tests were found in the literature. The experimental data, including the geometric and material parameters and the raw load-deformation data from these experimental investigations, was compiled and input into a commercial database program for analysis.

A schematic of a single bolt lap plate connection test is shown in Figure 30. The method in which the load was applied to the plates and the method in which deformation was measured varied depending on the experimental investigator. Generally, the free ends of the connection were bolted to a testing assembly that was placed in a universal type testing machine to apply the load. The deformation was measured as the change in the distance from a fixed point on one plate to a fixed point on the opposite plate.

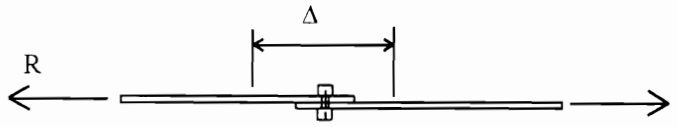

Figure 30 Typical Single Bolt Lap Plate Connection Tests

The following sections present a brief summary of each of the four experimental investigations. In some cases it was necessary to make assumptions about and adjustments to the data so that the tests could be included in the analysis. The assumptions and adjustments made are also discussed briefly in the following sections.

5.2.1 Lap Plate Connection Tests Reported by Karsu (1995)

Karsu (1995) reported a total of 61 lap plate connection tests. Each test actually consisted of two lap plate connections that were pulled at the same time. The average load and deformation measurements for the two connections were used.

Parameters which were varied in the experimental study included bolt diameter, plate thickness of both plates in the connection, bolt end distance, and plate edge condition. Washers were placed under both the nut and bolt head. Electronic potentiometers were used to measure the deformation.

The test specimens were assembled and put into a testing rig. The bolts were snugged up and then a pre-load was applied to the specimen. While the pre-load was applied the bolts were fully tensioned by turn-of-nut. The pre-load was then removed and the test was started from zero load. This process was intended to eliminate any sudden slips in the connection during the test.

The deformations of interest in this research are the local bolt and plate deformations and not the overall elastic plate deformations between points of measurement. The data reported by Karsu (1995) included elastic deformations. Consequently, a method of estimating these deformations was developed and they were removed from the data.

5.2.2 Lap Plate Connection Tests Reported by Gillet (1978)

Gillet (1978) reported a total of 75 lap plate connection tests. Load-deformation data was available for only 66 of these tests. Parameters varied in the experimental study included bolt grade and diameter, steel grade, plate thickness, and end distance.

The test plates were fabricated by a local steel fabricator. The plates were sheared and the bolt holes were punched to standard sizes. Two dial gages were used to measure deformations, one in front and one in back of the specimen.

The test specimens were assembled and put into the testing rig. The bolts were snugged up and then a pre-load of 5 kips was applied to the specimen. While the pre-load was applied the bolts were fully tensioned by turn-of-nut. The pre-load was then removed and the test was started from zero load. This process eliminated any sudden slips in the connection during the test.

Three assumptions about this testing program have been made so that the tests could be included in the analysis. First, no material properties were given for the 5/8-in. thick plates used in the test program. It was assumed that the steel properties of these plates were consistent with other A36 steel properties given in the report and the average of the A36 steel properties given was used.

Second, in some cases the mode of failure was not clear. The mode of failure for a group of tests was reported rather than for the individual tests. In some cases, two modes of failure were indicated for the same group of tests. In these cases, a failure mode was assumed based on the options given for the group and a comparison of the load-deformation behaviors for the tests in the group.

Lastly, it was assumed that the bolt threads were excluded from the shearing plane. This was based on a comparison of the expected bolt shearing load to the test load reported.

5.2.3 Lap Plate Connection Tests Reported by Caccavale (1975)

Caccavale (1975) reported 11 lap plate connection tests. The plate thickness was the only parameter varied; and, washers were placed under the nuts of the bolts.

The author did not specifically report failure modes of specimens. However, the author does indicate that "The test results show that under these conditions no visible mark of shear deformation occur in the bolt." This would tend to indicate some sort of plate failure. For analysis purposes it was assumed that plate bearing/tearout failures occurred.

Because of the way that deformations were measured in these tests, it is highly likely that the initial deformation readings included test setup deformations which were not intended to be measured. Because of this measurement problem, only the strength characteristics from this data is included in subsequent development and verification work.

5.2.4 Lap Plate Connection Tests Reported by Sarkar and Wallace (1992)

Sarkar and Wallace (1992) reported 16 lap plate connection tests. Parameters that were varied included the bolt type, plate thickness and end distance.

The report did not indicate how the bolts had been tightened. Based on a comparison to the test data from Karsu (1995) and Gillet (1978) it is believed that the bolts were only tightened to the snug condition and the tests are treated as such for analysis purposes in this report.

5.3 Plate and Bolt Strength Predictive Models

There were primarily five failure modes associated with the single bolt lap plate connections: bearing, tearout, splitting, plate buckling, bolt shear. The first four of these failure modes are associated with the plate and were described in Section 4.2.5.1. The last failure mode is associated with the bolt. Methods of predicting the plate strength and bolt strength are presented and evaluated in the following sections. Experimental strength values from the tests given by Karsu (1995), Gillet (1978), Caccavale (1975), and Sarkar and Wallace (1992) were used to evaluate the plate and bolt strength predicting methods.

5.3.1 Plate Strength

A discussion of plate failure modes and an evaluation of existing models for predicting plate strength were presented in Chapter 4. It was shown that plate failure modes included bearing, tearout, splitting, and plate buckling. It was also shown that for the first three of these failure modes the strength prediction based on the AISC Specification (*Load and*, 1993) provided the best correlation with single bolt-single plate test strengths. Consequently, this is the only model that will be evaluated in the next section.

A comparison of test load to predicted load is presented in Table 18. The test load is defined as the load when the specimen failed or when the test was stopped. The predicted load is based on the AISC Specification (*Load and*, 1993). Only tests that failed by bearing, tearout, or splitting were considered.

Table 18 Plate Strength To Predicted Strength

	Average	COV	No.
All Plate Failures			
All Researchers	1.02	12.0%	85
Gillet	0.97	14.0%	36
Karsu	1.07	7.8%	36
Caccavale	1.07	8.9%	11
Sarkar and Wallace	0.88	5.1%	2
Bearing / Tearout Failures			
All Researchers	1.06	10.0%	43
Gillet	0.98	12.1%	10
Karsu	1.09	8.3%	22
Caccavale	1.07	8.9%	11
Sarkar and Wallace	-	-	-
Splitting Failures			
All Researchers	0.99	13.1%	42
Gillet	0.96	14.8%	26
Karsu	1.06	6.9%	14
Caccavale	-	-	-
Sarkar and Wallace	0.88	5.1%	2

The following observations are made based on review of Table 18.

- Bearing/Tearout failures had mean strengths about 7% higher than splitting failures. This is partly attributable to the very low test strengths reported by Sarkar and Wallace (1992).
- Evaluation of bearing/tearout failures shows the predicted strength is about 6% conservative. A comparison of the specification equation to bearing/tearout strength for single bolt single plate specimens in Chapter 4 showed an average ratio of 0.998. This may be an indication of a slight increase in plate strength associated with the single bolt lap plate connections compared to the single plate single bolt type specimens. One possible reason for the increased strength is the confinement of the steel in front of the bolt provided by the bolt nut and head and washers if present. Another reason may be that some load was being carried by friction between the two plates which leads to calculated bearing stresses higher than the real bearing stresses (Fisher and Struik, 1974). However, it should be noted that the upper limit on the bearing stress was shown by Perry (1981) to be unaffected by bolt tension.

- Considering all the researcher's data, there is good correlation between the test load and the predicted load.
- Most of the variation results from the tests conducted by Gillet (1978).
- Splitting failures are physically very different than tearout failures. The current expression given in the AISC Specification (*Load and*, 1993) is based on the physical behavior associated with tearout. Despite this, the expression appears to correlate very well with the test strengths associated with splitting failures as well.

The only general conclusion that can be made based on this evaluation is that the current expression given in the AISC Specification (*Load and*, 1993) for determining tearout strength correlates well with all the test data considered.

5.3.2 Bolt Strength

There are basically five bolt shear strength models that have been recommended over the last 25 years. These models were primarily developed from bolt shear tests where the bolt was in double shear. The basic differences in these models lie in the value of the ultimate shearing stress and the value of the root area in the threaded portion of the bolt. These models are summarized in Table 19 along with statistical results from a comparison of test to predicted strength. There were a total of 71 single bolt lap plate tests that failed by bolt shear.

Table 19 Evaluation of Bolt Shear Strength Models

Model	F_{vb}/F_{ub}	A_{bv}/A_b	Average Test/Predict	COV
Fisher and Struik (1974)	0.62	0.75	1.05	12%
Fisher et al (1978)	0.75 / 0.67*	**	0.89	12%
AISC (1986)	0.60	0.75	1.09	12%
Kulak et al (1987)	0.62	0.70	1.07	14%
AISC (1993)	0.50	0.80	1.28	11%

* A325 / A490 Bolts

** Was not stated. Assumed to be 0.70 for evaluation purposes.

Considering the ratio of test strength-to predicted strength, all the models except Fisher et al (1978) were conservative. The latest edition of the AISC Specification (LRFD 1993) is overly conservative because the new model assumes long joint behavior which is generally less efficient than a single bolt joint. Overall the model suggested by Fisher and Struik (1974) compared the best; but, predictions using the AISC Specification (*Load and*, 1986) are also satisfactory. The coefficient of variation for all the models except perhaps that recommended by Kulak et al (1987) are in line with the expected coefficient of variation of 10% (Fisher et al, 1978).

Based on the above comparison, it appears that the average shearing strength of the bolts in the single bolt lap connections is slightly higher than would be expected based on equations developed from double shear bolt tests. One possible reason for this is an inclined shearing angle. A visual inspection of the bolts that sheared in the tests reported by Karsu (1995) showed that the shearing angle was inclined, similar to the tests reported by Munse et al (1954). A second possible reason for the increased load may be frictional forces between the plates resulting from tension in the bolt. The bolt tension could be a result of the original pre-tensioning or the result of prying forces developed by the deforming plates or some combination of these two.

Without additional testing and analysis, trying to include either of these possible effects to increase the bolt load capacity does not seem justifiable at this time. In general, it is believed that the model given in AISC Specification (*Load and*, 1986) is sufficiently accurate and precise for purposes of the current research.

5.4 High Strength Bolt Load-Deformation Behavior

A method for approximating the load-deformation behavior of the bolt isolated from the plate and friction behavior is developed in the following sections.

5.4.1 Characterization of Load-Deformation Behavior

Wallaert and Fisher (1965) conducted 174 elemental bolt shear tests. Single bolts were tested in double shear. Fisher (1965) developed the following expression to represent the load-deformation behavior of the bolt shear tests conducted by Wallaert and Fisher (1965):

$$R = R_{ult} [1-e^{-\mu\Delta}]^{\lambda} \quad \text{(Eq 37)}$$

The equation parameters R_{ult}, μ, and λ were determined for a number of the bolt shear tests and these values were reported in Fisher (1965). The author recognized that R_{ult} corresponded well with the bolt shearing strength. The author also recognized that the parameter μ was primarily influenced by the type of connected material and that λ was basically unaffected by the type of connected material. It is believed that Equation 37 can sufficiently approximate isolated bolt load-deformation behavior. The specific values of λ and μ are developed in the following section.

5.4.2 Equation Parameters

Some of the tests by Wallaert and Fisher (1965) had bolts that were only tightened to the snug condition. The load-deformation behavior of these tests should be primarily comprised of the bolt and plate behaviors (i.e. little if any influence by friction). Using the curve parameters reported by Fisher (1965) the load vs. deformation for one of the tests with a snug tight bolt was plotted. Next, using the plate component behavior model, developed in Chapter 4, the load-deformation behavior of the plates were determined. For each load the estimated plate deformations were subtracted from the test deformations (assumed given by the curve parameters). The remaining load-deformation behavior was then assumed to be that associated with the bolt alone. Based on a non-linear regression analysis of this load-deformation behavior, it was determined that a value of μ of approximately 34 and a value of λ of 1.0 seemed appropriate.

When λ has a value of 1.0 it can be shown that μ is a scaling factor for the initial stiffness of the load-deformation response (i.e. the initial stiffness is μ times the bolt strength R_{ult}). EC3 Annex J (1994) gives an estimate for initial bolt stiffness for a snug tight bolt in single shear. The exact expression given in EC3 Annex J (1994) can be rearranged in terms of bolt shear strength. When this is done the scaling factor for the initial stiffness is given as 52.2.

Based on the analysis of the test reported by Fisher (1965) and the initial stiffness given by EC3 Annex J (1994), it appears that a value of μ somewhere between 34 and 52.2 and a value of λ of 1.0 seems justifiable. To determine the most appropriate value of μ, the single bolt lap plate connection tests with snug tight bolts were evaluated.

The final value of μ was determined by calibrating the predicted load-deformation behavior for single bolt lap plate connections against the test data reported by Sarkar and Wallace (1992). The load-deformation response for each of these tests was simulated using the plate-bolt-plate springs in series. The plate spring behaviors were approximated using the plate behavior model developed in Chapter 4 and the bolt spring behavior was approximated using Equation 37 with R_{ult} equal to the test strength and λ equal to 1.0. The best value of μ was then determined through visual and numerical analysis. Based on this analysis, a final value of μ equal to 50 seemed most appropriate and agrees well with the value derived from EC3 Annex J (1994).

5.4.3 Failure Deformation

The last step in characterizing the bolt component behavior was to determine the deformation in the bolt at failure. First, the failure deformations of the test specimens reported by Wallaert and Fisher (1965) with A514 steel plates were considered. It was assumed that the majority of the deformation at failure in these specimens was deformation in the bolt and not in the plate (because of the extremely high plate strength). Based on the results of these tests, the bolt deformation at failure was found to be approximately 1/8-in. Measurements were made on sheared bolts from the tests

conducted by Karsu (1995). These measurements confirmed, that for A325 bolts, a bolt deformation of about 1/8-in. at failure is a reasonable value.

5.4.4 Conclusion

It is recognized that the load-deformation behavior of the bolt is most likely dependent on many parameters which are not included in the above study. However, for the scope of the current research the suggested simple representation of this behavior is believed satisfactory.

5.5 Frictional Behavior

A method for approximating the frictional behavior isolated from the plate and bolt behavior is developed in the following sections.

5.5.1 Characteristics of Behavior

Frank and Yura (1981) conducted 77 elemental slip tests using steel plates with blasted surfaces and single bolts in double shear. A special test setup that insured the only resistance to load was the frictional resistance between the plates was used. A typical load-deformation response has been reproduced from Frank and Yura (1981) and is presented in Figure 31.

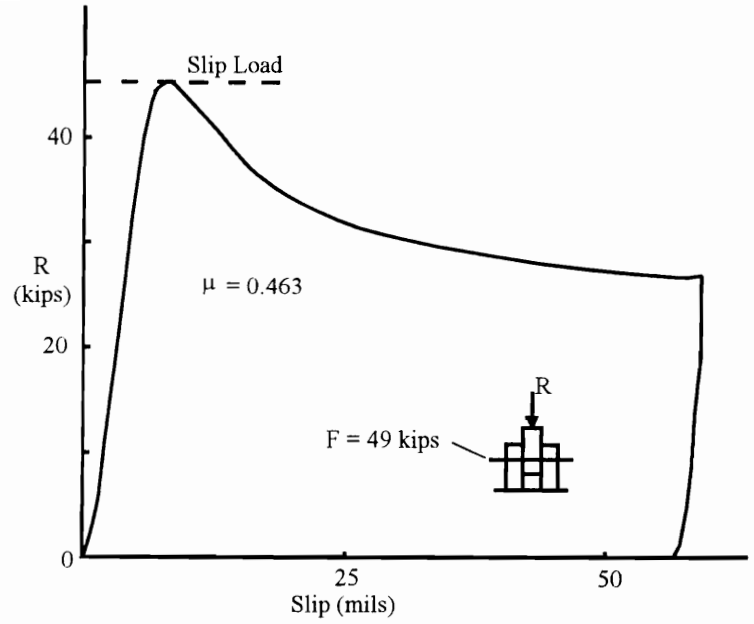

Figure 31 Frictional Load-Slip Behavior Reported by Frank and Yura (1981)

There are two important observations based on the test behavior presented in Figure 31. First, the test specimen exhibited a linear behavior up to very near the slipping load. Second, after the slipping load was reached the load resistance degraded with increased slip. Based on these observations it appears that there are three characteristic behaviors associated with the load-slip response: initial stiffness, slip load, and post slip behavior. The only literature found at this time deals with the slip load which is discussed in the following section.

5.5.2 Existing Methods For Predicting Slip Load

Fisher et al (1978) did a statistical study of the slip resistance associated with the use of high strength bolts. The results showed that the average slip resistance of a high strength bolt with a single shear plane in mild steels with clean mill scale surfaces and where the bolts had been tightened by turn-of-nut method is given by

$$R_n = \alpha A_{bt} F_{ub} \qquad \text{(Eq 38)}$$

Where α was 0.33 and 0.29 for A325 and A490 bolts respectively. The coefficient of variation was determined as 24% for both A325 and A490 bolts. A_{bt} is the tension area of a bolt usually taken as 75% of the gross area of the bolt "A_b".

The current AISC Specification (*Load and*, 1993) specifies that the minimum bolt tension should be 70% of the minimum tensile strength of the bolt. Based on this and some additional assumptions, which are not completely described, the slip load for A325 and A490 bolts in standard holes under service loads and for steel with clean mill scale surfaces is given as 17 A_b and 21 A_b, respectively. The constants, 17 and 21, have units of ksi. When designing for factored loads the constants for the slip load change to 23.5 and 29.4 for A325 and A490 bolts respectively.

5.5.3 Quantification Of Characteristic Behavior Based on Test Results

The frictional behavior for each of the single bolt lap plate tests with fully tensioned bolts reported by Karsu (1995) and Gillet (1978) was determined. This was done by approximating the plate-bolt-plate behavior with the plate model developed in Chapter 4 and the bolt model developed in the previous section. This approximate plate-bolt-plate behavior was subtracted from the test behavior. It is assumed that the remaining load-deformation behavior is the frictional behavior. An example of this behavior is shown in Figure 32.

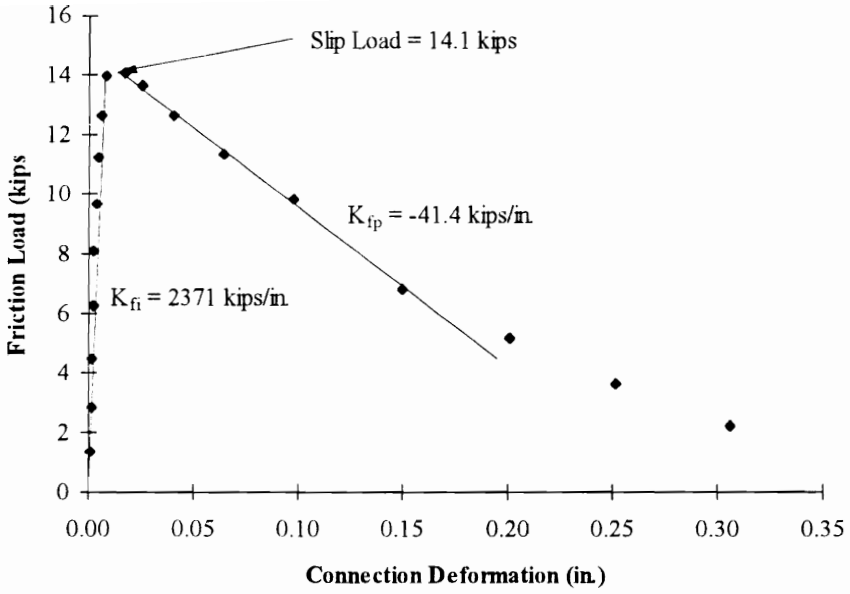

Figure 32 Experimental Friction Load-Deformation Behavior Test 4 Reported by Gillet (1978)

As can be seen in Figure 32 the basic shape of the load-deformation response is similar to that reported by Frank and Yura (1981). The only significant difference between the above isolated behavior and that reported by Frank and Yura (1981) is that the post slip load resistance continues to degrade until there is little or no frictional load transfer.

Based on the values of the initial stiffness (K_{fi}), the post stiffness (K_{fp}), and the slip load (R_f) determined from the test data, methods for approximating each of these quantities were developed. First, based on a combination of the AISC Specification (*Load and*, 1993) requirements for bolt tightening and the recommended coefficients for A325 vs. A490 bolts given by Fisher et al (1978), the following expression for the slip load was derived.

$$R_f = \alpha\ (0.7\ F_{ub})\ (0.75\ A_b)\ \mu \qquad \text{(Eq 39)}$$

Where

α = 1.0 for A325 bolts and 0.88 for A490 bolts

μ = Friction coefficient (0.33 for clean mill scale surfaces)

Next, the deformation when slip started to occur was determined to have an average value 0.0076-in. with a COV of 47% The initial frictional stiffness (K_{fi}) is determined by dividing R_f by 0.0076-in.

Finally, the post slip stiffness (K_{fp}) was related to the combined thickness of t_1 and t_2. This relationship is best represented by determining the deformation at which the frictional resistance could be assumed to be zero (Δ_{fu}).

$$\Delta_{fu} \begin{cases} (t_1 + t_2) < 0.5" & \Delta_{fu} = 0.4" \\ .0.5" \le (t_1 + t_2) \le 1.5" & \Delta_{fu} = 0.4" - (t_1 + t_2 - 0.5)\ 0.3 \\ 1.5" < (t_1 + t_2) & \Delta_{fu} = 0.1" \end{cases} \quad \text{(Eq 40)}$$

The post slip stiffness is then determined by dividing R_f by Δ_{fu}.

5.6 Deformation at Failure

To evaluate the ductility of lap plate connections (and eventually of beam-girder connections), it is important to be able to estimate the deformation at failure. First, the source of test data and how failure deformations were defined is discussed. Next, the component method for predicting the deformation at failure is developed and discussed. Finally, the component method is evaluated against the test data.

5.6.1 Data For Evaluation and Development of Models

The deformation at failure was determined for each set of test data reported by Karsu (1995), Gillet (1978), and Sarkar and Wallace (1992). The deformation at failure was defined as the test deformation just prior to a significant loss in load carrying capacity resulting from a plate or bolt failure.

When a bolt failure occurs the deformation at failure is easily defined. However, when plate failure occurs the deformation at failure is less easily defined because of the long plastic plateaus. In addition, many of the tests were stopped before any reduction in load carrying capacity was observed. These tests do not provide useful data for evaluating

the deformation at failure. Consequently, it is convenient to separate the tests into bolt failures and plate failures. When considering bolt failures, all of the failure deformations were used in the evaluation and development of models. When considering plate failures, only the tests with bearing/tearout or splitting failures were considered. Of these only the tests reported by Karsu (1995) were used. This is because all but two of the tests reported by Sarkar and Wallace (1992) failed by bolt shear and the tests reported by Gillet (1978) were typically stopped at a deformation limit of around 0.3-in. In many of the tests reported by Gillet (1978) it is believed that additional deformations could have been sustained without loss of load.

5.6.2 Component Model

Using the component model, the deformation at failure can be determined by combining the deformations of the plate-bolt-plate series. First, the plate or bolt that limits the strength of the series must be determined. The deformation for this component is then determined based on the assumed failure deformation for the plate or bolt. The remaining component deformations are determined using the plate and bolt component behaviors developed previously.

The failure deformation for bolts was previously determined to be 1/8-in (Section 5.4.3). The plate failure deformation has never been determined. Based on the normalized plate load-deformation behavior developed in Chapter 4, it was possible to determine the plate deformation associated with the maximum plate load. In normalized form, this deformation is given as

$$\overline{\Delta}_f = 22.87 \qquad \text{(Eq 41)}$$

It is assumed that this deformation is a reasonable estimate of the plate deformation at failure.

5.6.3 Evaluation of Component Model Failure Deformation Predictions

Failure deformations for tests failing by plate bearing/tearout or splitting and reported by Karsu (1995) were calculated using the component model. The average test to predicted ratio for the component model was 1.23 with a coefficient of variation of 23%. Failure deformations for tests failing by bolt shear and reported by Karsu (1995), Gillet (1978), and by Sarkar and Wallace (1992) were calculated using the component model. The average test to predicted ratio for the component model was 1.06 with a coefficient of variation of 47%.

5.7 Parametric Model of Lap Plate Load-Deformation Behavior

The component model is ideally applicable to a broad spectrum of parameter values and is not, in general, restricted to the range of parameters for which there are tests. However, this flexibility comes at the price of increased complexity; and, a computer program would be needed to readily implement the model.

Parametric equations are typically easy to use but are limited to the range of parameters tested. However, given the large number of tests collected in this report and the wide range and number of parameters included in the tests, the development of parametric equations seems like a reasonable way of providing a second method by which the load-deformation behavior can be approximated. Because the majority of the test data collected was for tests with fully tensioned bolts, parameter equations are only developed for connections with fully tensioned bolts.

The simplest method of representing the non-linear load-deformation behavior of the single bolt lap plate connections is with a continuous non-linear parametric equation. Thus the Richard Equation was chosen. To determine relationships between the connection parameters and the equation parameters, a detailed graphical and numerical study of the test data was conducted. Based on this study the following relationships were determined (note: all units are in kips and inches):

$$R_n = R_{np} \leq R_{nb} \qquad \text{(Eq 42)}$$

$$K = 5751\ t_1 d_b + 1213 \quad \text{(Eq 43)}$$

$$K_p = 9\ \{\ R_{np} / R_{nb}\ \}^{2.9} \quad \text{(Eq 44)}$$

$$R_{transition} = 0.14\ F_{ub}\ d_b^2 + 12 t_1/d_b \le R_n \quad \text{(Eq 45)}$$

$$R_o = R_n - 0.25\ K_p \ge R_{transition} \quad \text{(Eq 46)}$$

$$R_1 = R_{transition}(t_2/t_1)^{0.1} \le 0.98\ R_o \quad \text{(Eq 47)}$$

$$n = \frac{-\ln(2)}{\ln\left(\frac{R_1}{R_o} - \frac{K_p}{K - K_p}\right)} \le 3 \quad \text{(Eq 48)}$$

R_{np} and R_{nb} are the plate and bolt strengths respectively. In the above equations, upper and lower bounds have been placed on some of the load constants to avoid having predicted loads above the nominal strength of the connection (i.e. the increased strength over the plate strength resulting from friction, which was seen for thin plate combinations, is ignored). In addition, only positive plastic slopes are assumed.

5.8 Evaluation of Load-Deformation Models

In the previous sections of this chapter a component model and a parametric model of single bolt lap plate connection load-deformation behavior were developed. In this section previously existing models for predicting the load-deformation behavior are presented. This is followed by a numerical evaluation of the accuracy and precision with which each model is able to predict the experimental load-deformation results.

5.8.1 Existing Models

A model for the load-deformation behavior of high strength bolts is given in AISC Manual Vol. II (*Manual of* 1993). This model is used for determining the strength of eccentric loaded bolted connections and is given by:

$$R = R_{ult}\left(1 - e^{-\mu\Delta}\right)^{\lambda} \quad \text{(Eq 49)}$$

Where:

$\mu = 10$

$\lambda = 0.55$

R_{ult} = Bolt strength

e = Base of natural logarithm

The equation was developed by Fisher (1965) and will be referred to as the Fisher Equation from here on. The values of the coefficients were determined by Crawford and Kulak (1971) based six identical elemental bolt tests.

Karsu (1995) recommended a model that uses the four different sets of Richard Equation coefficients. The coefficients to be used depended on the plate thickness of the thinner plate in the connection (t_1) and/or whether bolt or plate failure occurred. The recommended coefficients are summarized in Table 20. These coefficients are based on data that was normalized by the test strength; consequently, it is necessary to multiply the resulting value from the Richard Equation by the plate or bolt strength to obtain the estimated load.

Table 20 Normalized Richard Equation Coefficients (Karsu, 1995)

Failure & Plate Thickness	K	K_p	R_o	n
Plate Failure				
t_1 = 0.125-in.	25.42	-0.226	1.234	1.56
t_1 = 0.25-in.	20.34	-0.0286	1.07	1.11
t_1 = 0.375-in.	20.14	0.0368	1.02	1.11
Bolt Failure	26.3	0.061	1.13	0.66

5.8.2 Benchmarks For Evaluation of Models

In the following section, each of the methods for approximating the load-deformation behavior of single bolt lap plate connections are evaluated against the test data. Values for the coefficient of variation and the L_2 Norm are determined for each method. Without having something to compare these numbers, to it is difficult to determine if the method is good or bad. Two different benchmark evaluations were

conducted to determine variations and norms by which the results of the subsequent evaluations are compared.

It is assumed that the best any method could come to approximating the load-deformation behavior is if that method were able to predict the coefficients for either the Richard Equation or Fisher Equation that would minimize the L_2 Norm for each group of identical tests. The first benchmark is based on this assumption. Non-linear regression was used to determine the best (minimize the L_2 Norm) equation coefficients for the Richard and Fisher Equations for each group of identical tests. Next, using these coefficients, the load at each test deformation was calculated. These loads were then compared to the test loads to determine values of the coefficient of variation (of test over predict) and the L_2 Norm. The first benchmark will be referred to as Benchmark Level 1.

The second benchmark considers the current inability to predict connection strength. The assumption is that if the basic shape of the load-deformation curve is correct but the calculated connection strength is wrong then the variation and norm values may be large despite the fact that the basic shape is being predicted very well. To determine what part of the variation and norm values is attributable to poor predictions of the connection strength, a second set of benchmark values were determined. These were determined by multiplying the original estimated loads (at each test deformation) by the ratio of predict over test strength. The new values were then evaluated to determine revised COV and L_2 Norm values. The second benchmark will be referred to as Benchmark Level 2.

5.8.3 Evaluation of Models

The component, parametric, and existing models for predicting the load-deformation behavior of a single bolt lap plate connection were evaluated against the experimental load-deformation data. For each experimental load-deformation point, the load was calculated using each of the different methods. The ratio of test load over predicted load was then determined. The average, COV, and L_2 Norm were then

determined and are presented in Table 21. Because of the way the benchmarks were determined, the models are grouped under Richard Equation methods or Fisher Equation methods with the exception of the component model which does not use a continuous non-linear analytical curve.

Table 21 Evaluation Of Load-Deformation Models (Ratio of Test over Predicted)

Method	Fully Tensioned Bolts			Snug Tight Bolts		
	Average	COV	L_2 Norm (kips)	Average	COV	L_2 Norm (kips)
Component Method	1.02	20%	140	0.92	25%	43
Richard Equation Methods						
Parametric	1.09	21%	167	-	-	-
Karsu Unified Curves	1.20	30%	231	-	-	-
Benchmark Level 1	0.99	11%	52	-	-	-
Benchmark Level 2	1.04	16%	160	-	-	-
Fisher Equation Methods						
AISC Vol II	1.67	41%	339	0.88	31%	63
Benchmark Level 1	0.96	23%	85	1.00	14%	13
Benchmark Level 2	0.99	31%	189	1.13	17%	40

In general, the component method does the best job of predicting the load-deformation behavior. The parametric relationships for the Richard equation provide good estimates with less complexity than the component method.

5.9 Summary, Conclusions, and Recommendations

5.9.1 Summary and Conclusions

The objective of the study presented in this chapter was to develop two models for approximating the load-deformation behavior of a high strength bolt in a single bolt lap plate connection: a component model and a parametric model.

First, data from four independent testing programs that studied single bolt lap plate connections was collected. Second, existing plate and bolt strength models were evaluated against the experimental data. Based on this evaluation it was shown that bolt shearing strength is best predicted by the rules given in the AISC Specification (*Load and*,

1986); and, the current rules given in the AISC Specification (*Load and*, 1993) are overly conservative when considering a single bolt in shear.

Next, to develop the component model, bolt and frictional behavior models were developed. The bolt behavior is given by:

$$\frac{R}{R_n} = 1 - e^{-6.25 \bar{\Delta}} \qquad \text{(Eq 50)}$$

Where

$\bar{\Delta} = \Delta / \Delta_f$

And

$\Delta_f = 1/8\text{-in.}$

The frictional behavior is approximated by a bi-linear model which is summarized in Figure 33.

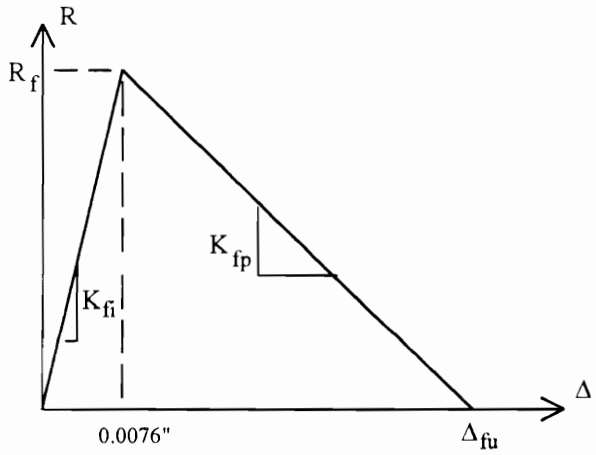

Figure 33 Bi-Linear Representation of Friction Load-Deformation Behavior

Where

$R_f = \alpha\ (0.7\ F_{ub})\ (0.75\ A_b)\ \mu$

α = 1.0 for A325 bolts and 0.88 for A490 bolts

μ = Friction coefficient (0.33 for clean mill scale surfaces)

F_{ub} = Minimum specified tensile strength of the bolt

A_b = The area associated with the nominal diameter of the bolt

$$\Delta_{fu} \begin{cases} (t_1 + t_2) < 0.5" & \Delta_{fu} = 0.4" \\ .0.5" \le (t_1 + t_2) \le 1.5" & \Delta_{fu} = 0.4" - (t_1 + t_2 - 0.5)\ 0.3 \\ 1.5" < (t_1 + t_2) & \Delta_{fu} = 0.1" \end{cases}$$

t_1 = Thickness of the thinner of the two plates connected (in.)

t_2 = Thickness of the thicker of the two plates connected (in.)

A method for predicting the failure deformation using the component model was also developed. Comparisons of predicted failure deformation to test failure deformation indicated that the failure deformation is a highly variable quantity and in general difficult to predict.

To provide a simpler method for approximating the single bolt lap plate connection load-deformation behavior, a parametric model was developed for lap plate connections with fully tensioned bolts. This parametric model uses the Richard Equation where the equation parameters are given by:

$$R_n = R_{np} \le R_{nb} \quad \text{(Eq 51)}$$

$$K = 5751\ t_1 d_b + 1213 \quad \text{(Eq 52)}$$

$$K_p = 9\ \{ R_{np} / R_{nb} \}^{2.9} \quad \text{(Eq 53)}$$

$$R_{transition} = 0.14\ F_{ub}\ d_b^2 + 12 t_1 / d_b \le R_n \quad \text{(Eq 54)}$$

$$R_o = R_n - 0.25\ K_p \ge R_{transition} \quad \text{(Eq 55)}$$

$$R_1 = R_{transition} (t_2/t_1)^{0.1} \le 0.98\ R_o \quad \text{(Eq 56)}$$

$$n = \frac{-\ln(2)}{\ln\left(\frac{R_1}{R_o} - \frac{K_p}{K - K_p}\right)} \le 3 \quad \text{(Eq 57)}$$

Finally, the component model, parametric model, and two existing models for predicting the load-deformation behavior of single bolt lap plate connections were evaluated against the test data. In general, both the component and parametric models provided good predictions of the load-deformation behavior.

5.9.2 Recommendations

The frictional component behavior was based on the assumption that the bearing behavior of the bolts and plates could be satisfactorily approximated with the component method. A much better understanding of this behavior could be obtained based on the load-displacement histories of actual friction tests such as those conducted by Frank and Yura (1981). It is recommended that the data from the Frank and Yura (1981) tests be obtained. This data was not included in the report by Frank and Yura (1981) nor in the thesis that the report was based on (Perry, 1981). In addition, new tests considering thinner plates and possibly specially designed lap plate connection tests that avoid initial bearing should be conducted. The data from the Frank and Yura (1981) tests and the new tests could be used to develop a better understanding of the friction behavior. Also, literature from the area of tribology should be consulted. A brief literature review in this area produced at least one paper (Simkins, 1967) that may provide some insight into the pre- and post-slip frictional behaviors.

There were only 16 lap plate connection tests with bolts in the snug tight condition. Additional tests should be conducted. These tests would provide a better basis for evaluation of models for predicting the load-deformation behavior. In addition, they could be used to gain a better understanding of the bolt component load-deformation behavior. Finally, when combined with the database of connection tests that had fully tightened bolts a much better understanding of the frictional component behavior could be obtained.

It has been shown that the shape of the load-deformation behavior and the deformation at failure are not constant values; however, this is the assumption made when using the current ultimate strength method for analysis of eccentrically loaded bolt groups. An analytical study of the effect of varying shape and failure deformation on the load capacity of eccentric bolt groups should be conducted to determine if using constant shape and failure deformation values provides sufficient accuracy and safe results. The parameter model based on the Richard Equation could be used for this study.

6. Behavior and Modeling of PR Steel Beam-Girder Connections

This chapter summarizes the report by Rex and Easterling (1996(e)) on the behavior and modeling of partially restrained steel beam-girder connections.

6.1 Introduction

6.1.1 General

The primary hypothesis of this dissertation is that a PR beam-girder connection can be modeled as a combination of connection components as illustrated in Figure 34. This hypothesis is verified for bare steel PR beam-girder connections in this chapter. In addition, a simplified method of modeling bare steel PR connections is developed.

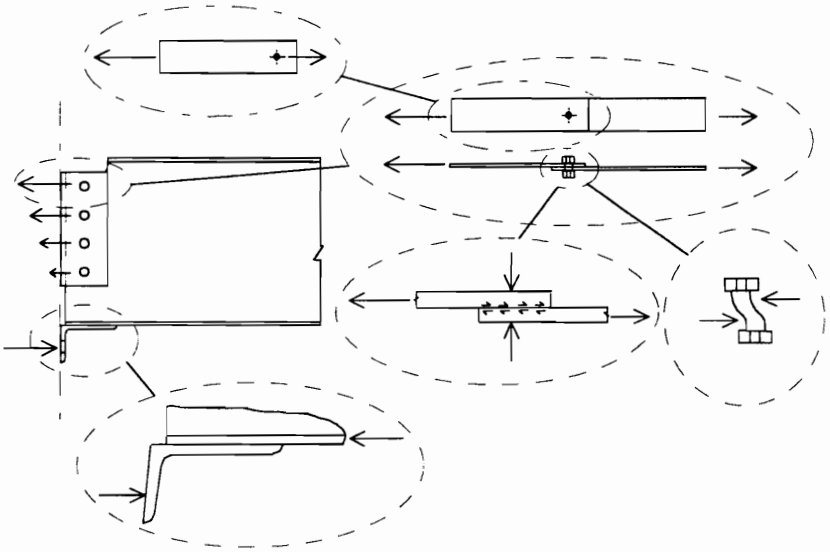

Figure 34 Primary Components of Proposed Beam-Girder Connection

6.1.2 Objectives And Methods

The primary objective of the study presented in this chapter is to present the required details needed to implement the component model and to verify that the model can be used to accurately approximate the moment-rotation behavior of bare steel PR beam-girder connections. A secondary objective of the study is to develop a model which is simpler to use than the component model. These objectives are achieved by:

1. Conducting an experimental investigation of the moment-rotation behavior of bare steel PR connections.
2. Developing behavior models for components of the bare steel connection.
3. Developing and outlining one method by which the component model can be implemented.
4. Calibrating and verifying the component model results against the experimental test results.
5. Using the component model to help develop a simpler model for approximating the bare steel PR beam-girder connection moment-rotation behavior.

First, 17 full-scale bare steel connections were experimentally tested. The purpose of these tests was to provide experimental data for calibrating and verifying the component model. These tests varied a variety of connection parameters as well as the shear-to-moment ratio.

Second, behavior models for each of the fundamental components of the steel connection are needed before the component model can be implemented. Some of these behavior models were developed in previous chapters (plate bearing, bolt deformation, friction behavior). Behavior models for the remaining components are developed based on existing literature and basic mechanics.

Third, once behavior models for each of the components are available, a method of combining the component behaviors to model the moment-rotation behavior of the connection is needed. A method which uses an ultimate strength analysis is developed and outlined.

Fourth, some characteristics of the steel connections are not well understood, such as bolt and angle gaps. The component modeling is calibrated against the experimental data to determine estimates of these quantities. It is shown that the component model can provide very accurate approximations of the moment-rotation behavior if proper estimates of these quantities are known.

Fifth, because of the computational complexity associated with the component model, a simpler method of modeling the moment-rotation behavior is developed. This method is based on a combination of basic mechanics and a parametric analysis.

6.2 Experimental Investigation of PR Steel Beam-Girder Connections

6.2.1 Test Specimens

Seventeen full-scale steel connections were experimentally tested. A summary of the primary variables considered in the experimental program are presented in Table 22 and basic specimen details are given in Figure 35.

Each test beam was approximately 8-ft in length and two connections were fabricated on each beam, one at each beam end. One connection was tested at a time. Bolts were first brought to a snug tight condition by tightening them with a typical spud wrench. For the connections with fully tensioned bolts the turn-of-nut method (*Load and*, 1993) was used to control bolt tension. Connections 1 through 12 had the seat angle welded to the beam flange; while, connections 14a through 14e had the seat angle bolted to the beam flange.

Table 22 Steel Connection Experimental Test Variables

Connection	Shape	Distance To Load Point (in.)	Distance To Beam End (in.)	Number of Bolts	d_b (in.)	Bolt Tension	t_p (in.)
1	W18x35	36	2	5	1	Full	0.5
2	W18x35	36	2	4	1	Full	0.5
3	W18x35	36	1.5	4	1	Full	0.5
4	W18x35	36	2	4	1	Snug	0.5
5	W16x36	36	2	3	1	Full	0.5
6	W16x36	36	1.5	3	1	Full	0.5
7	W16x36	36	2	3	1	Full	0.5
8	W16x36	36	2	3	1	Snug	0.5
9	W10x45	36	2	2	1	Full	0.25
10	W10x45	36	2	2	0.875	Full	0.25
11	W10x45	36	2	2	1	Snug	0.25
12	W10x45	36	2	2	0.875	Snug	0.25
14a	W12x30	5	2	3	1	Full	0.5
14b	W12x30	10	2	3	1	Full	0.5
14c	W12x30	15	2	3	1	Full	0.5
14d	W12x30	20	2	3	1	Full	0.5
14e	W12x30	25	2	3	1	Full	0.5

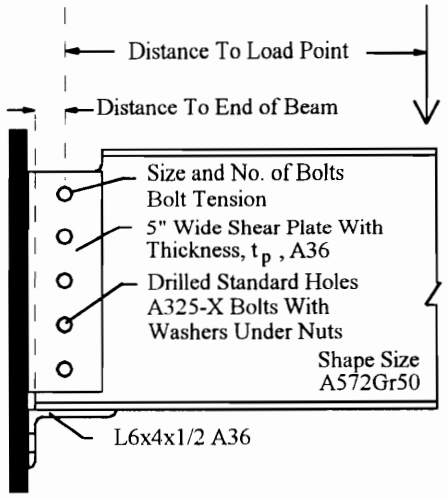

Figure 35 Steel Connection Experimental Test Variables

6.2.2 Instrumentation

The primary purpose of the test instrumentation was to measure the moment-rotation behavior of the connection. A schematic of the typical instrumentation used for all the connection tests is shown in Figure 36. The connection moment was determined by multiplying the load (read from the load cell) by the distance from the load to the centerline of the connection. The connection rotation was measured using a combination of potentiometers and dial gages. The displacement readings from the potentiometers and dial gages were properly added and then divided by the vertical distance between instruments to determine the connection rotation.

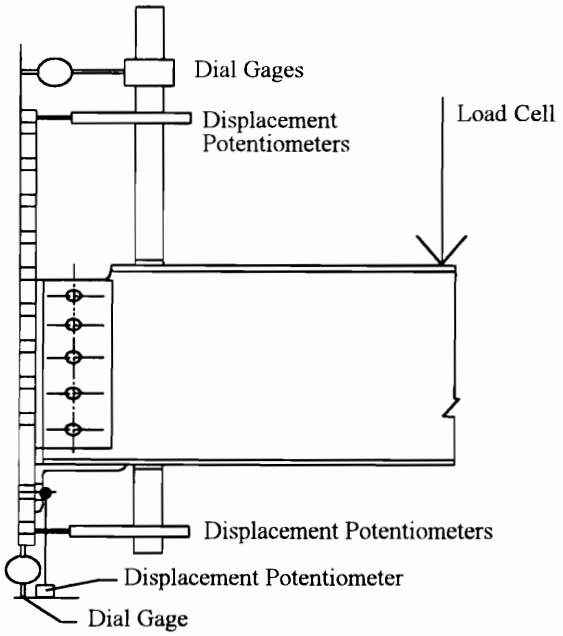

Figure 36 Typical Instrumentation

6.2.3 Test Setup

The basic test setup was a cantilever type test specimen intended to represent one-half of a symmetric beam-girder connection. A schematic of the test setup is shown in Figure 37.

To facilitate the ease with which the connections could be placed into and removed from the test setup the connections were actually attached to a large 1-in. thick removable steel plate rather than directly to the W21x101 column flange. The shear plate and seat angle were attached to the removable plate which was then attached to the column flange with bolts.

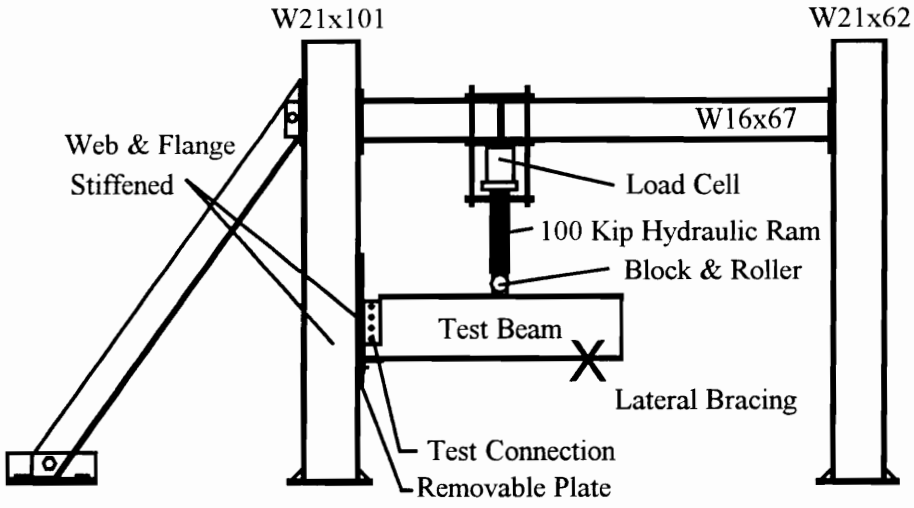

Figure 37 Test Setup

6.2.4 Test Procedure

The first stage of the test was load controlled while the second stage of the test was rotation controlled. After each load or displacement increment the connection was allowed to settle for approximately four to five minutes. Displacement and load readings were then taken. All tests were typically run from the start without any unloading until a reduction in load carrying capacity occurred (i.e. some sort of connection failure began). Connection #4 was the only test that was unloaded before failure. This test was unloaded to re-align a ram which was out of alignment. The test was then re-loaded to failure.

6.2.5 General Results

The principle results, that are of interest for this study, are the results characterizing the moment-rotation behavior. The typical characterizing values are the ultimate moment (M_{ult}), ultimate rotation (ϕ_{ult}), and the initial stiffness (K_i). These quantities along with the ultimate shear load (V_{ult}) are summarized in Table 23. In addition, comparisons of the ultimate shear load and moment to the calculated shear and moment capacity of the beam as per the AISC Specification (*Load and*, 1993) are given.

Table 23 Summary of Connection Results

Connection	V_{ult} (kips)	V_{ult} / V_n	M_{ult} (k-in.)	M_{ult} / M_p	ϕ_{ult} (rad)	K_i (k-in./rad)
1	43	0.30	1556	0.51	0.079	186262
2	41	0.28	1460	0.48	0.079	129196
3	35	0.24	1257	0.41	0.079	148449
4	41	0.28	1479	0.48	0.070	62035
5	31	0.25	1099	0.39	0.101	55649
6	25	0.20	904	0.32	0.085	65291
7	31	0.25	1117	0.40	0.090	98127
8	30	0.24	1081	0.38	0.119	26919
9	11	0.10	389	0.14	0.134	37780
10	10	0.10	371	0.13	0.098	22833
11	11	0.10	384	0.14	0.113	12607
12	11	0.10	380	0.14	0.133	19348
14a	94	1.06	470	0.24	0.134*	47381
14b	58	0.65	580	0.29	0.121*	88783
14c	41	0.46	618	0.31	0.113**	67202
14d	32	0.36	641	0.32	0.103**	60173
14e	26	0.30	656	0.33	0.087**	90594

* Near ultimate load shear yielding of web caused rotation readings to be exagerated.
** Near ultiamte load top rotation gages lost contact with support resulting in rotation readings smaller than actual

In general, the rotation capacity of all the connections was extremely high with the minimum ϕ_{ult} for Connection #4 of 70 mrad. The rotation capacity is seen to increase with a reduced number of bolts and a reduced distance to the top bolt. Connection moment

resistance approached 50% of the plastic moment capacity for the largest connections. Applied shear was typically 20 to 40% of the nominal beam web shear capacity except for connections #14a and #14b. The load point for these connections was only 5 and 10-in. from the connection respectively. The shear load for #14a exceeded the shear capacity of the beam web which resulted in the connection test being stopped before any true connection failure occurred.

6.2.6 Failure Modes

All of the connection tests except #14a were run until a significant drop in load carrying capacity occurred. Connection #14a was stopped because of limitations of the test setup after achieving large rotations and because of excessive shear yielding of the beam web. In general there were six failure modes:

1. Tension rupture of beam web between two top bolt holes
2. Tension rupture of beam web between top bolt hole and bottom edge of beam cope
3. Tear-out failure of beam web between top bolt hole and end of beam
4. Tension rupture of shear plate between top bolt hole and top of plate
5. Shear yielding of beam web
6. Local buckling of bottom beam flange

Only the first four of these failure modes resulted in loss of load carrying capacity. Failure modes five and six were simply noted as they initiated and progressed during the test but the tests were not stopped until one of the first four failure modes occurred (except for #14a). A summary of the failure modes for each connection is given in Table 24.

Table 24 Summary of Connection Failure Modes

Connection / Mode	1	2	3	4	5	6	7	8	9	10	11	12	14a	14b	14c	14d	14e
1	X				X		X	X						X	X	X	X
2		X		X													
3			X			X											
4									X	X	X	X					
5													X	X			
6	X	X	X		X		X	X									

6.2.7 Angle Gaps

In most of the connection tests there was a horizontal gap between the heel of the seat angle and the connection support. This type of erection tolerance had not been seen in previous connection tests conducted by the writer nor had any mention of such a gap been reported in similar experimental investigations conducted by others. The importance of this initial gap was not understood until after the connection tests had been completed. In addition, no gaps were noticed until after the first five connection tests had been completed. Unfortunately, this resulted in insufficient attention to the size and behavior of the angle gap.

6.2.8 Effect of Shear-Moment Ratio

Connections #14a to #14e were designed to determine what effect the shear-moment ratio (ratio of shear over moment) would have on the moment-rotation behavior of the connections. All the connection details were identical except for the location of the applied load which varied from 5-in. to 25-in. from the centerline of the connection. The moment-rotation test data for all five connections is presented in Figure 38.

Review of Figure 38 indicates two possible effects. First, the moment capacity of the connection increases with increasing distance to the inflection point. However, there is little change in the moment capacity between connections with inflection points at 10-in. or beyond. This indicates that the shear-moment ratio has little influence on the connection moment-rotation behavior when the inflection point is beyond some critical distance. For this particular connection that distance appears to be between 5-in. and 10-in. Second, the rotation capacity appears to increase as the inflection distance decreases. This apparent increase in rotation capacity is the result of errors in the rotation measurements (as described in the footnotes of Table 23) in the later stages of these tests and is believed invalid.

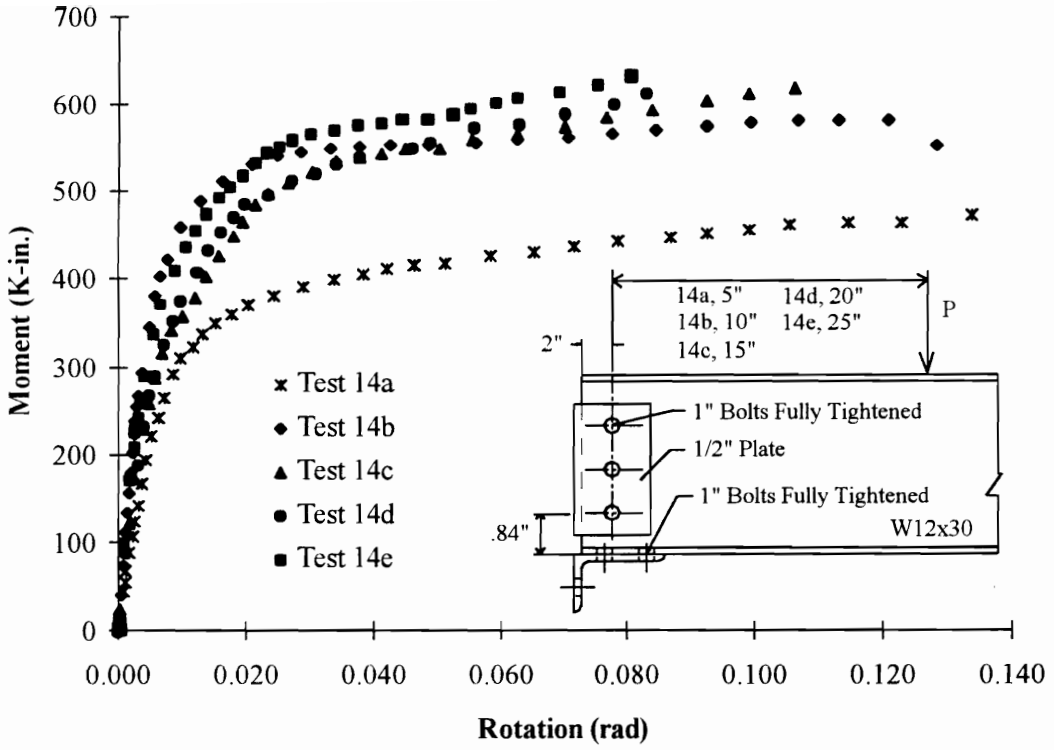

Figure 38 Moment-Rotation Behavior Connections #14a to #14e

Based on the results previously given in Table 23, there are no consistent observations of the effect of shear-moment ratio on the initial connection stiffness with the one possible exception of K_i for Connection #14a being significantly lower than the other four connections in the group.

The primary conclusion from these five connection tests is that the shear-moment ratio has little influence on the connection behavior if the inflection point is located outside some critical distance. Further analysis and experimental work to better understand this behavior is needed.

6.3 Behavior Models For Connection Components

For the bare steel connection the major components are a high strength bolt in single shear and the seat angle. The behavior of these components are based on the behavior of more fundamental components such as:

- Plate bearing
- Bolt bending, bearing, and shearing
- Friction between plates
- Bolt hole gaps
- Fillet welds
- Axial shortening of the seat angle
- Seat angle bending resulting from angle gaps
- Axial elongation of the shear plate at the gross and net sections
- Axial elongation of the beam web at the gross and net sections

6.3.1 Frictional Behavior Between Plates

A behavior model for friction resistance developed between two plates bolted together with a high strength bolt was developed in Chapter 5. This model was based on experimental results from single bolt lap plate connection tests. It is assumed that this model is valid for use in the full steel connection with one exception.

The average deformation when the frictional resistance is attained was determined to be 0.0076-in. with a COV of 46% based on the single bolt lap plate tests. In Section 6.5.1, it will be determined that a deformation value of 0.015-in. is more appropriate. The difference in these values is believed to be attributable to two reasons: uneven bolt tensioning in the full connection and differing plate surface conditions.

6.3.2 Plate-Bolt-Plate Bearing Behavior

As the plates in the connection start to move relative to each other, bearing forces are developed by contact between the bolt hole in one plate against the bolt and in turn by

contact between the bolt and the bolt hole of the second plate. Behavior models for this plate-bolt-plate series were developed in Chapters 4 and 5 based on results from studies of single bolt single plate connections and single bolt lap plate connections. It is assumed that these behavior models are valid with one exception.

In the studies of single bolt, single plate connections and single bolt, lap plate connections, any gaps between the bolt shank and the bolt hole where intentionally eliminated. In full steel connections these gaps cannot be eliminated and are assumed to exist in most bolted connections. The effect of the "bolt gap" is that no load can be developed by the plate-bolt-plate series until the bolt gap is closed by relative movement between the plates. This results in a load-deformation behavior with zero bearing load resistance in the initial stage.

6.3.3 Fillet Weld Behavior

An evaluation of available methods for predicting the strength and load-deformation behavior of fillet welds was conducted. Based on this evaluation, the method given in the AISC Specification (*Load and*, 1993) is recommended. This method is a modification of the method developed by Miazga and Kennedy (1989) and Lesik and Kennedy (1990). The weld strength is given by:

$$\frac{P_\theta}{P_0} = 1 + 0.5\ \mathrm{Sin}^{1.5}\theta \qquad \text{(Eq 58)}$$

Where

P_θ = Strength of weld loaded at angle θ

$P_0 = 0.6\ F_{exx}\ A_w$ = Strength of weld loaded at $\theta = 0$

F_{exx} = Nominal weld electrode strength

A_w = Effective area of weld throat

The weld load-deformation behavior is given by:

$$\frac{P}{P_\theta} = [\rho(1.9 - 0.9\,\rho)]^{0.3} \qquad \text{(Eq 59)}$$

Where:

$\rho = \Delta/\Delta_u$

$\Delta_u = 0.209(\theta+2)^{-0.32} D$ = Deformation at ultimate load of fillet weld

$\Delta_f = 1.087(\theta+6)^{-0.65} D$ = Deformation at fracture of fillet weld

D = Leg size of fillet weld (in.)

6.3.4 Seat Angle Behavior

The seat angle in the proposed beam-girder connection is essentially designed to resist axial loads passing from the bottom flange of the beam to the seat angle and then in turn to the girder web as shown in Figure 39. There are two primary sources of flexibility: axial shortening of the outstanding leg of the angle and flexural bending of the leg which is adjacent to the girder web. The flexural bending occurs only if there is a gap between the heel of the seat angle and the web of the girder and then only until this gap is closed. Two simple mechanical models for approximating these flexibility's are also shown in Figure 39.

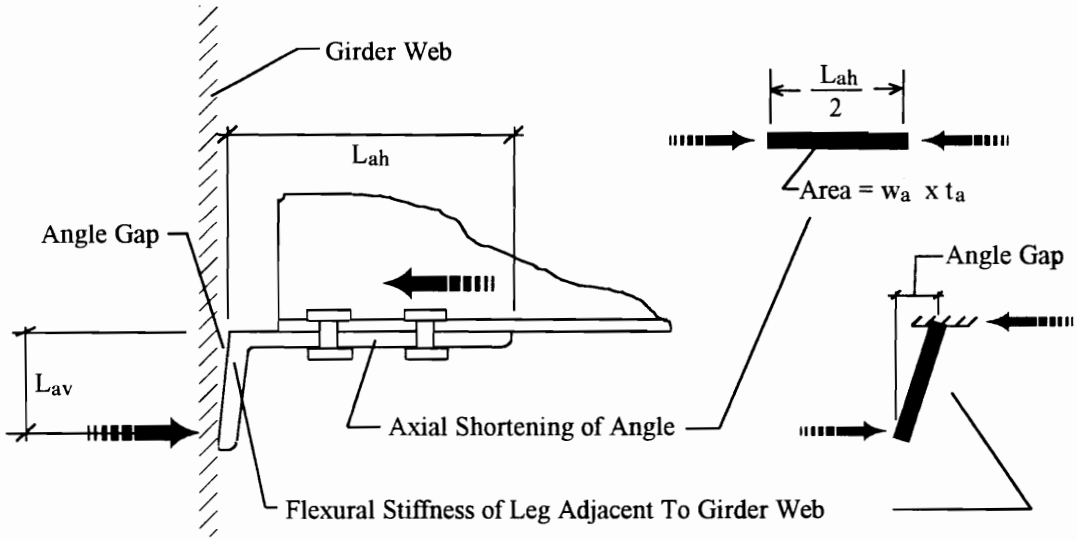

Figure 39 Modeling Seat Angle Flexibility

The axial shortening is modeled as a truss element where the area is equal to the cross-sectional area of the angle and the length is equal to the outstanding leg length (L_{ah})

divided by two. Holes in the angle leg are ignored as they would typically be filled with a bolt which would act to carry the compression load across the hole. The constitutive behavior of the truss element is based on the typical stress-strain model of mild steel developed in Chapter 2.

The flexural stiffness is modeled as a cantilevered beam subject to a concentrated load where the moment of inertia is based on the angle cross-sectional properties and the length is assumed to be the vertical distance from the top of the angle to the location where the bolts attach the angle to the girder web (L_{av}). The flexural stiffness is assumed to increase many orders of magnitude when the angle gap closes. This leads to a bi-linear behavior model of the flexural behavior. The flexural stiffness is assumed to remain elastic until the angle gap closes.

6.3.5 Shear Plate and Beam Web Net and Gross Tension Behavior

When the component model is implemented, the bolt deformations in the web and shear plate will be treated as a combination of vertical and horizontal deformations. The vertical deformations put the steel in the web and plate in vertical shear while the horizontal deformations typically put the steel in the web and plate in horizontal tension (occasionally compression). The flexibility of the shear plate and beam web in shear has been assumed to be small and ignored for modeling. However, the horizontal flexibility and strength are believed to be significant, particularly, the horizontal tension behavior of the net section around the bolt hole. Consequently, the horizontal tension behavior has been included in the model.

As shown in Figure 40, two truss elements for both the web and plate are used to model the gross and net section horizontal tension behavior. The constitutive behavior of the truss element is based on the typical stress-strain model of mild steel developed in Chapter 2.

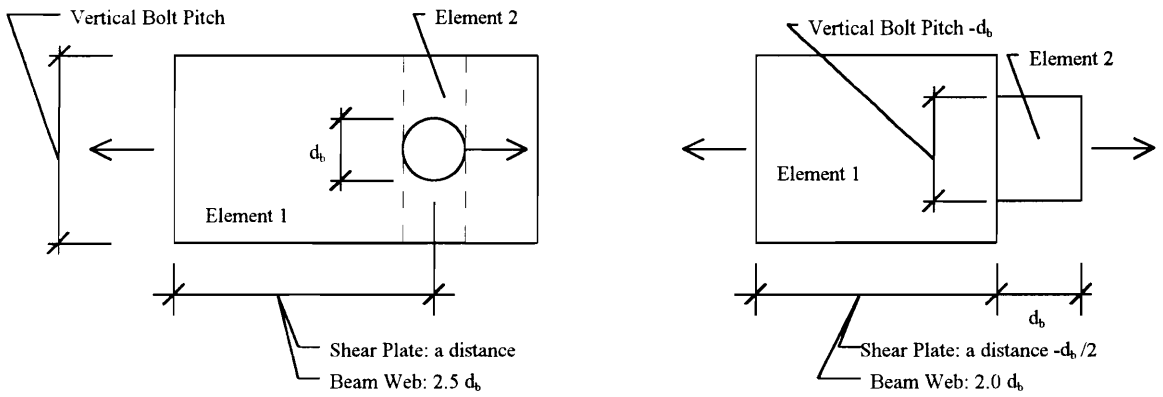

Figure 40 Modeling Shear Plate And Beam Web Flexibility

6.4 Implementation of the Component Model

A method of combining the behavior models of each connection component is needed so that the moment-rotation behavior of the connection can be modeled. One such method is outlined in the following.

6.4.1 Combination Elements

The first step in combining the connection component behaviors is to create combination elements at each critical level in the connection and/or direction of deformation. For the proposed steel beam-girder connection there are essentially three combination element behaviors: horizontal web bolt behavior, vertical web bolt behavior and horizontal seat angle behavior. Schematics of these combination elements and the components of each element are shown in Figure 41.

First, at the level of each bolt in the beam web, the behavior of the fillet weld attaching the shear plate to the girder web, the shear plate and beam web axial stiffness, and the high strength bolt stiffness are combined to create a single Horizontal Web Bolt load-deformation behavior. In addition, the friction behavior, plate bearing, web bearing, and bolt behavior are combined to create a single Vertical Web Bolt load-deformation behavior. Each web bolt behavior will be identical except for differences in the bolt gap.

Second, at the level of the seat angle the behavior of the angle in flexure, the angle under axial compression, and the beam flange-to-seat angle connection (fillet welds or high strength bolts) are combined to create a single Seat Angle load-deformation behavior and moment-deformation behavior. The moment-deformation behavior is needed because the ultimate strength analysis of the overall connection (described in the next section) assumes that the angle resistance is located at the top of the seat angle. However, before the angle gap closes the actual resistance is located at a distance L_{av} below the top of the seat angle. The moment-deformation behavior accounts for this discrepancy. The moment is equal to the value of the load for a given deformation multiplied by L_{av} until the gap closes. Once the gap closes the moment is assumed to be zero.

Each combination element is represented by a single load-deformation behavior which is continuous from the initial behavior to failure. The failure deformation and load associated with a combination element is assumed to be limited by the component that fails. For example, if bolt shear failure occurs then the failure load is the bolt shear strength and the failure deformation is the bolt shear failure deformation combined with the deformations of the other components in the web bolt combination element that occur at the failure load.

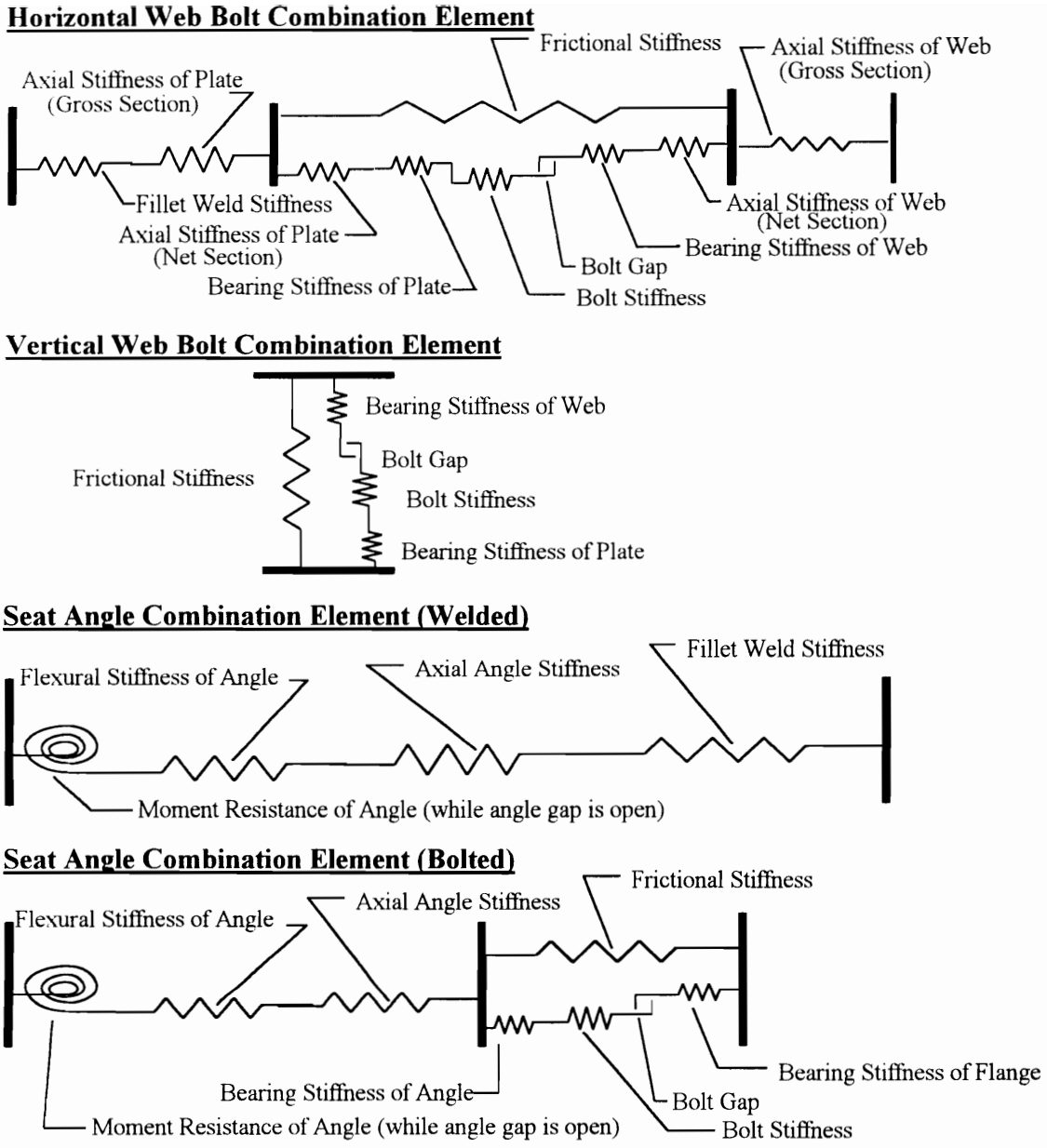

Figure 41 Combination Elements

6.4.2 Ultimate Strength Analysis

Now that the individual connection components have been combined into combination elements, the next step is to combine the combination element behaviors to determine the moment-rotation behavior of the overall connection. The method used to

combine the combination element behaviors is similar to the ultimate strength method for determining the load capacity of an eccentrically loaded bolt group. This method is fully described in the AISC Manual Vol. II (*Manual of*, 1993).

The physical connection and the resulting ultimate strength model are shown in Figure 42. There are two primary differences between the basic ultimate strength analysis and the analysis used. First, the single non-linear load-deformation behavior of the bolt is replaced by the horizontal and vertical web bolt combination element behaviors. Second, the seat angle combination element is added to the analysis. The seat angle is assumed to only resist load in the x direction and seat angle deformation is assumed to be the x component of the total deformation at the angle based on the same analysis technique used to determine the total deformation at each bolt location.

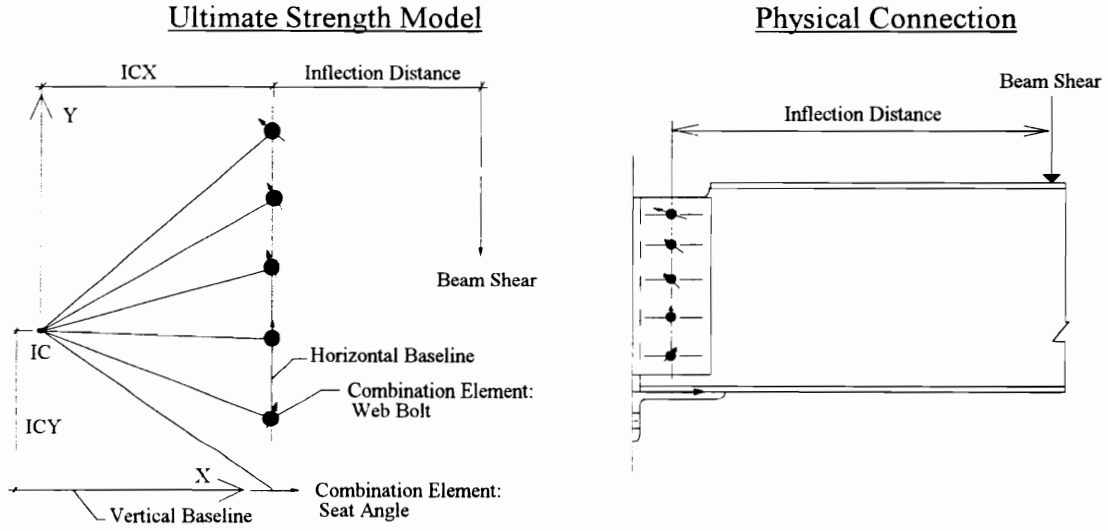

Figure 42 Modified Ultimate Strength Method

6.4.3 Special Considerations

When using the ultimate strength analysis method to determine the connection moment-rotation behavior there are two of special considerations that must be addressed. First, because the web bolts are represented by two combination element behaviors, which in a real connection are not independent of each other, an interaction between the two

behaviors must be assumed. Second, because the above analysis does not consider compatibility with the attached beam, there are believed to be limits to the applicability of the analysis.

6.4.3.1 Interaction of Horizontal and Vertical Web Bolt Behaviors

The web bolts in the modified ultimate strength analysis are represented by two different load-deformation relationships because of the different behavior in the horizontal direction compared to the vertical direction. It is necessary to develop a method of estimating how the vertical and horizontal behaviors interact so that the behavior of a bolt deforming at some angle to the horizontal or vertical may be determined. An elliptical interaction has been assumed for the current model. This interaction curve is shown in Figure 43. The nomenclature in Figure 43 is defined as follows:

R_{nv} = Maximum resistance in the vertical direction

R_{nh} = Maximum resistance in the horizontal direction

V = Load resistance in the vertical direction

H = Load resistance in the horizontal direction

R_n = Maximum resistance in the direction of deformation

θ = Angle of deformation with respect to the horizontal

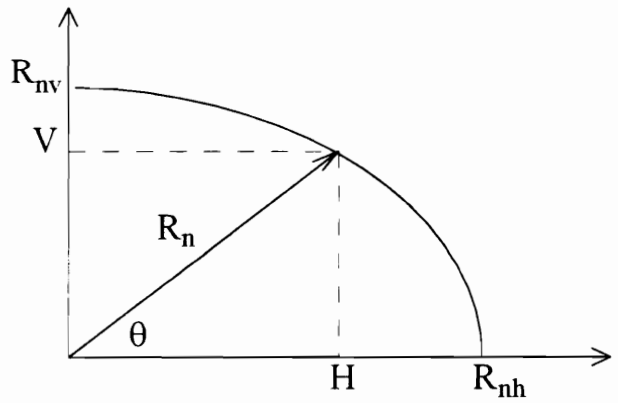

Figure 43 Elliptical Interaction Between Horizontal and Vertical Web Bolt Behavior

In the ultimate strength analysis, the load resistance must be determined based on the total deformation and the angle of deformation. A two step process is used to determine the load resistance. First, using the value of the total deformation and the vertical and horizontal combination element behaviors, the maximum load resistance in the vertical and horizontal directions respectively (R_{nv} and R_{nh}) are determined. These two values define the boundaries of the ellipse (i.e. the ellipse expands as the deformation increases up to the limiting load capacity in each direction). Second, R_n is determined from the angle of deformation.

$$R_n = \frac{1}{\sqrt{\left(\frac{\text{Cos}\,\theta}{R_{nh}}\right)^2 + \left(\frac{\text{Sin}\,\theta}{R_{nv}}\right)^2}} \qquad \text{(Eq 60)}$$

There is no general proof that the interaction between vertical and horizontal behavior is elliptical; however, it can be shown that the interaction is elliptical if the vertical and horizontal behaviors are limited by the bolt shearing strength. In this case, the limiting strength is the bolt shear strength and is independent of the angle of deformation. This results in an elliptical interaction surface in which both legs of the ellipse are equal (i.e. a circle).

6.4.3.2 Shear Failure of PR Connections

The ultimate strength analysis of the connection does not consider compatibility with the attached filler beam. In the analysis, a constant inflection point is assumed; however, if compatibility with the attached beam were considered, the inflection point would vary because of the non-linear behavior of the connection. If the inflection point, chosen for the analysis, is too close to the connection then the connection may fail in shear rather than in moment. A connection fails in shear when the deformation limit of one of the vertical web bolt combination elements is reached during the analysis. A connection fails in moment when the deformation limit of one of the horizontal web bolt combination elements or the seat angle combination element is reached.

Real connections can fail in shear and that alone is not a problem. The problem is that the ultimate strength analysis of the connection inherently assumes that increased shear on the connection reduces the moment capacity and the rotation capacity of the connection. In the extreme, the connection could fail in shear without any connection rotation if the inflection point was chosen at the location of the connection centerline. The problem with this is that the beam end must rotate and if the beam end rotates then the connection has to develop moment resistance which then will decrease the shear capacity of the connection. In situations where the connection is failing in shear, the only way to do a proper analysis is to include beam compatibility; however, if designing with PR connections, the beam cannot be chosen without an estimate of the connection behavior. Consequently, the design could become very iterative.

To avoid this problem with the connection analysis, one very simple rule can be applied. The maximum shear on the connection must be "small" compared to the connection shear strength to ensure that the connection fails in moment before it fails in shear. To determine what connection shear values could be considered "small" a brief parametric study was conducted. Based on this study, it was determined that steel connections fail in shear if the shear ratio exceeded 83% on average. Where the shear ratio is the ratio of applied shear over the basic connection shear strength. The basic connection shear strength is the summation of the strength for each vertical web bolt combination element. The actual shear ratios ranged from 76% to 87% with a COV of 3.8%. A conservative value for the maximum allowable shear ratio of 75% is recommended to ensure that shear failure will not occur in the connection.

6.5 Calibration and Evaluation of Component Model

6.5.1 Calibration of Component Model

The component model was used to determine approximations to the moment-rotation behavior of each of the experimental connections. In doing so, the component

model was calibrated to the experimental results by varying values of the bolt gaps, angle gap, L_{av}, and Δ_s (for frictional behavior). The resulting values of the bolt gaps, angle gap, and L_{av} are presented in Table 25. The average slipping deformation "Δ_s" was determined to be approximately 0.015-in.

Table 25 Connection Properties Determined By Model Calibration

Connection	L_{av} (in.)	Angle Gap (in.)	Bolt Gap Web Bolt #1 (in.)	Bolt Gap Web Bolt #2 (in.)	Bolt Gap Web Bolt #3 (in.)	Bolt Gap Web Bolt #4 (in.)	Bolt Gap Web Bolt #5 (in.)
1	1.8	0.0500	0.0800	0.1000	0.0200	0.0000	0.1250
2	2.0	0.0600	0.0400	0.1000	0.0400	0.1250	N/A
3	2.0	0.0600	0.0500	0.0450	0.0300	0.1250	N/A
4	2.0	0.0400	0.0800	0.0400	0.0000	0.0500	N/A
5	2.3	0.0600	0.0300	0.0800	0.0300	N/A	N/A
6	2.0	0.0625	0.0313	0.0313	0.0625	N/A	N/A
7	1.9	0.0600	0.0300	0.0800	0.0250	N/A	N/A
8	2.2	0.0625	0.0000	0.1000	0.0500	N/A	N/A
9	2.0	0.0300	0.0800	0.1000	N/A	N/A	N/A
10	2.3	0.0600	0.0313	0.0313	N/A	N/A	N/A
11	2.0	0.0250	0.0313	0.0000	N/A	N/A	N/A
12	2.0	0.0150	0.0050	0.0000	N/A	N/A	N/A
14a	1.2	0.0100	0.1250	0.0313	0.0250	N/A	N/A
14b	2.0	0.0200	0.0000	0.0000	0.0000	N/A	N/A
14c	1.7	0.0250	0.0313	0.0300	0.0000	N/A	N/A
14d	1.7	0.0300	0.0313	0.0200	0.0000	N/A	N/A
14e	2.0	0.0200	0.0000	0.0000	0.0000	N/A	N/A

6.5.2 Evaluation of Component Model

The component model moment-rotation behavior was compared to the test results for each experimental connection. The primary moment-rotation behavior characteristic values (M_{ult}, ϕ_{ult}, K_i) are summarized and evaluated in Table 26. In general there was very good agreement between the predicted and the experimental behavior; however, there were some discrepancies. Some possible reasons for differences between the predicted and experimental behavior include:

- Poor modeling of the angle flexural stiffness.
- High variability associated with bolt friction behavior .
- Not including local buckling of bottom flange in component model.

- Poor estimates of web bolt failure deformations.

Table 26 Model Vs. Test Results For Primary Moment-Rotation Characteristics

Connection	Model M_{ult} (k-in.)	Model ϕ_{ult} (mrad)	Model K_i (k-in./rad)	Model / Test M_{ult}	Model / Test ϕ_{ult}	Model / Test K_i
1	1622	65	203883	1.04	0.82	1.09
2	1510	65	140346	1.03	0.82	1.09
3	1199	44	140346	0.95	0.56	0.95
4	1514	60	42476	1.02	0.86	0.68
5	1011	70	78030	0.92	0.69	1.40
6	802	47	85468	0.89	0.55	1.31
7	1013	70	85966	0.91	0.78	0.88
8	1015	72	21720	0.94	0.61	0.81
9	327	91	35452	0.84	0.68	0.94
10	357	160	28706	0.96	1.63	1.26
11	318	75	14683	0.83	0.66	1.16
12	340	148	16606	0.89	1.11	0.86
14a	448	93	58570	0.95	0.69	1.24
14b	550	92	49382	0.95	0.76	0.56
14c	572	92	55001	0.93	0.81	0.82
14d	576	92	57524	0.90	0.89	0.96
14e	584	91	65217	0.89	1.05	0.72
Statistics			Mean	0.93	0.82	0.98
			COV	7%	31%	24%
			Max	1.04	1.63	1.40
			Min	0.83	0.55	0.56

6.6 Simplified Method For Approximating Moment-Rotation Behavior

In the previous section it was shown that the component method is able to provide moment-rotation approximations that agree well with experimental results. However, the complexity of the model does not lend itself to hand or even spreadsheet calculations. Consequently, it was decided to develop a simpler method of providing moment-rotation approximations.

When a complex model is reduced to a simpler one there are simplifying assumptions involved. The first of these assumptions is that the moment-rotation behavior

can be represented by a single continuous analytical expression. The Richard Equation was chosen for the following reasons:

- The equation is continuous and easy to use.
- The equation is able to accurately represent the moment-rotation behavior for most connections.
- Three of the four connection parameters relate very well to definable moment-rotation characteristics such as K, K_p, and M_{ult} which are the initial stiffness, final stiffness, and moment capacity of the connection, respectively.

To limit the number of connection parameters that have to be considered in the development of a simplified method, a variety of assumptions and/or simplifications were made:

1. The seat angle or the connection between the seat angle and the bottom flange will not fail.
2. All bolts are fully tensioned per the AISC Specification (*Load and*, 1993)
3. The friction resistance will not be considered in determining the moment capacity of the connection.
4. All bolts have 1/16-in. bolt gap.
5. The weld attaching the shear plate to the girder web will not fail.
6. There is no angle gap.
7. The connection will not fail in shear.
8. The seat angle is welded to the beam bottom flange.

The following sections develop and present methods for relating the connection parameters to the Richard Equation parameters. The first three relationships developed for M_0, K, and K_p are based on a combination of basic mechanics and assumptions about the connection behavior. The last relationship, which is developed for the curvature parameter "n" , is purely parametric.

6.6.1 Moment Capacity, M_0

A three stage method of determining the connection moment capacity has been developed. First, the shear carried by each bolt in the web is determined. Next, the remaining bolt capacity in the horizontal direction is determined for each web bolt. Finally, the connection moment is determined.

6.6.1.1 Distribution of Connection Shear To Bolts

Based on observations from the experimental connection tests and the ultimate strength analysis of the connections, it is clear that the bolts closest to the center of connection rotation carry more shear than the bolts far away from the center of connection rotation. Based on the assumption about the seat angle strength, it is assumed that the center of connection rotation will be close to the bottom of the beam when the connection is near failure. Consequently, it has been assumed that the shear load (V) carried by each bolt in the beam web will be inversely proportional to the vertical distance between the bolt and the bottom of the beam. In general, for bolt j of N_w bolts, this is given by:

$$V_j = \left\{ \frac{\frac{1}{Y_j}}{\sum_{i=1}^{N_w} \frac{1}{Y_i}} \right\} V_{ult} \leq R_{nv} \qquad \text{(Eq 61)}$$

Where

$$R_{nv} = \min \begin{vmatrix} \text{Vertical Bearing Strength of Web} \\ \text{Vertical Bearing Strength of Plate} \\ \text{Bolt Shear Strength} \end{vmatrix}$$

V_{ult} = The ultimate shear applied to the connection and

Y_j = The vertical distance from bolt j to the top of the seat angle

The upper limit of R_{nv} is imposed to ensure that the calculated shear load on the bolt does not exceed the vertical load carrying capacity of the bolt. If the calculated shear

load does exceed the vertical load capacity, then it is necessary to revise the vertical distances Y_j until the shear is redistributed such that no single bolt shear load exceeds R_{nv}.

6.6.1.2 Determine Remaining Horizontal Capacity of Each Bolt

Once the shear load on each bolt is determined the horizontal load capacity (H) of each bolt can be determined. Based on the vertical and horizontal bolt behavior interaction the remaining horizontal capacity is given by:

$$H_j = \frac{R_{nh}}{R_{nv}} \sqrt{R_{nv}^2 - V_j^2} \qquad \text{(Eq 62)}$$

Where

$$R_{nh} = \left| \begin{array}{l} \text{Horizontal Bearing Strength of Web} \\ \text{Horizontal Bearing Strength of Plate} \\ \text{Horizontal Net Tension Strength of Web} \\ \text{Horizontal New Tension Strength of Plate} \\ \text{Bolt Shear Strength} \end{array} \right|_{\min}$$

6.6.1.3 Determine Connection Moment Capacity

The connection moment capacity (M_0) can be determined by summing the individual moment contributions of each web bolt. This is given by:

$$M_0 = \sum_{j=1}^{Nw} H_j Y_j \qquad \text{(Eq 63)}$$

It is important to note that the values of Y_j used to determine the moment capacity must be the real values of Y_j and not the imaginary ones used to determine the distribution of the shear load in the connection.

6.6.2 Initial Stiffness, K

The initial stiffness of the connection (K) can be approximated by combining initial stiffness values for the major connection elements. For the bare steel connection the major connection elements are the seat angle and each of the web bolts.

For a welded seat angle with no angle gap, the initial stiffness of the angle is assumed to be the initial stiffness of the weld. The weld stiffness is derived from the weld load-deformation model given in the AISC Specification (*Load and*, 1993) with the exception that f(p) is assumed to be 8.234 Δ/Δ_{max} as given in the original paper by Lesik and Kennedy (1990). The resulting angle stiffness is given by:

$$K_{ia} = F_{exxa} (20.9 L_0 + 106.6 L_{90}) \quad \text{(Eq 64)}$$

The bolt stiffness, when a bolt gap is present, is assumed to be the frictional stiffness of the bolt which is given by:

$$K_{iw} = R_f / 0.015 \quad \text{(Eq 65)}$$

Because the initial stiffness of each of the elements is essentially elastic, an elastic combination of the element stiffness is appropriate. This can be expressed in equation form as:

$$K = \sum_{j=0}^{Nw} K_j (h + Y_j)^2 \quad \text{(Eq 66)}$$

Where h is the elastic center of rotation given by:

$$h = -\frac{\sum_{j=0}^{Nw} K_j Y_j}{\sum_{j=0}^{Nw} K_j} \quad \text{(Eq 67)}$$

K_j and Y_j are the estimated initial stiffness and location respectively of each of the major connection elements.

6.6.3 Final Stiffness, K_p

When the connection is near the ultimate moment strength, the center of rotation is assumed to be near the bottom of the beam. With this assumption, the final stiffness of the connection can be determined by the sum of the products of the web bolt final stiffness values by the square of the distance from the bolt to the seat angle.

$$K_p = \sum_{j=1}^{Nw+1} K_{pj} Y_j^2 \quad \text{(Eq 68)}$$

K_{pj} is the web bolt plastic stiffness (K_{pb}). Based on the parametric model developed for single bolt lap plate connections in Chapter 5, it is assumed that the web bolt plastic stiffness is given by:

$$K_{pb} = 9\left\{ \min \left[\frac{\text{Plate or Web Horizontal Net Tension Strength}}{\text{Plate or Web Horizontal Bearing Strength}} \right] \frac{}{\text{Bolt Shear Strength}} \right\}^{2.9} \quad \text{(Eq 69)}$$

6.6.4 Curvature Parameter, n

A parameter analysis was used to determine a relationship between the connection parameters and the curvature parameter in the Richard Equation. There were three basic stages to this analysis. The first stage considered the effect of varying the web bolt parameters. Based on the results of the first stage analysis, 11 web bolt parameter combinations were determined for use in stages two and three. In stage two, the effect of varying the number of bolts in the web was considered. Both stages one and two only considered the behavior of the connections with fairly low applied shear to basic connection shear capacity ratios (10% to 20% typically). The results of these two stages provide an upper bound on the value of n. Stage three considered the effect of increasing shear on the connection. Here the ratio of applied shear to the basic shear capacity was varied from very low values up through values that would cause shear failure in the connection. The results of these three stages of analysis were used to develop a relationship between the connection parameters and the curvature parameter in the Richard Equation.

$$n = (1.67\ \Psi_1^2 - 0.71\ \Psi_1 + 0.72)\ \alpha_1\ \alpha_2 \quad \text{(Eq 70)}$$

Where:

$\Psi_1 = R_f / R_{nh}$

α_1 = Correction factor accounting for number and spacing of bolts

$\alpha_1 = 1 + 0.0327\ P_w\ \beta_1\ \beta_2$

$\beta_1 = 0.35\ e^{2.09\,\Psi_1}$

$\beta_2 = 1.2 - 2.27 / N_w$

α_2 = Correction factor accounting for shear ratio

$$\alpha_2 = \frac{\beta_3 - 1}{0.45}\Psi_2 \quad 1.67 - 0.67\,\beta_3 \leq 1.0$$

Ψ_2 = Shear ratio = $V_{ult} / (N_w R_{nv})$

$\beta_3 = 1.304 - 0.768\ \Psi_1 \leq 1.0$

6.6.5 Evaluation of Parameter Relationships

When the simplified method is compared to component model results, that are consistent with the assumptions made in the development, there is generally good correlation between the two. To illustrate this point, the component model and simplified method were used to determine the moment-rotation behavior for five different connections which had a wide range of connection parameters. The resulting moment-rotation approximations are shown in Figure 44. The primary discrepancy between the two occurs when the bolts slip into bearing. This creates a behavior which is characterized by a reduction and then an increase in connection stiffness. The Richard Equation is not capable of replicating such behavior. Aside for this discrepancy the component model and simplified method agree reasonably well.

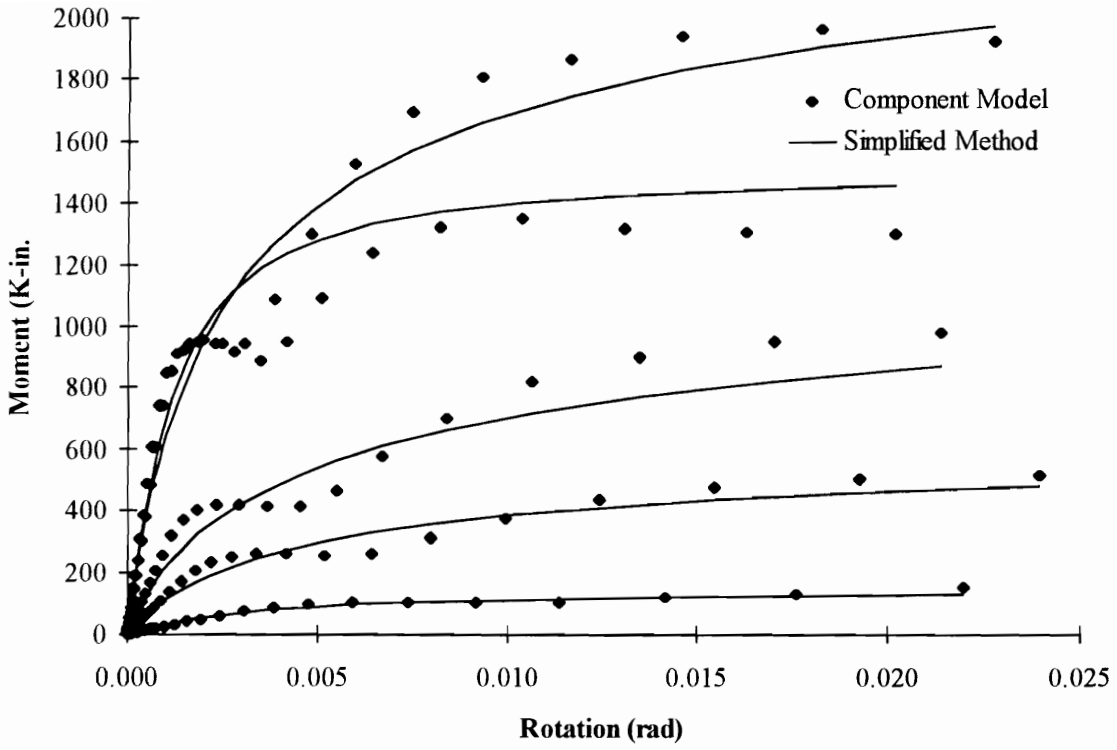

Figure 44 Comparison of Component and Simplified Model

6.7 Summary, Conclusions, and Recommendations

6.7.1 Summary and Conclusions

The primary objective of the study presented in this chapter was to present the required details needed to implement the component model and to verify that the model can be used to accurately approximate the moment-rotation behavior of bare steel PR beam-girder connections. A secondary objective of the study is to develop a model which is simpler to use than the component model. These objectives were achieved through a number of steps.

First, an experimental study of 17 full-scale bare steel connections was presented. The purpose of these tests was to provide experimental data for calibrating and verifying

the component model. Based on the results of the experimental study the following conclusions were reached:

- The shear-moment ratio has no significant influence on the connection moment-rotation behavior until this ratio becomes relatively high.
- Because of angles which are rolled out-of-square, as well as, connection fit-up problems it is possible that there will be a gap between the heel of the seat angle and the support. The effect of this gap is not well understood.
- In general the rotation capacity of a connection decreases with increasing connection height; however, all connections tested had rotational capacities at or above 79 mrad which should provide sufficient ductility for the development of plastic collapse mechanisms.
- The moment capacity of the experimental connections ranged from 13 to 51% of the plastic moment capacity of the associated beam.

Second, behavior models for each of the fundamental components of the steel connection were presented and/or developed. Some modifications were made to previously existing component behavior models to account for bolt gaps and differences in frictional behavior.

Third, a method of combining the component behaviors to model the moment-rotation behavior of the connection was presented. This method utilizes an analysis similar to the ultimate strength analysis given in the AISC Manual Vol. II (*Manual of*, 1993). To ensure that the results of this analysis are valid it is suggested that the applied connection shear be less than 75% of the basic connection shear capacity.

Fourth, the component model was used to develop approximations of the moment-rotation behavior of the experimental connections. In general, the approximate behaviors were very close to the experimental behaviors; however, in order for the model and experimental results to agree two modifications to the model were made. First, bolt and angle gaps were included in the model and the values of these gaps were calibrated for

each experimental connection. Second, the frictional stiffness which had been determined from single bolt lap plate connection tests had to be reduced.

Fifth, a method for approximating the moment-rotation behavior of the beam-girder connection which is simpler yet less flexible than the component method was developed. Using a combination of basic mechanics and parametric analysis, relationships between the connection parameters and the four equation parameters of the Richard Equation were developed.

6.7.2 Recommendations

Angle gaps have not been discussed in any research on PR connections that the writer is aware of. The effect of the angle gap on the connection behavior is not well understood. A rather crude method of accounting for the reduction in stiffness associated with the angle gap was used for purposes of the component model. However, this crude approximation of the behavior has no experimental basis and results in an angle behavior which is highly unlikely in reality. A better understanding of the angle behavior associated with an angle gap is needed. Both experimental and analytical studies could be conducted to develop such an understanding.

Local buckling of the bottom flange occurred in a number of the connection tests. A method of accounting for the reduction in connection stiffness that occurs because of the local buckling or a method for ensuring that local buckling does not occur should be developed.

Currently, the behavior of the bolts attaching the beam web to the shear plate is approximated by single bolt lap plate behavior. This approximation is probably sufficient when the direction of bolt deformation is directly toward the end of the beam or edge of the shear plate. However, when the direction of deformation differs from this, it is unclear whether the single bolt lap plate behavior sufficiently approximates the true behavior. A combination of experimental and analytical work in which the direction of bolt deformation is varied and a general method of accounting for this behavior is needed.

This work would also eliminate the need for an interaction relationship between horizontal and vertical web bolt load-deformation behavior.

The ultimate strength analysis used to implement the component method does not currently consider compatibility with the beam that the connection is attached to. As long as the connection does not fail in shear this is not a problem. However, if the connection fails in shear, then there must be a modification made to the analysis to consider compatibility with the attached beam. A method for modifying the analysis and the implications of revising the analysis should be developed and determined if the connections are going to be used in locations where there is a possibility of connection shear failure.

A more detailed study of the influence of each of the connection components on the moment-rotation behavior is needed. This study can be conducted using the component model. A more comprehensive parametric model of the connection should be developed based on this study. It is also recommended that confidence intervals on the moment-rotation behavior be determined through a statistical combination of the connection component behaviors (such as Monte Carlo simulations).

7. Behavior and Modeling of PR Composite Beam-Girder Connections

This chapter summarizes the report by Rex and Easterling (1996(f)) on the behavior and modeling of partially restrained composite beam-girder connections.

7.1 Introduction

7.1.1 General

The primary hypothesis of this dissertation is that a PR beam-girder connection can be modeled as a combination of connection components as illustrated in Figure 45. This hypothesis is verified for composite PR beam-girder connections in this chapter. In addition, a simplified method of modeling composite PR connections is developed.

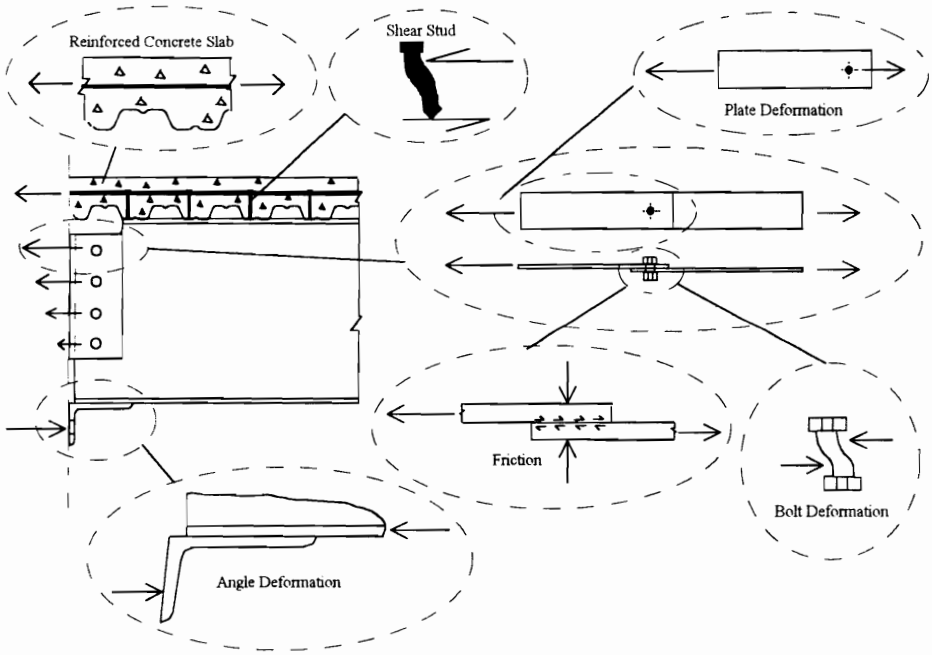

Figure 45 Primary Components of Proposed Beam-Girder Connection

7.1.2 Objectives And Methods

The primary objective of the study presented in this chapter is to present additional details needed to extend the component model, developed in Chapter 6, to composite beam-girder connections and to verify that the model can be used to accurately approximate the moment-rotation behavior. A secondary objective is to modify the simplified connection model, developed in Chapter 6, so that it can be used to approximate the moment-rotation behavior of composite connections. These objectives are achieved by:

1. Conducting an experimental investigation of the moment-rotation behavior of composite PR connections.
2. Developing and presenting the modifications to the component model, developed in Chapter 6, which are needed to extend the model to composite connections.
3. Verifying the component model results against the experimental test results.
4. Using the component model and the simplified model, developed in Chapter 6, to develop a simpler model for approximating the composite PR beam-girder connection moment-rotation behavior.

First, the details of an investigation in which four full-scale cruciform specimens were experimentally tested are presented. The specimens were designed to represent a portion of a typical steel framed composite floor system. The results of these tests provide experimental data for the development and verification of the component and simplified models. In addition, the results provide information about the effect that pre-loading the steel connection has on the moment-rotation behavior of the composite connection.

Second, the required modifications to the component model are presented. This includes a discussion of the behavior models for the composite slab components which were developed in Chapter 3. In addition, required modifications to the ultimate strength analysis of the connection to include the composite slab behavior are presented.

Third, approximations of the moment-rotation behavior of the experimental connections are developed using the component model. The approximate behaviors are then verified against the experimental results.

Fourth, because of the computational complexity associated with the component model, a simpler method of modeling the moment-rotation behavior is developed. The model is developed by making modifications to the simplified model developed in Chapter 6 to include the behavior of the reinforced composite slab.

7.2 Experimental Investigation of PR Composite Beam-Girder Connections

7.2.1 Test Specimens

Four full-scale composite beam-girder cruciform specimens were experimentally tested. These were labeled #5 through #8. Connections #5 and #6 were identical to each other as were connections #7 and #8. The primary details of the connections are shown in Figure 46. All bolts except for bolts used to attach the seat angle to the girder were pre-tensioned using the turn-of-nut method and round washers were placed under the nuts.

7.2.2 Instrumentation

The primary purpose of the test instrumentation was to measure the moment-rotation behavior of the connection. In addition, measurement of slip between the reinforced composite slab and the steel beam as well as beam and girder vertical deflections were measured. A schematic of the instrumentation used for all the connection tests is shown in Figure 47. In addition to the shown instrumentation, load cells were used to measure the load applied by the hydraulic ram and subsequently the moment and shear applied to the connections.

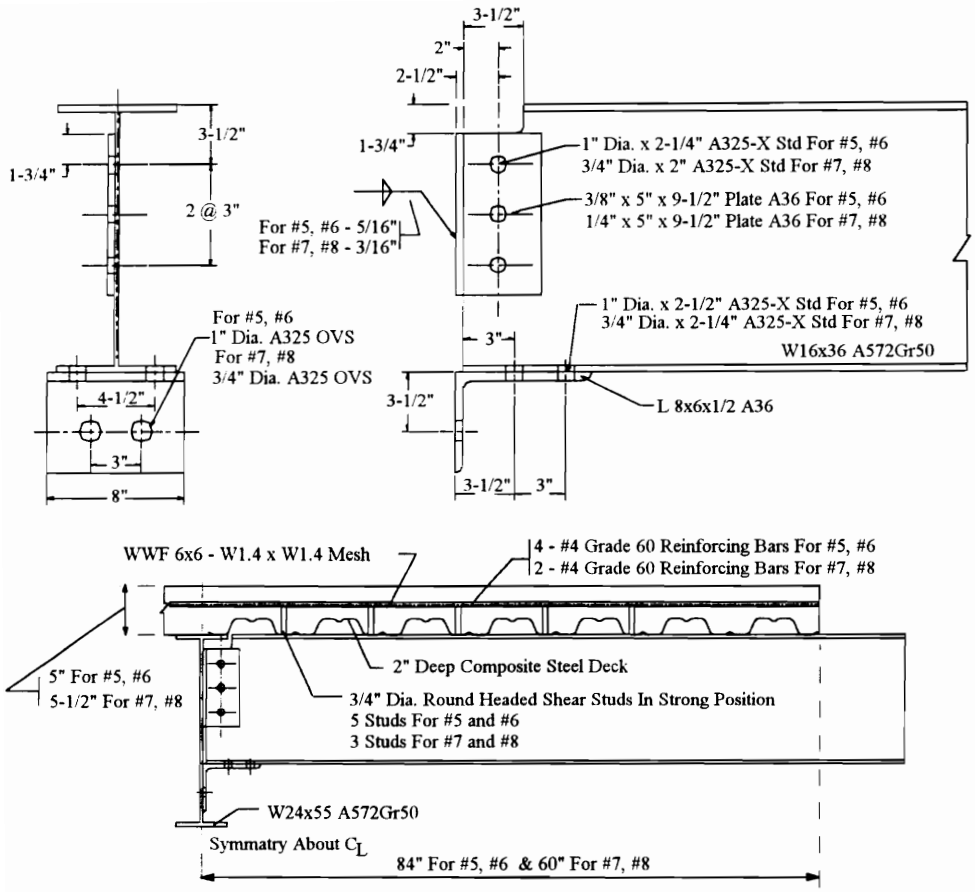

Figure 46 Details of Experimental Composite Connections

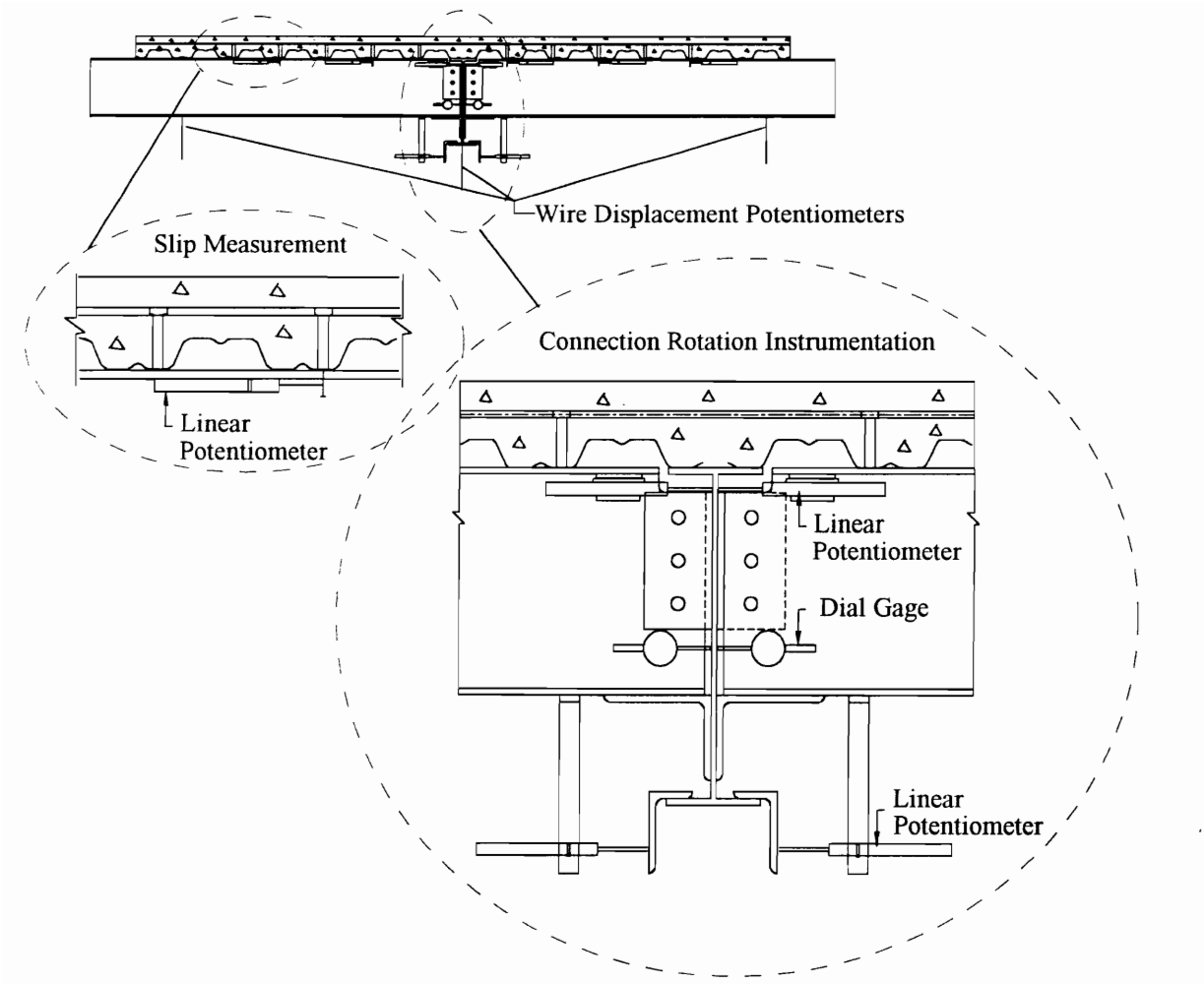

Figure 47 Instrumentation

7.2.3 Test Setup

The basic test setup was a cruciform type test specimen intended to represent a portion of a steel-framed composite floor system. The beams were attached to the girder with the connection details presented previously. The girder was then attached to two columns which were subsequently attached to the testing lab strong floor. Two different testing frames were used to load the test specimens. One test setup was used to apply the pre-load to Connections #5 and #7 immediately after concrete was cast, which simulated design dead load. This test setup was called the "Dead Load Setup." A different test

setup was used to load the composite connections to failure loading after concrete had cured for 28 days or longer. This test setup was called the "Live Load Setup." A schematic of the test specimen and loading setups are presented in Figure 48.

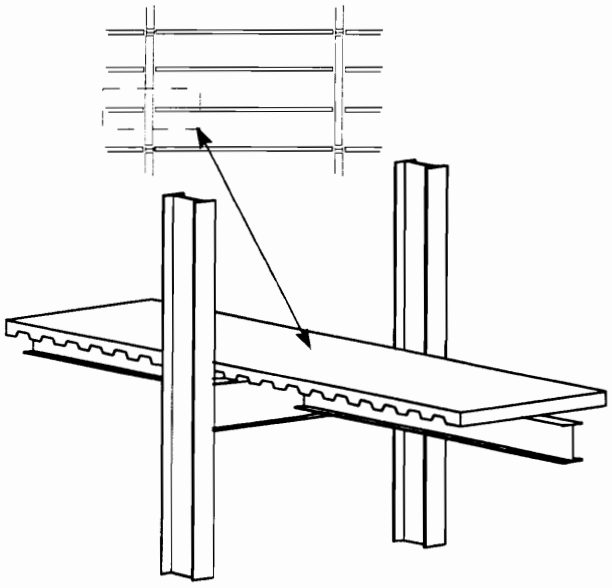

Test Specimen

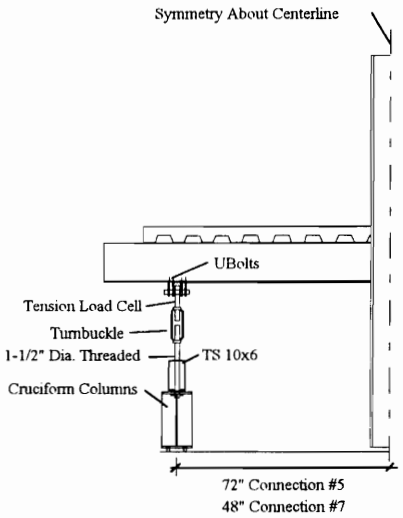

Dead Load Setup

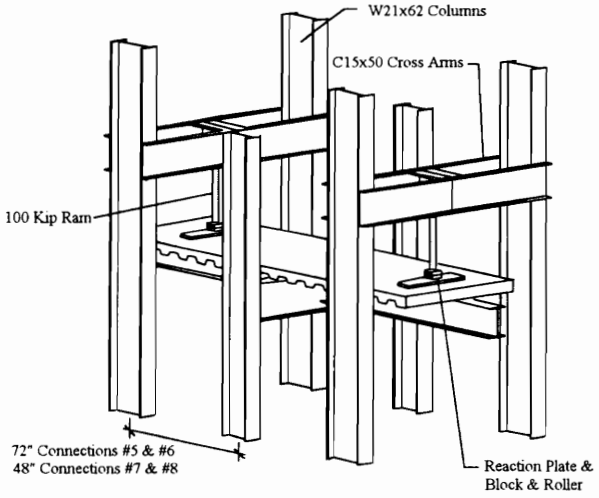

Live Load Setup

Figure 48 Test Setup

During the live load portion of the tests, the free end of the beam for Connections #6 through #8 was restrained against lateral movement with a lateral brace system attached to the top and bottom flange of the beam. These braces were not attached to connection #5 until near the end of the test. The lateral bracing system allows the beam end to have free vertical movement while preventing lateral movement. The brace is believed to provide the same lateral stability that would be provided by the rest of the beam in a real floor system.

7.2.4 Test Procedure

Un-shored construction techniques are used for the majority of composite beams currently built. Consequently, connections associated with these beams will have two distinct stages of behavior: before and after the concrete hardens. Before the concrete hardens, the only rotational resistance of the beam-girder connection will be provided by the bare steel connection. After the concrete hardens the composite connection will provide rotational restraint against all additional applied load. To determine what effect the initial loading of the steel connection (i.e. before concrete hardens) has on the moment-rotation behavior of the composite connection, two test procedures were used.

For Connections #5 and #7, the test procedure was designed to represent the loading history for un-shored construction. Immediately after placement of the concrete the dead load setup was used to apply a pre-load that simulated the connection loading which would occur based on a hypothetical design. After 28 days, the simulated dead load was removed and the live load test setup was used to test the connections to failure. Connections #6 and #8 were not loaded immediately after casting concrete. Rather, they were only loaded after the 28 day curing period for the concrete.

7.2.5 General Results

The principle results that are of interest for this study are the results characterizing the moment-rotation behavior. These results include the ultimate moment (M_{ult}), ultimate

rotation (ϕ_{ult}), and the initial stiffness (K_i). These quantities along with the ultimate shear load (V_{ult}) are summarized in Table 27. In addition, comparisons of the ultimate shear load and moment to the calculated shear and moment strength as per the AISC Specification (*Load and*, 1993) based on the measured steel properties for the bare steel beams are given. The values in Table 27 are the average values for the two sides of each connection test. In addition, K_i for the composite behavior of Connections #5 and #7 was determined by examining the moment-rotation data with moment values above the maximum moment applied during pre-load.

Table 27 Summary of Connection Results

Connection	V_{ult} (kips)	V_{ult} / V_n	M_{ult} (k-in.)	M_{ult} / M_p	ϕ_{ult} (rad)	K_i (k-in./rad)
#5 Steel	N/A	N/A	N/A	N/A	N/A	245221
#5 Comp	38	0.24	2618	0.74	0.096*	658486
#6	34	0.22	2388	0.68	0.075	1030683
#7 Steel	N/A	N/A	N/A	N/A	N/A	205270
#7 Comp	33	0.21	1486	0.42	0.077	628587
#8	31	0.20	1413	0.40	0.061	1070930

* Test setup limited rotation

Connections #6 and #8 failed when one of the reinforcing bars ruptured in tension. Connection #7 also failed because of reinforcing steel tension rupture; however, in addition to the reinforcing steel rupture, the shear plate ruptured immediately after the reinforcing steel ruptured. Connections #5 and #6 had larger bolts, a thicker shear plate, and more reinforcing steel than Connections #7 and #8. Because of these different connection details, the average moment capacity of #5 and #6 (2500 k-in.) is higher than the average moment capacity of #7 and #8 (1450 k-in.).

Despite the differences in connection details, the initial stiffness values associated with #5 and #6 were very similar to those determined for #7 and #8. There are two primary reasons for the small differences. First, the steel connection initial stiffness is primarily a function of frictional resistance. Ideally, the larger the bolt the higher the

frictional resistance. However, because of the high variability in bolt tensioning and steel surface conditions, the size of the bolt does not always determine the level of frictional resistance. Consequently, the size of the bolts did not have a significant effect on the initial stiffness. Second, the composite connection initial stiffness is primarily a function of the initial stiffness of the composite slab. Before cracking, the amount of reinforcing steel in the composite slab has little influence on the slab stiffness. Consequently, the amount of reinforcing steel did not have a significant effect on the initial stiffness.

7.2.6 Effect of Pre-Loading Composite Connections

The details of Connections #5 and #7 were identical to those of Connections #6 and #8, respectively; however, #5 and #7 were loaded immediately after the concrete was cast (i.e. before the concrete could cure) while #6 and #8 were not loaded until after the concrete had cured (i.e. not loaded until over 28 days after the concrete was cast). The reason for the differing loading sequences was to determine what, if any, effect the pre-load had on the composite connection behavior.

A comparison of the moment-rotation behavior for all four connections is given in Figures 49 and 50. The overall behavior up to 50 mrad of rotation is plotted in Figure 49 and the initial behavior of each connection is plotted in Figure 50. The moment-rotation behavior for Connections #5 and #7 have been plotted assuming that the behavior of the connections after removing the pre-load is the composite connection behavior. For comparison purposes the test data after removal of the pre-load has been shifted back to the origin.

7.2.6.1 General

There is one general observation based review of Figures 49 and 50. The overall moment-rotation behaviors of the connections that were pre-loaded are stiffer than the those for the connections that were not pre-loaded. In some regions of the moment-

rotation behavior this effect is minimal; in particular, there is no effect of pre-load on the initial behavior before slab cracking.

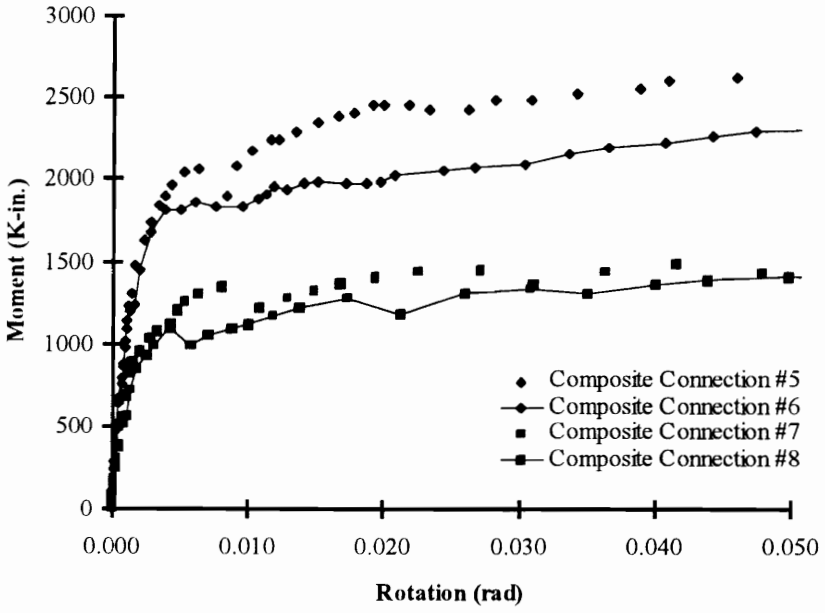

Figure 49 Overall Composite Connection Behavior For All Connections

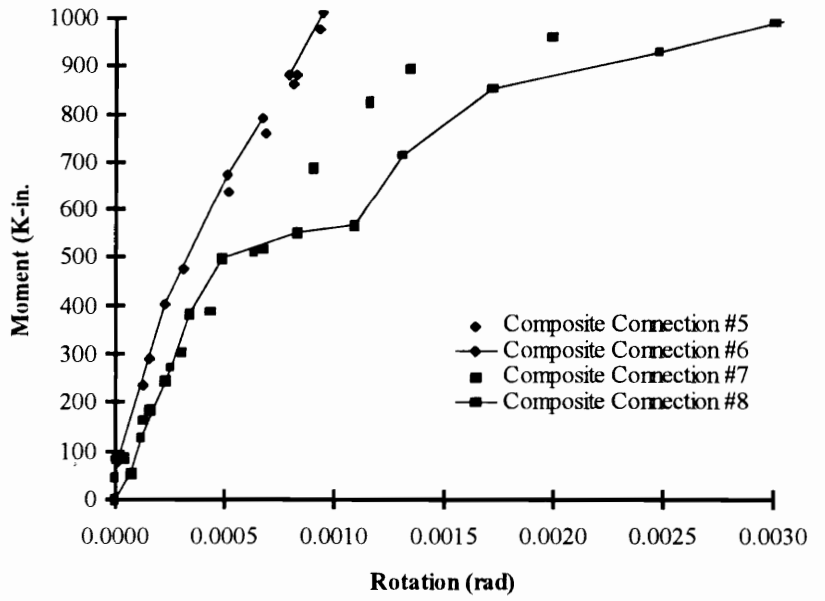

Figure 50 Initial Composite Connection Behavior For All Connections

The first observation is explained by the difference in the composite slab forces at similar moments. Because of the pre-load on the steel connection the composite slab force is zero or in compression for moments at or below the pre-load moment for the connections that were pre-loaded. This would not be true for the connections that were not pre-loaded. Consequently, the moment that is associated with a slab force sufficient to crack the slab will be higher if the connection is pre-loaded. This would be true for initial and subsequent moments associated with different levels of slab cracking.

7.2.6.2 Moment Capacity

Ideally, because of plastic behavior in the steel connection and composite slab, the ultimate moment capacity of the connections which are pre-loaded should be very similar to those which are not pre-loaded. This is true for Connections #7 and #8 which had moment capacities of 1486 and 1413 k-in. respectively (a difference of only 5%). However, based on the test data, this does not appear to be true for Connections #5 and #6 which had moment capacities of 2618 and 2388 k-in., respectively (a difference of 9%).

The reason for the larger difference in moment capacities is believed to be attributable to the interaction of the stay in place steel forming (pour stop) used for casting the test specimens. Connection #5 was tested with stay-in-place steel forming that ran continuous over the girder. Because the forming was continuous over the girder it was able to act similar to the reinforcing steel and visual observations during the test clearly indicated that the forming was carrying load. The forming was cut on each side of the girder in Connection #6 to eliminate the possibility of the forming carrying load.

7.2.6.3 Rotation Capacity

In general, the connections which were pre-loaded had higher rotational capacities than the connections which were not pre-loaded. The major reason for the different rotational capacities is the difference in the elongation of the composite slab for a given rotation. If the composite slab limits the connection ductility (as was the case for all the connections tested in this report) then the pre-loaded connections should fail at a rotation

equal to the failure rotation of the connection which is not pre-loaded plus the pre-load rotation. The pre-load rotation of Connection #7 was approximately 8.5 mrad. Consequently, #7 should have failed at a rotation of 8.5 mrad greater than the failure rotation of #8. The actual increase was 16 mrad. The additional ductility is believed to be a result of differences in cracking patterns of the two slabs.

7.2.6.4 Conclusion

The primary reason it is necessary to understand the effect of pre-loading the bare steel connection is to evaluate how the behavior of the composite connection can be determined. If there is no effect, then composite connection behavior based on tests or analysis which disregards the initial loading of the steel connection can be used. However, if there is an effect (which there appears to be), then some judgment must be used when determining the composite connection behavior.

In general, the composite behavior of the connections which were not pre-loaded was conservative compared to the composite connection behavior of the connections which were pre-loaded (i.e. the moment-rotation behavior was softer and the connection ductility was reduced). Based on this observation, it appears that it is conservative to use the composite connection behavior determined without consideration of the steel connection pre-load. This is a very important conclusion in that the amount of pre-load (i.e. the moment and rotation) imposed on the steel connection will in general depend on the attached beams geometry and loading. If these have to be considered when determining the composite behavior of the connection, the complexity of determining the behavior increases significantly.

It should be noted that the above conclusion is based on the assumption that failure of the connection occurs in the composite slab. If the connection capacity (both moment and rotation) is limited by an element of the steel connection, then using a composite connection behavior which is based on an analysis or test that ignores steel connection pre-load will most likely be unconservative.

7.3 Behavior Models For Connection Components

The behavior models for the connection components are the same as those presented in Section 6.3 for bare steel connections with the addition of three behavior models needed for the reinforced composite slab:

- Reinforcing Steel,
- Concrete Tension Stiffening, and
- Shear Studs.

Behavior models for these components were developed in Section 3.3.

7.4 Implementation of the Component Model

A method of combining the behavior models of each connection component was presented in Section 6.4 for steel connections. Modifications of this method required to include the composite slab behavior are presented in the following.

7.4.1 Combination Elements

The first step in combining the connection component behaviors is to create combination elements at each critical level in the connection and/or direction of deformation. The critical levels and combination elements for the composite connection are the same as those of the bare steel connection with the addition of a composite slab combination element.

At the level of the composite slab the behavior of the reinforced concrete slab and the shear studs are combined as shown in Figure 51. The reinforced concrete slab behavior is assumed to be the parallel combination of the reinforcing steel and concrete tension stiffening behavior. The concrete slab is then combined with the shear stud behavior where the shear stud behavior is assumed to be a parallel combination of all the shear studs in the negative moment region. The composite slab combination element behavior is represented by a single multi-linear load-deformation behavior. This representation is developed as outlined in Section 3.4.1.

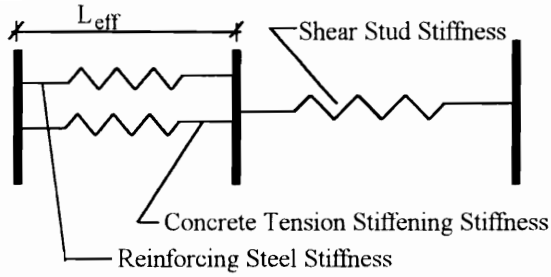

Figure 51 Composite Slab Combination Element

7.4.2 Ultimate Strength Analysis

A method of combining the component behaviors to model the moment-rotation behavior of a bare steel connection was presented in Section 6.4.2. This method utilizes an analysis similar to the ultimate strength analysis given in the AISC Manual Vol. II (*Manual of*, 1993). The only modification needed to use the same method to model the moment-rotation behavior of composite connections is that the composite slab combination element has to be included. The resulting model is shown in Figure 52 where the composite slab combination element is treated in a similar fashion to the seat angle combination element. It is assumed that the composite slab only resists load in the x direction and deformations are assumed to be the x component of the total deformation at the slab based on the same analysis technique used to determine the total deformation at each bolt location.

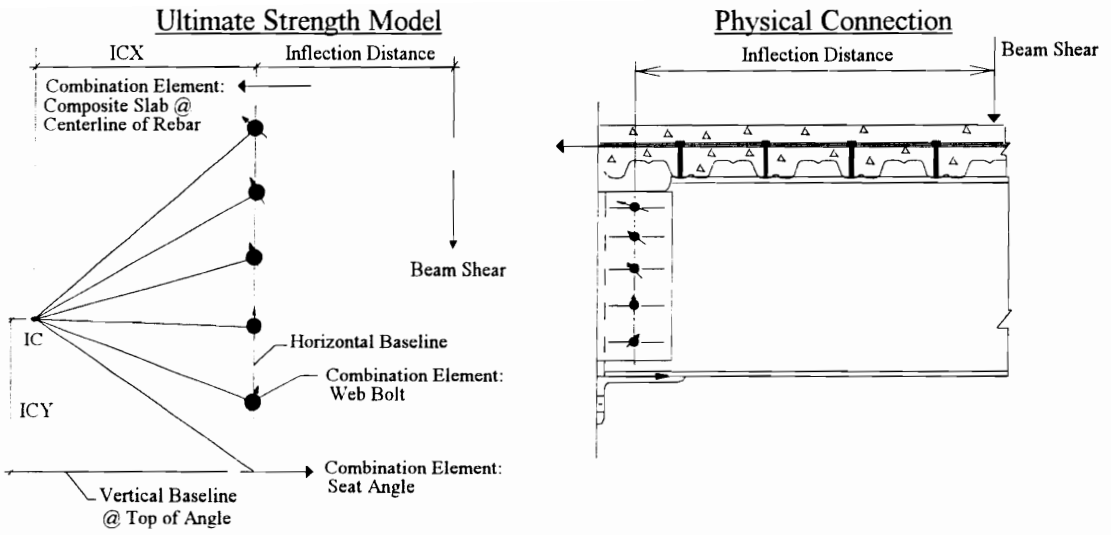

Figure 52 Modified Ultimate Strength Model

7.4.3 Special Considerations

As discussed in Section 6.4.3.2, the ultimate strength analysis of the connection does not consider compatibility with the attached beam. As a result, the analysis may be invalid if the connection fails in shear rather than in moment. For bare steel connections, it was determined that if the shear ratio was below 75% then the connection would fail in moment before failing in shear. The shear ratio is the ratio of applied shear-to-the basic shear strength of the connection, which is the summation of the vertical strength of all the web bolts.

Because composite connections behave differently than the bare steel connections, it was decided to conduct a brief parametric study to determine if the upper limit of 75% on the shear ratio was also applicable to composite connections. The results of this study showed that composite connections would fail in shear if the shear ratio exceeded 82% on average. The actual ratios ranged from 76% to 88% with a COV of 3.8%. Based on these results it appears that the upper limit on ratio of 75% is also applicable to composite connections.

7.5 Evaluation of Component Model

The component model was used to develop approximations to the moment-rotation behavior of the experimental connections. It was assumed that bolt and angle gap values were zero. The resulting approximations were then compared to the test data. A graphical comparison of the moment-rotation behavior for connections #5 and #7 is presented in Figure 53. The primary moment-rotation behavior characteristic values (M_{ult}, ϕ_{ult}, K_i) are summarized and compared in Table 28. In general there was very good agreement between the predicted and the experimental behavior; however, there were some discrepancies.

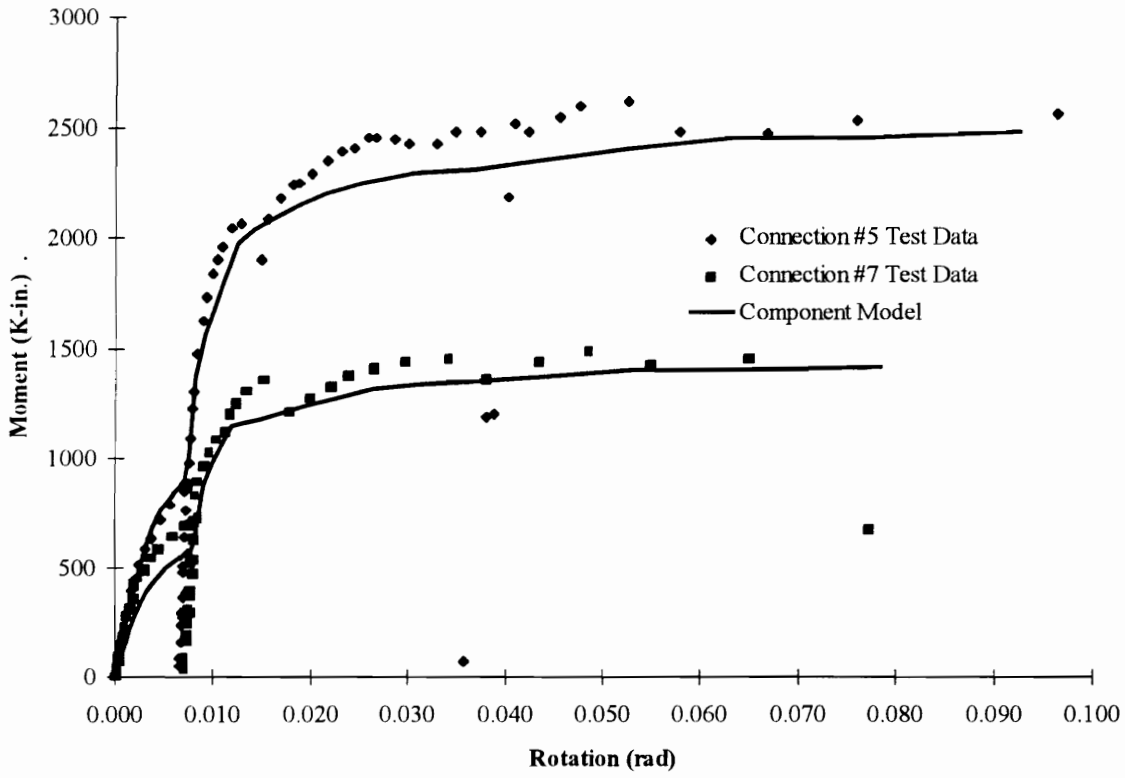

Figure 53 Comparison of Component Model and Test M-ϕ Behavior

First, the test behavior of the steel connection for #7 was stiffer than the component model behavior. However, the differences only occur in the later stages of

behavior. The reason for this difference is that it was over two hours between when the concrete was cast and when the pre-loading was finished. Undoubtedly some concrete setting occurred during this time which could have caused some load to be carried by the reinforcing steel. Even a small load developed in the reinforcing steel multiplied by the moment arm between the reinforcing steel and the seat angle causes the test connection moment resistance to increase noticeably.

Second, initial stiffness values from the component model were much smaller than the initial stiffness values of the composite connection behaviors. The primary reason for this is that the component model only uses the effective area of concrete around each reinforcing bar to determine the tension resistance of the concrete. However, before the concrete cracks, the actual area of concrete resisting tension forces is much larger than the effective area around each bar. Consequently, the tension forces carried by the concrete would be much higher in the experimental test than in the component model resulting in an increased connection stiffness.

Table 28 Model Vs. Test Results For Primary Moment-Rotation Characteristics

Connection	Model M_{ult} (k-in.)	Model ϕ_{ult} (mrad)	Model K_i (k-in./rad)	Model / Test M_{ult}	Model / Test ϕ_{ult}	Model / Test K_i
5 Steel	N/A	N/A	220147	N/A	N/A	0.90
5 Comp	2482	92	351335	0.95	0.96	0.53
6	2472	72	675443	1.04	0.96	0.66
7 Steel	N/A	N/A	142333	N/A	N/A	0.69
7 Comp	1417	78	295665	0.95	1.01	0.47
8	1398	62	429200	0.99	1.02	0.40
Statistics			Mean	0.98	0.99	0.61
			COV	0.04	0.03	0.29
			Max	1.04	1.02	0.90
			Min	0.95	0.96	0.40

7.6 Simplified Model For Approximating Moment-Rotation Behavior

A model for approximating the moment-rotation behavior of the bare steel beam-girder connection which is simpler yet less flexible than the component model was developed in Section 6.6. It is desirable to expand this method for use with composite connections. The additional assumptions and modifications required to do this are presented in the following.

7.6.1 Assumptions and Simplifications

To limit the number of connection parameters that were considered in the development of a simplified model for bare steel connections, a variety of assumptions and/or simplifications were made. Additional assumptions and/or simplifications were made to expand the model for use with composite connections.

1. Only #4 Grade 60 reinforcing steel is used.
2. Only strong position studs are used, there is only one stud per deck rib, and shear stud spacing is constant along beam.
3. Only ¾-in. diameter shear studs are used.
4. S_0 is at least 12-in.
5. The composite slab strength is always limited by the strength of the reinforcing steel.

7.6.2 Moment Capacity, M_0

The three stage method of determining the bare steel connection moment capacity presented in Section 6.6.1 is the same with one exception. The additional moment resistance provided by the reinforced composite slab is added to the moment resistance of the bare steel connection.

$$M_0 = M_0 \text{ (for bare steel connection)} + R_{nslab}\, Y_r \qquad \text{(Eq 71)}$$

Where:

$$R_{nslab} = \min \begin{vmatrix} A_r\, F_{ur} \\ N_{studs}\, Q_{sol} \end{vmatrix}$$

Y_r = Distance from the top of the seat angle to the center of the reinforcing steel

The above method was used to estimate the moment capacity of each of the experimental connections. The ultimate shear applied during the test was used as V_{ult} for determining the moment capacity. The results are given in Table 29. In general, the method provided good estimates of the moment capacity.

Table 29 Comparison of Simplified Moment Capacity to Experimental Moment Capacity

Connection	M_0 (k-in)	M_{ult} (k-in)	M_0/M_{ult}
5	2618	2517	1.04
6	2388	2517	0.95
7	1486	1429	1.04
8	1413	1429	0.99
		Average	1.00
		COV	0.04

In addition to comparing M_0 to the moment capacity of the experimental connections, it was also compared to the moment capacity determined by the component model. As will be described later, a parameter analysis was used to determine the relationship between connection parameters and the curvature parameter in the Richard Equation. A comparison between the moment capacity determined from the component model and M_0 determined as outlined above was made for 971 of the connections included in the parameter analysis. The ratio of M_0 to the moment capacity determined by the component method was determined for each connection. The average for the 971 connections was 1.03 with a COV of 2.9%. The minimum ratio was 0.95 and the maximum ratio was 1.11. None of the connections considered failed in shear.

7.6.3 Initial Stiffness, K

The method outlined in Section 6.6.2 for determining the initial stiffness of bare steel connections is easily modified so that it can be used to determine the initial stiffness of composite connections. This is done by including the initial stiffness of the composite slab in the elastic combination of the component stiffness values.

$$K = \sum_{j=0}^{N_{w+1}} K_j \left(h + Y_j\right)^2 \qquad \text{(Eq 72)}$$

Where h is the elastic center of rotation given by:

$$h = -\frac{\sum_{j=0}^{N_{w+1}} K_j Y_j}{\sum_{j=0}^{N_{w+1}} K_j} \qquad \text{(Eq 73)}$$

Where K_j and Y_j for j equal to N_{w+1} are K_{islab} and Y_r. For a slab with shear stud strength higher than reinforcing steel strength an approximate value of K_{islab} was derived in Section 3.4.2.

$$K_{islab} = \frac{P_{slab1}}{\delta_{slab1} - \frac{\ln\left\{1 - \left(\frac{P_{slab1}}{N_{studs} Q_{sol}}\right)^{2.5}\right\}}{18}}$$

7.6.4 Final Stiffness, K_p

The method outlined in Section 6.6.3 for determining the final stiffness of bare steel connections is easily modified by adding the final stiffness of the composite slab to the final stiffness determined for the bare steel connection.

$$K_p = K_p \text{ (Bare steel connection)} + K_{pslab} Y_r \qquad \text{(Eq 74)}$$

For a slab with shear stud strength higher than reinforcing steel strength an approximate value of K_{pslab} was derived in Section 3.4.2.

$$K_{pslab} = 150 A_r / S_0 \qquad \text{(Eq 75)}$$

7.6.5 Curvature Parameter, n

For bare steel connection with low shear ratios (Ψ_2), the value of the curvature parameter was previously determined in Section 6.6.4 as

$$n = (1.67\ \Psi_1^2 - 0.71\ \Psi_1 + 0.72)\ \alpha_1 \qquad \text{(Eq 76)}$$

Where:

$\Psi_1 = R_f / R_{nh}$

α_1 = Correction factor accounting for number and spacing of bolts

$\alpha_1 = 1 + 0.0327\ P_w\ \beta_1\ \beta_2$

$\beta_1 = 0.35\ e^{2.09\ \Psi_1}$

$\beta_2 = 1.2 - 2.27 / N_w$

It was decided that, rather than develop all new parametric relationships between the composite connection parameters and the curvature parameter, correction factors which would modify the value of the curvature parameter based on Equation 76 would be developed instead. These correction factors were developed based on the results of a three stage parameter study. The first stage considered the effect of varying levels of composite slab strength with low values of the connection shear ratios (Ψ_2). The second stage considered the effect of varying Y_r with low values of Ψ_2. The third stage considered the effect of varying Ψ_2 from low values to values that would cause shear failure in the connection. Based on the results of this study the following correction factors were derived.

$$\alpha_3 = \beta_4 - \beta_5\ \Psi_1 \qquad \text{(Eq 77)}$$

Where:

α_3 = Correction factor accounting for the composite slab

$\beta_4 = (-0.82 - 0.27\ \Psi_3)\ \Psi_4^2 + (0.9 + 0.75\ \Psi_3)\ \Psi_4 + 1.25$

$\beta_5 = (-0.93 - 0.15\ \Psi_3)\ \Psi_4^2 + (1.21 + 0.53\ \Psi_3)\ \Psi_4 + 0.51$

$$\Psi_3 = \frac{N_{studs}\, Q_{sol}}{N_w\, R_{nh}}$$

$$\Psi_4 = \frac{A_r\, F_{ur}}{N_w\, R_{nh}}$$

$$\alpha_4 = \frac{{\Psi_2}^{0.022}\ {\Psi_3}^{0.003}\ {\Psi_4}^{0.232}}{{N_w}^{0.02}\ {\Psi_1}^{0.217}} \qquad \text{(Eq 78)}$$

Where:

α_4 = Correction factor accounting for shear ratio

For $\Psi_2 < 0.3$, α_4 should be taken as 1.0

7.6.6 Evaluation of Parameter Relationships

The parameter relations developed in the previous section were used to estimate the moment-rotation behavior of the experimental connections. These approximate moment-rotation behaviors were plotted against the test results. Review of these plots showed that the model provided a conservative estimate of the behavior up to around 30 mrad. Beyond this rotation, the estimate typically became unconservative. The estimate is initially conservative because the parameter equations were developed assuming a 1/16-in. bolt gap. It is believed that the bolt gaps for the experimental tests were much smaller than this value. The estimate becomes unconservative in the later stages because the value of n was calibrated for rotations up 20 mrad.

When the simplified model is compared to component model results that are consistent with the assumptions made in the development of the simplified model there is generally good correlation between the two. To illustrate this point the component model and simplified model were used to determine the moment-rotation behavior for four different connections which had a wide range of connection parameters. The resulting moment-rotation approximations are shown in Figure 54. There is generally good agreement between the component model and simplified model.

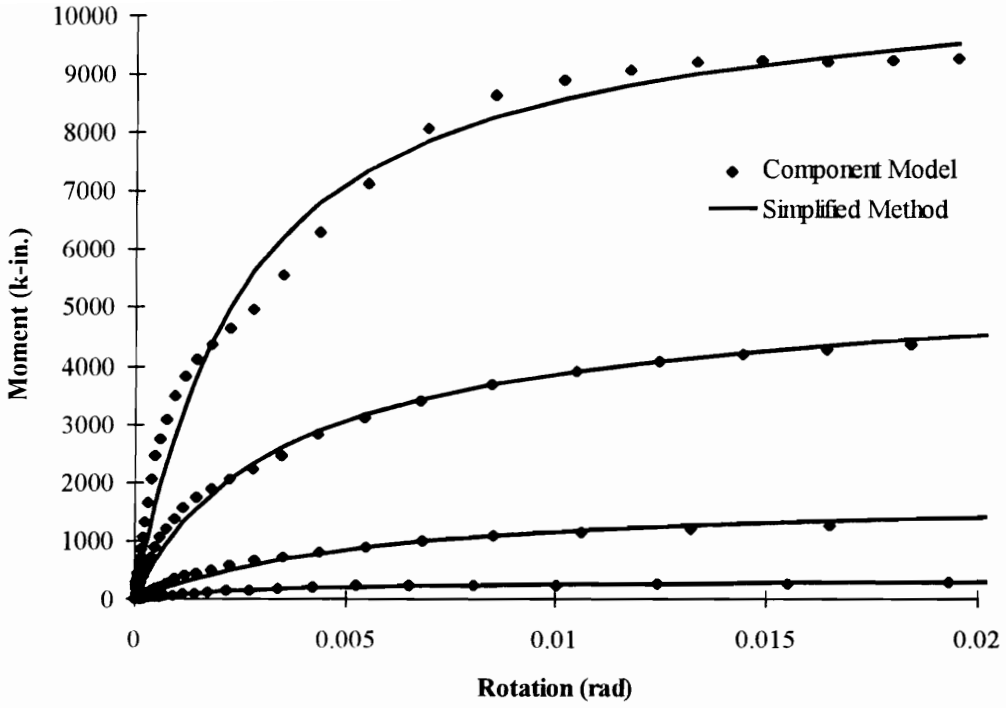

Figure 54 Comparison of Component and Simplified Model

7.7 Summary, Conclusions, and Recommendations

7.7.1 Summary and Conclusions

The primary objective of the study presented in this chapter was to present additional details needed to extend the component model, developed in Chapter 6, to composite beam-girder connections and to verify that the model can be used to accurately approximate the moment-rotation behavior. A secondary objective was to modify the simplified connection model, developed in Chapter 6, so that it can be used to approximate the moment-rotation behavior of composite connections. These objectives were achieved through a number of steps.

First, an experimental study of the moment-rotation behavior of composite PR connections was presented. The results of these tests provided experimental data for the

development and verification of the component and simplified models. In addition, the results provided information about the effect that pre-loading the steel connection has on the moment-rotation behavior of the composite connection. Observations regarding the effect of pre-loading include:

- The overall composite connection moment-rotation behavior for the connections that were pre-loaded was generally stiffer than for connections that were not pre-loaded. The moment resistance of the steel connection developed during pre-loading is believed to be the cause of this increase in composite connection stiffness.
- The initial portion of the moment-rotation behavior appears to be unaffected by pre-loading.
- If connection rotational ductility is limited by the ductility of the composite slab, then the overall connection ductility increases if connections are pre-loaded. The increase in ductility is generally attributed to the initial rotation of the bare steel connection, under the pre-load, which occurs before the composite slab cures.

Based on these observations, it appears conservative to use the composite connection moment-rotation behavior from experiments or analysis which do not consider the effect of connection pre-load. However, if connection ductility is limited by a part of the steel connection then this conclusion is most likely invalid.

Second, the component model developed in Chapter 6 for steel connections was modified to include the effect of the composite slab. These modifications included adding three behavior models which are used to develop a new combination element for the composite slab behavior. The composite slab combination element was then added to the ultimate strength analysis to determine the moment-rotation behavior of the composite connection. To ensure that the results of this analysis are valid, it was shown that the suggested upper limit for the shear ratio of 75% for bare steel connections was also applicable to composite connections. Comparisons between the results of the component model and the data from the experimental connection tests suggests that the component

model is very capable of approximating the moment-rotation behavior of composite connections.

Third, because of the computational complexity associated with the component model, a simplified model for determining the moment-rotation behavior was developed. The model was developed by making modifications to the simplified model developed in Chapter 6 to include the behavior of the reinforced composite slab.

7.7.2 Recommendations

The effective length (L_{eff}) used to determine axial deformation in the composite slab has only been proven to work for experimental tests in which the length of the slab in tension was constant from the start to the end of the test. These tests include the composite slab tests presented in Chapter 3 and the composite connection tests presented in this chapter. Because the length of slab in tension will change (as a result of varying inflection point), an analytical study showing what effect a changing slab length has on the composite slab behavior and consequently the connection behavior should be conducted.

The ultimate strength analysis used to implement the component method does not currently consider compatibility with the beam that the connection is attached to. As long as the connection does not fail in shear, this is not a problem. However, if the connection fails in shear, then there must be a modification made to the analysis to consider compatibility with the attached beam. A method for modifying the analysis and the implications of revising the analysis should be developed and determined if the connections are going to be used in locations where there is a possibility of connection shear failure.

A more detailed study of the influence of each of the connection components on the moment-rotation behavior is needed. This study can be conducted using the component model. A more comprehensive parametric model of the connection should be developed based on this study. It is also recommended that confidence intervals on the moment-rotation behavior be determined through a statistical combination of the connection component behaviors (such as Monte Carlo simulations).

REFERENCES

Annual Book of ASTM Standards-Part 4, ASTM Committee A-1 on Steel, American Society for Testing and Material, Philadelphia, Pa., 1988, ASTM A307 *Standard Test Methods and Definitions For Mechanical Testing of Steel Products.*

ANSYS User's Manual (1992) Volume 1 Procedures For Revision 5.0.

Astaneh, A., Call, S. M., and McMullin, K. M. (1989). "Design of Single Plate Shear Connections." AISC Engineering Journal, 26(1), 21-32.

Beer, F. P. and Johnston, Jr. E. R. (1981). *Mechanics of Materials*, McGraw-Hill

Bernuzzi, C., Noe', S., and Zandonini, R. (1991). "Semi-Rigid Composite Joints: Experimental Studies," *Connections in Steel Structures II: Behavior, Strength, and Design*, ed. R. Bjorhovde, A. Colson, G. Haaijer, and J.W.B. Stark, ASCE, 189-200.

Boresi, A. P., Schmidt, R. J. and Sidebottom, O. M. (1993). "Advanced Mechanics of Materials," Fifth Edition, John Wiley & Sons.

Bowman, M. D. and Quinn, B. P. (1994). "Examination of Fillet Weld Strength." AISC Engineering Journal, 31(3), 98-108.

Butler, L. J. and Kulak, G. L. (1971). "Strength of Fillet Welds as a Function of Direction of Load," Welding Journal, 50(5), 231s-234s.

Butler, L. J., Pal, Shubendu, S., and Kulak, G. L. (1972). "Eccentrically Loaded Welded Connections," Journal of the Structural Division, 98(ST5), 989-1005.

Buttry, K. E. (1965). "Behavior of Stud Shear Connectors in Lightweight and Normal-Weight Concrete," *MS Thesis, University of Missouri*

Caccavale, S. E. (1975). "Ductility of Single Plate Framing Connections," M. S. Thesis University of Arizona.

Collins, M. P. and Mitchell, D. (1991). *Prestressed Concrete Structures*, Prentice Hall, 142-154.

Crawford, S. F. and Kulak, G. L. (1971). "Eccentrically Loaded Bolted Connections," *Journal of the Structural Division*, **97**(ST3), 765-783.

Easterling, W. S., Gibbings, D. R. and Murray, T. M. (1993). "Strength of Shear Studs in Steel Deck on Composite Beams and Joists," *AISC Engineering Journal*, **30**(2), 44-55.

Eurocode 3: Design of Steel Structures (1993) Commission of The European Communities.

Eurocode 3: Design of Steel Structures, Part 1.1 Revised Annex J Joints and Building Frames (1994) Commission of The European Communities.

Fisher, J. W. (1965). "Behavior of Fasteners and Plates With Holes," *Journal of Structural Division*, **91**(ST6), 265-286.

Fisher, J. W. and Struik J. H. A. (1974). *Guide to Design Criteria for Bolted and Riveted Joints,* John Wiley & Sons

Fisher, J. W., Galambos, T. V., Kulak, G. L., and Ravindra, M. K. (1978) "Load and Resistance Factor Design Criteria For Connectors," *Journal of Structural Division*, **104**(ST9), 1427-1441.

Fisher, J. W., Ramseier, P. O., and Beedle, L. S. (1963). "Tests of A440 Steel Joints Fastened With A325 Bolts," *IABSE Publications*, Zurich, Switzerland, Vol. 23, 135-157.

Frank, K. H. and Yura, J. A. (1981). "An Experimental Study of Bolted Shear Connections", Report No. FHWA/RD-81/148, US. Department of Transportation, Federal Highway Administration.

Galambos, T. V. and Ravindra, M. K. (1978). "Properties of Steel For Use In LRFD," *Journal of the Structural Division*, **104**(ST9), 1459-1468.

Gillett, P. E. (1978), "Ductility and Strength of Single Plate Connections," Ph.D. Dissertation, The University of Arizona.

Johnson, R. P. and Huang, D. (1994). "Resistance to Longitudinal Shear of Composite Beams With Profiled Sheeting," Research Report CE48 University of Warwick Department of Engineering.

Johnson, R. P., Greenwood, R. D., and VanDalen, K. (1969). "Stud Shear Connectors in Hogging Moment Regions of Composite Beams," *The Structural Engineer*; **47**(9), 345-350.

Karsu, B. (1995) "The Load Deformation Response of Single Bolt Connections," M. S. Thesis Virginia Polytechnic Institute and State University.

Kulak, G. L. and Timler, P. A. (1984). "Tests on Eccentrically Loaded Fillet Welds," Structural Engineering Report No. 124, Department of Civil Engineering, University of Alberta, Edmonton, Alberta.

Kulak, G. L., Fisher, J. W., and Struik, J. H. A. (1987*). Guide to Design For Bolted and Riveted Joints*, 2nd Edition, John Wiley & Sons, New York, NY, 1987.

Lesik, D. F. and Kennedy, D. J. L. (1990). "Ultimate Strength of Fillet Welded Connections Loaded in Plane," *Canadian Journal of Civil Engineering*, **17**(1), 55-67.

Lewis, B. E. (1994). "Edge Distance, Spacing, and Bearing in Bolted Connections", *DRAFT* Report, Oklahoma State University.

Load and Resistance Factor Design Specification for Structural Steel Buildings, (1993). American Institute of Steel Construction, Chicago, Illinois.

Load and Resistance Factor Design Specification for Structural Steel Buildings (1986). American Institute of Steel Construction, Chicago, Illinois.

LRFD Cold-Formed Steel Design Manual (1991). American Iron and Steel Institute, (AISI), Washington, D.C.

Lyons, J. C., Easterling, W. S. and Murray, T.M. (1994). "Strength Of Headed Shear Studs," Vols. I and II, Report CE/VPI-ST 94/07, Virginia Polytechnic Institute and State University, Blacksburg, VA.

Manual of Steel Construction Load and Resistance Factor Design (1986). American Institute of Steel Construction, Chicago, Illinois.

Manual of Steel Construction Volume I and II Load and Resistance Factor Design (1993). American Institute of Steel Construction, Chicago, Illinois.

Miazga, G. S. and Kennedy, D. J. L. (1989). "Behavior of Fillet Welds As A Function Of The Angle Of Loading," Canadian Journal of Civil Engineering, 16(), 583-599.

Minutes of the June 3, 1994 meeting of the Research Council on Structural Connections, Proposal by J.A. Yura and K.H. Frank.

Mirza, S. A. and MacGregor, J. G. (1979). "Variability of Mechanical Properties of Reinforcing Bars," *Journal of the Structural Division*, **105**(ST5), 921-937.

Munse, W. H., Wright, D. T., and Newmark, N. M. (1954) "Laboratory Tests of High Tensile Bolted Structural Joints" Proceeding of ASCE, **80**(441) May, p 441-1 to 441-38.

Oehlers and Coughlan (1986) "Shear Stiffness of Stud Shear Connections in Composite Beams," Journal of Constructional Steel Research, Vol. 6, p273-284.

Ollgaard, J. G., Slutter, R. G., and Fisher, J. W. (1971). "Shear Strength of Stud Connectors in Lightweight and Normal Weight Concrete." *AISC Engineering Journal*, **8**(2), 55-64.

Perry, W. C. (1981). "The Bearing Strength of Bolted Connections," M. S. Thesis University of Texas at Austin.

Read, D. R. and Frank, K. H. (1993) "Statistical Analysis of Tensile Data For Wide-Flange Structural Shapes," Unpublished Report From University of Texas at Austin, 1-17.

Rex, C. O. (1994). "Behavior of Composite Semi-Rigid Beam-To-Girder Connections," MS Thesis, Virginia Polytechnic Institute and State University, Blacksburg, VA.

Rex, C. O. and Easterling, W. S. (1995). "Partially Restrained Composite Beam-To-Girder Connections." *AISC Engineering Journal*, **32**(4), 145-158.

Rex, C. O. and Easterling, W. S. (1996(a)). "Behavior and Modeling of Mild and Reinforcing Steel," Report CE/VPI-ST 96/12, Virginia Polytechnic Institute and State University, Blacksburg, VA.

Rex, C. O. and Easterling, W. S. (1996(b)). "Behavior and Modeling of a Reinforced Composite Slab as Part of a Partially Restrained Composite Beam-Girder Connection," Report CE/VPI-ST 96/13, Virginia Polytechnic Institute and State University, Blacksburg, VA.

Rex, C. O. and Easterling, W. S. (1996(c)). "Behavior and Modeling Of A Single Plate Bearing On A Single Bolt," Report CE/VPI-ST 96/14, Virginia Polytechnic Institute and State University, Blacksburg, VA.

Rex, C. O. and Easterling, W. S. (1996(d)). "Behavior and Modeling of Single Bolt Lap Plate Connections," Report CE/VPI-ST 96/15, Virginia Polytechnic Institute and State University, Blacksburg, VA.

Rex, C. O. and Easterling, W. S. (1996(e)). "Behavior and Modeling of Partially Restrained Steel Beam-Girder Connections," Report CE/VPI-ST 96/16, Virginia Polytechnic Institute and State University, Blacksburg, VA.

Rex, C. O. and Easterling, W. S. (1996(f)). "Behavior and Modeling of Partially Restrained Composite Beam-Girder Connections," Report CE/VPI-ST 96/17, Virginia Polytechnic Institute and State University, Blacksburg, VA.

Richard, R. M. and Elsalti, M. K. (1991). "PRCONN, Moment-Rotation Curves for Partially Restrained Connections." Users manual for program developed at The University of Arizona Department of Civil Engineering and Engineering Mechanics.

Richard, R. M., Gillett, P. E., Kriegh, J. D., and Lewis, B. A. (1980). "The Analysis & Design of Single-plate Framing Connections," *AISC Engineering Journal*, 2nd Qtr., 38-52.

Salmon, C. G. and Johnson, J. E. (1990). Steel Structures: Design and Behavior, Third Edition, Harper and Row, New York.

Sarkar, D. and Wallace, B. (1992). *Design of Single Plate Framing Connections, DRAFT* Report No. FSEL/AISC 92-01, Fears Structural Engineering Laboratory, University of Oklahoma.

Simkins, T. E. (1967). "The Mutuality of Static and Kinetic Friction," Lubrication Engineering, American Society of Lubrication, Vol. **23** (21), 26-31.

Specification for Structural Steel Buildings Allowable Stress Design and Plastic Design (1989). American Institute of Steel Construction, Chicago, Illinois.

Sublett, C. N., Easterling, W. S. and Murray, T.M. (1992). "Strength Of Welded Headed Studs In Ribbed Metal Deck On Composite Joists," Report No. CE/VPI-ST 92/03, Virginia Polytechnic Institute and State University, Blacksburg, VA, 257 pages.

Swannell, P., and Skewes, I. C. (1979). "The Design of Welded Brackets Loaded In-Plane: General Theoretical Ultimate Load Techniques and Experimental Program," AWRA Report P6-1-78. Australian Welding Research, 7, 55-70.

Tate, M. B. and Rosenfeld, S. J. (1946). "Preliminary Investigation of the Loads Carried by Individual Bolts in Bolted Joints," Technical Note No. 1051, National Advisory Committee for Aeronautics, Washington, D. C., 1-68.

Vogt, F. (1947). "Load Distribution in Bolted or Riveted Structural Joints in Light-Alloy Structures," Technical Note No. 1135, National Advisory Committee for Aeronautics, Washington, D. C.

Wallaert, J. J. and Fisher, J. W. (1965). "The Shear Strength of High-Strength Bolts," *Journal of the Structural Division*, **91**(ST3), 99-125.

Wang, C. K. and Salmon, C. G. (1985). *Reinforced Concrete Design*, Fourth Edition, Harper & Row, New York.

Zandonini, R. (1989). "Semi-Rigid Composite Joints," Strength and Stability Series, Vol. 8, *Connections*, ed. R. Narayanan, Elsevier, London, 63-120.

VITA

Clinton Owen Rex was born in Lima, Ohio on the 5th of August 1968. He graduated valedictorian of Ada High School in 1987. He graduated Summa Cum Laude with his Bachelor of Science in Civil and Environmental Engineering from The University of Cincinnati in 1992. As an undergraduate, he worked for a variety of engineering firms including Peterman and Associates (Engineering and Surveying Consultants), Turner Construction Company (General Contractors), and Dames & Moore (Environmental Consultants). In the fall of 1992 he entered The Charles Edward Via, Jr. Department of Civil Engineering in pursuit of a Master of Science in Civil Engineering which he received in the Spring of 1994. After receiving the Master of Science degree, he remained at The Charles Edward Via, Jr. Department of Civil Engineering in pursuit of a Doctor of Philosophy in Civil Engineering. He was a Via Fellow while pursuing both the M.S. and Ph.D. degrees. He is now working for Stanley D. Lindsey and Associates which is a structural engineering firm in Atlanta, Georgia.